

The crossover from the Macroscopic Fluctuation Theory to the Kardar-Parisi-Zhang equation controls the large deviations beyond Einstein's diffusion

Alexandre Krajenbrink*

Quantinuum and Cambridge Quantum Computing, Cambridge, UK

Pierre Le Doussal

*Laboratoire de Physique de l'École Normale Supérieure, CNRS,
ENS & PSL University, Sorbonne Université, Université de Paris, 75005 Paris, France*

(Dated: April 12, 2022)

We study the crossover from the macroscopic fluctuation theory (MFT) which describes 1D stochastic diffusive systems at *late times*, to the weak noise theory (WNT) which describes the Kardar-Parisi-Zhang (KPZ) equation at *early times*. We focus on the example of the diffusion in a time-dependent random field, observed in an atypical direction which induces an asymmetry. The crossover is described by a non-linear system which interpolates between the derivative and the standard non-linear Schrodinger equations in imaginary time. We solve this system using the inverse scattering method for mixed-time boundary conditions introduced by us to solve the WNT. We obtain the rate function which describes the large deviations of the sample-to-sample fluctuations of the cumulative distribution of the tracer position. It exhibits a crossover as the asymmetry is varied, recovering both MFT and KPZ limits. We sketch how it is consistent with extracting the asymptotics of a Fredholm determinant formula, recently derived for sticky Brownian motions. The crossover mechanism studied here should generalize to a larger class of models described by the MFT. Our results apply to study extremal diffusion beyond Einstein's theory.

Introduction For one-dimensional stochastic systems with a diffusive scaling at large time, such as the symmetric exclusion process (SEP), the macroscopic fluctuation theory (MFT) [1] provides a powerful framework to describe the large deviations of the density and current [2]. Upon introduction of an asymmetry or driving, such as in the asymmetric exclusion process (ASEP) [3], the diffusive scaling breaks down above some scale, and the large scale behavior of the model is usually described by the Kardar-Parisi-Zhang (KPZ) universality class [4]. A paradigmatic member of this class is the KPZ equation [5], which can be obtained as the continuum limit of the ASEP with a weak asymmetry [6]. The large deviations for the KPZ equation at short time can be described using the so-called weak noise theory (WNT) [7–9]. It is a close cousin of the MFT, both reduce the calculation of large-deviation rate functions to solving saddle point partial non-linear differential equations, not always an easy task. A natural question is to understand, in presence of a small but relevant asymmetry, the nature of the crossover from the MFT to the WNT. We can expect that it should be somewhat subtle since the MFT describes the large deviations at large time, while the WNT describes the large deviations for the KPZ equation at short time.

Recently, exact solutions of the WNT equations were obtained by us [10, 11]. It required to extend the inverse scattering method of [12, 13] to mixed-time boundary conditions on the so-called $\{P, Q\}$ system, a close cousin of the non-linear Schrodinger equation (NLS). In this paper we show on an example that the crossover from the MFT to the WNT can be realized as the crossover from the derivative non-linear Schrodinger equation (DNLS) [14] to the NLS equation. We focus on a model for the diffusion of a particle (also called a tracer) at position $y(\tau)$ convected by a centered Gaussian random field $\eta(y, \tau)$ which is white noise in time and short-range correlated in space, described by a Langevin equation

$$\frac{dy(\tau)}{dt} = \sqrt{2}\eta(y(\tau), \tau) + \chi(\tau), \quad (1)$$

where χ is a standard white noise in time. Equivalently, the probability density function (PDF) for the particle position in a given realization of η , $q_\eta(y, \tau) = \langle \delta(y(\tau) - y) \rangle_\chi$, obeys the Fokker-Planck equation

$$\partial_\tau q_\eta(y, \tau) = \partial_y^2 q_\eta(y, \tau) - \partial_y (\sqrt{2}\eta(y, \tau) q_\eta(y, \tau)). \quad (2)$$

This model, and its discrete random walk versions, has been revisited recently [15–20]. The typical behavior is rather dull, and given by the random

field average $\overline{q_\eta(y, \tau)}$ which yields standard diffusion $y \sim \sqrt{\tau}$. However, in the space-time directions which are *atypical* for the random walk, e.g. $y \sim v\tau$, it exhibits interesting sample to sample fluctuations related to the KPZ class [15]. In fact, in the small v regime (more precisely for $y \sim \tau^{3/4}$), it maps to the KPZ equation itself (as predicted in [16, 18] and proved in [20], see also [17]). These predictions found interesting applications in quantum models with noise, for observables dominated by atypical trajectories [21]. They also lead to interesting predictions for extremal diffusion [15, 16, 20, 22], i.e. for the position of the maximum of N independent particles, see below. It turns out that Eq. (2) also arises from a lattice gas model of heat transfer, the Kipnis-Marchioro-Presutti (KMP) model [23], to which the MFT has been applied [1, 24–36]. Hence we anticipate a crossover from the MFT to the WNT when focusing on less and less typical directions. It is an interesting and open question to understand how the large-time large deviations of this model match the short-time large deviations of the KPZ equation.

In this paper we show that this crossover is described by the so-called interpolating system, see (11) below. Using inverse scattering methods we provide the solution for this system and obtain the large deviation function of a particular observable. At the end we sketch how the result agrees with the asymptotic behavior of a Fredholm determinant formula for this observable obtained in [19] for a related model of sticky Brownian motions. We consider a particle which is at position $y = 0$ at time $\tau = 0$ and study the statistics of the probability $Z(Y, T)$ that at time $\tau = T$ it is found to the right of $y = Y$

$$Z(Y, T) = \mathbb{P}(y(T) > Y | y(0) = 0) \quad (3)$$

We also need to introduce $H(Y, T)$ the logarithm of this probability, our observable of interest here. It also equals

$$Z(Y, T) = e^{H(Y, T)} = \int_Y^{+\infty} dy q_\eta(y, T) \quad (4)$$

with $q_\eta(y, 0) = \delta(y)$. Note that $H(Y, T) \in [-\infty, 0]$ since $Z = Z(Y, T) \in [0, 1]$. $Z(Y, T)$ is itself a random variable that fluctuates depending on the realization of $\eta(y, \tau)$, which from now on is a standard white noise in space and time. We consider the diffusive scaling so that Y, T are large, with $Y = \xi\sqrt{T}$, where $\xi = \mathcal{O}(1)$ is fixed and plays the role of the asymmetry parameter. We are interested in the tails of the PDF of $Z = Z(Y, T)$, equivalently of $H = H(Y, T)$, which

take the large deviation forms for $T \gg 1$

$$\mathcal{P}(Z) \sim e^{-\sqrt{T}\hat{\Phi}(Z)}, \quad \mathcal{P}(H) \sim e^{-\sqrt{T}\Phi(H)}, \quad (5)$$

where $\Phi(H) = \hat{\Phi}(Z = e^H)$ is the rate function which we want to compute, together with its (implicit) dependence in ξ .

We perform a change of variable $y = x\sqrt{T}$, $\tau = tT$, and $\sqrt{T}q_\eta(y, \tau) = Q_{\tilde{\eta}}(x, t)$ so that (2) becomes

$$\partial_t Q_{\tilde{\eta}} = \partial_x^2 Q_{\tilde{\eta}}(x, t) - T^{-1/4} \partial_x (\sqrt{2}\tilde{\eta}(x, t) Q_{\tilde{\eta}}(x, t)) \quad (6)$$

where $\tilde{\eta}$ is a standard white noise and $Z(Y, T) = \int_\xi^{+\infty} dx Q_{\tilde{\eta}}(x, 1)$. To obtain $\Phi(H)$ in (5) we will first calculate the rate function $\Psi(z)$ which is defined from the generating function

$$\overline{\exp(-z\sqrt{T}Z(Y, T))} \sim \exp(-\sqrt{T}\Psi(z)) \quad (7)$$

Since Z is a random variable taking values in $[0, 1]$, $\Psi(z)$ is defined for any real z , with $\Psi'(z) \in [0, 1]$ [37]. Using (5) one can compute the expectation value in the l.h.s of (7) for $T \gg 1$ via a saddle point method and obtain the relation

$$\Psi(z) = \min_{H \leq 0} [\Phi(H) + ze^H] = \min_{Z \in [0, 1]} [\hat{\Phi}(Z) + zZ] \quad (8)$$

which shows that $\Psi(z)$ and $\Phi(H)$ are Legendre transforms [38]. The minimum in (8) is attained at $H = H(z)$ which is a solution of $\Phi'(H) = -ze^H$. Anticipating, a remarkable feature of the present problem is that for $\xi > \sqrt{8}$ this equation has more than one solution, which leads to different possible branches for $\Psi(z)$. In that case, we will call the "optimal" $\Psi(z)$ the function defined from (8) (and (7)), i.e. as a global minimum, which will thus exhibit a *first-order transition*, with a jump in $\Psi'(z)$. Our strategy will be to compute all branches of $\Psi(z)$, which allow to reconstruct $\Phi(H)$ and $\hat{\Phi}(Z)$.

Interpolating system. To do so we note that, as in [10], the l.h.s of (7) can be represented as a path integral

$$\iint \mathcal{D}Q \mathcal{D}P e^{-\sqrt{T}(S[P, Q] + z \int_\xi^{+\infty} dx Q(x, 1))} \quad (9)$$

where the associated dynamical action is

$$S[P, Q] = \int_0^1 dt \int_{\mathbb{R}} dx [P(\partial_t - \partial_x^2)Q - Q^2(\partial_x P)^2] \quad (10)$$

and $P\sqrt{T}$ is the response field. In the large T limit the path integral in (9) is controlled by its saddle point. Taking the functional derivatives w.r.t. $\{P, Q\}$, introducing the field $R(x, t) = \partial_x P(x, t)$, and performing a Galilean transformation $x \rightarrow x - \xi t$ to bring back ξ to zero (see details in [37]), we arrive

at the system of coupled equations

$$\begin{aligned} \partial_t Q &= \partial_x^2 Q + 2\beta \partial_x(Q^2 R) + 2gQ^2 R \\ -\partial_t R &= \partial_x^2 R - 2\beta \partial_x(QR^2) + 2gQR^2 \end{aligned} \quad (11)$$

with $\beta = -1$ [39] and $g = -\beta\xi/2$ and with the mixed-time boundary conditions

$$Q(x, t=0) = \delta(x) \quad , \quad R(x, t=1) = \Lambda\delta(x) \quad (12)$$

with $\beta\Lambda = ze^{-\frac{\xi^2}{4}}$ [40]. Once this system is solved, the value of $\Psi(z)$ is obtained from the saddle point via [37]

$$\Psi'(z) = \int_0^{+\infty} dx Q(x, 1) e^{-\frac{1}{2}x\xi - \frac{\xi^2}{4}} \quad (13)$$

and $\Psi(0) = 0$, where $Q(x, 1)$ is the z -dependent solution of the above system. This system interpolates between (i) the $\{P, Q\}$ system for $\beta = 0$ (with P called R here), i.e. the cousin of the NLS equation [12, 13] which controls the WNT of the KPZ equation [10, 11], and (ii) the cousin of the DNLS equation [14] for $g = 0$, which controls the MFT for this model for $\xi = 0$ [41]. Thus as $\xi = \frac{Y}{\sqrt{T}}$ is increased, g increases and in the limit of large ξ , which corresponds to atypical directions, one recovers the large deviations associated to the KPZ equation (see below). Remarkably, this interpolating system is again integrable [42]. We will thus extend the inverse scattering analysis of our previous work [10, 11] on the $\{P, Q\}$ system. Note in passing that the functions $Q(x, t)$ and $R(x, t)$ are not even for $\beta \neq 0$ but as in the $\{P, Q\}$ system they still enjoy the symmetry

$$R(x, t) = \Lambda Q(-x, 1-t). \quad (14)$$

Inverse scattering solution of the interpolating system. It is a simple generalization of our previous works [10, 11] so we will sketch it. The Lax pair of linear differential equation reads $\partial_x \vec{v} = U_1 \vec{v}$, $\partial_t \vec{v} = U_2 \vec{v}$ where $\vec{v} = (v_1, v_2)^\top$ is a two component vector (depending on x, t, k) where

$$U_1 = \begin{pmatrix} -\frac{ik}{2} & -(g + i\beta k)R(x, t) \\ Q(x, t) & \frac{ik}{2} \end{pmatrix}, \quad U_2 = \begin{pmatrix} A & B \\ C & -A \end{pmatrix} \quad (15)$$

with $A = \frac{k^2}{2} - (g + i\beta k)QR$, $B = -(g + i\beta k)((ik - \partial_x)R + 2\beta QR^2)$, $C = (\partial_x + ik)Q + 2\beta Q^2 R$. One can check that the compatibility condition $\partial_t U_1 - \partial_x U_2 + [U_1, U_2] = 0$ recovers (11). Let $\vec{v} = e^{k^2 t/2} \phi$ with $\phi = (\phi_1, \phi_2)^\top$ and $\vec{v} = e^{-k^2 t/2} \bar{\phi}$ be two independent solutions of the linear problem such that at $x \rightarrow -\infty$, $\phi \simeq (e^{-ikx/2}, 0)^\top$ and $\bar{\phi} \simeq (0, -e^{ikx/2})^\top$. Assuming from now on that

$\{Q, R\}$ vanish at infinity, the $x \rightarrow +\infty$ behavior of these solutions defines scattering amplitudes

$$\phi \underset{x \rightarrow +\infty}{\simeq} \begin{pmatrix} a(k, t) e^{-\frac{ikx}{2}} \\ b(k, t) e^{\frac{ikx}{2}} \end{pmatrix}, \quad \bar{\phi} \underset{x \rightarrow +\infty}{\simeq} \begin{pmatrix} \tilde{b}(k, t) e^{-\frac{ikx}{2}} \\ -\tilde{a}(k, t) e^{\frac{ikx}{2}} \end{pmatrix} \quad (16)$$

Plugging this form into the ∂_t equation of the Lax pair at $x \rightarrow +\infty$, one finds a very simple time dependence, $a(k, t) = a(k)$ and $b(k, t) = b(k)e^{-k^2 t}$, $\tilde{a}(k, t) = \tilde{a}(k)$ and $\tilde{b}(k, t) = \tilde{b}(k)e^{k^2 t}$. Another normalization relation is obtained from the Wronskian of the two solutions, $a(k)\tilde{a}(k) + b(k)\tilde{b}(k) = 1$.

Integrating the ∂_x equation of the Lax pair successively for $\bar{\phi}$ and ϕ at $t = 0$ and at $t = 1$, using (12), allows to obtain (see [37])

$$\tilde{b}(k) = (g + i\beta k)\Lambda e^{-k^2}, \quad b(k) = 1 \quad (17)$$

and

$$\begin{aligned} a(k) &= 1 - (g + i\beta k)\Lambda Q_-(k) \\ \tilde{a}(k) &= 1 - (g + i\beta k)\Lambda Q_+(k) \end{aligned} \quad (18)$$

where we have defined the half-Fourier transforms

$$Q_\pm(k) = \int_{\mathbb{R}^\pm} dx Q(x, 1) e^{-ikx} \quad (19)$$

From the normalization relation one also obtains

$$a(k)\tilde{a}(k) = 1 - b(k)\tilde{b}(k) = 1 - (g + i\beta k)\Lambda e^{-k^2} \quad (20)$$

which $Q_\pm(k)$ must satisfy. For $\beta = 0$ this equation was first obtained by us in Ref. [10] and used recently in [43]. As noted there, it is akin to the Fourier transform of the Wiener-Hopf formulae obtained in [35, Eqs. (S65)–(S66)]. Our Eq. (20) is thus the natural extension to arbitrary g, β .

Taking these relations in the large k limit we obtain that $Q(x, 1)$ has a jump at $x = 0$, with some relation between the right and left values $Q(0^\pm, 1)$. We now follow similar manipulations as in the recent work [41], the details are given in [37]. As $k \rightarrow \infty$ one has

$$Q_\pm(k) \simeq \pm \frac{1}{ik} Q(0^\pm, 1) \quad (21)$$

$$a(k) \simeq 1 + \beta\Lambda Q(0^-, 1) \quad (22)$$

$$\tilde{a}(k) \simeq 1 - \beta\Lambda Q(0^+, 1) \quad (23)$$

Equation (20) at $k \rightarrow \infty$ thus implies a first relation

$$(1 - \beta\Lambda Q(0^+, 1))(1 + \beta\Lambda Q(0^-, 1)) = 1 \quad (24)$$

The complete solution of (20) is given by [37]

$$\begin{aligned} a(k) &= (1 + \beta\Lambda Q(0^-, 1)) e^{\Phi_+(k)} \\ \tilde{a}(k) &= (1 - \beta\Lambda Q(0^+, 1)) e^{\Phi_-(k)} \end{aligned} \quad (25)$$

where

$$\begin{aligned}\Phi_{\pm}(k) &= \pm \int_{\mathbb{R}} \frac{dq}{2i\pi} \frac{\log(1 - (g + i\beta q)\Lambda e^{-q^2})}{q - k \mp i0^+} \\ &= \pm \int_{\mathbb{R}} \frac{dq}{2i\pi} \frac{\log(1 - (g + i\beta q)\Lambda e^{-q^2})}{q - k} \\ &\quad + \frac{1}{2} \log(1 - (g + i\beta k)\Lambda e^{-k^2})\end{aligned}\quad (26)$$

The first expression for $\Phi_{\pm}(k)$ is valid for k in the complex upper/lower half plane including the real line, while the second is valid for real k only. In the limit $\beta \rightarrow 0$ one has $Q(0^+, 1) = Q(0^-, 1)$ and one recovers the same formula as first obtained in [10]. In the limit $g \rightarrow 0$ one recovers the recent result in [41].

We still need to determine the two unknown constants $Q(0^{\pm}, 1)$ which are related by (24). Combining (18) and (25) we obtain the relation

$$(g + i\beta k)\Lambda Q_{\mp}(k) = 1 - (1 \pm \beta\Lambda Q(0^{\mp}, 1))e^{\Phi_{\pm}(k)} \quad (27)$$

which is valid for $\Im(k) \in \mathbb{R}^{\pm}$. Taken at $k = \frac{ig}{\beta} = -i\frac{\xi}{2}$ one obtains

$$1 \pm \beta\Lambda Q(0^{\mp}, 1) = e^{-\Phi_{\pm}(ig/\beta)} \quad (28)$$

where, for $g/\beta \neq 0$

$$\Phi_{\pm}(ig/\beta) = \pm\beta \int_{\mathbb{R}} \frac{dq}{2\pi} \frac{\log(1 - (g + i\beta q)\Lambda e^{-q^2})}{g + i\beta q} \quad (29)$$

are opposite real numbers, so that (28) is compatible with (24). As discussed below and in [37], Eqs. (26) and (29) are valid only for $\Lambda g < 1$.

Specialization to the MFT problem. We now compute $\Psi(z)$ from Eq. (13) and replace $\beta = -1$, $g = -\beta\frac{\xi}{2}$ and $\beta\Lambda = ze^{-\xi^2/4}$. We note that the r.h.s. of (13) is equal to

$$\Psi'(z) = Q_+(k = -i\frac{\xi}{2})e^{-\frac{\xi^2}{4}} = 1 - Q_-(k = -i\frac{\xi}{2})e^{-\frac{\xi^2}{4}} \quad (30)$$

where the second equality comes from the conservation of probability (see (S64)). These quantities can be obtained taking derivatives. Taking a derivative w.r.t. k of (27) at $k = \frac{ig}{\beta} = -i\frac{\xi}{2}$ and using (28) one obtains (see details in [37])

$$z\Psi'(z) = \int_{\mathbb{R}} \frac{dq}{2\pi} \frac{\log(1 - z(iq - \frac{\xi}{2})e^{-q^2 - \frac{\xi^2}{4}})}{(iq - \frac{\xi}{2})^2} + z\Theta(-\xi) \quad (31)$$

where here and below we use the convention that $\Theta(0) = 1/2$ and the principal part is needed only for

$\xi = 0$. Integrating over z one obtains

$$\Psi(z) = -\int_{\mathbb{R}} \frac{dq}{2\pi} \frac{\text{Li}_2(z(iq - \frac{\xi}{2})e^{-q^2 - \frac{\xi^2}{4}})}{(iq - \frac{\xi}{2})^2} + z\Theta(-\xi) \quad (32)$$

where the last term guarantees analyticity of $\Psi(z)$ in ξ . Denoting here $\Psi_{\xi}(z)$ to indicate the dependence in ξ and performing the change $q \rightarrow -q$ in the integrand we see that it obeys the symmetry

$$\Psi_{-\xi}(z) = \Psi_{\xi}(-z) + z \quad (33)$$

which is expected from the definition (7), since upon the symmetry $y \rightarrow -y$ in (2) and (4), the PDF of $Z(Y, T)$ must be the same as the PDF of $1 - Z(-Y, T)$. For $\xi = 0$ one can check (see [37]) that (32) is consistent with the result in [41].

Expanding (32) in series of z one predicts the cumulants of the probability $Z = Z(Y, T)$ in (3). The first one is the typical value $\bar{Z} = Z_{\text{typ}}(\xi) = e^{H_{\text{typ}}(\xi)}$ (i.e. in a typical random field η)

$$\begin{aligned}Z_{\text{typ}}(\xi) = \Psi'(0) &= -\int_{\mathbb{R}} \frac{dq}{2\pi} \frac{e^{-q^2 - \frac{\xi^2}{4}}}{iq - \frac{\xi}{2}} + \Theta(-\xi) \\ &= \frac{1}{2} \text{Erfc}\left(\frac{\xi}{2}\right) = \int_{\xi}^{+\infty} \frac{dx}{\sqrt{4\pi}} e^{-\frac{x^2}{4}}\end{aligned}\quad (34)$$

as expected since the mean (and typical) behavior is standard diffusion. The second cumulant is predicted as $\overline{Z(Y, T)^2}^c \simeq -T^{-1/2}\Psi''(0) = \frac{1}{4\sqrt{2\pi T}}e^{-\frac{\xi^2}{2}}$, as confirmed by a direct weak-noise expansion, see Section VIII D in [37].

Branch cuts, branches of $\Psi(z)$ and the rate function $\Phi(H)$. We will determine in this section the rate function $\Phi(H)$ for $\xi \geq 0$ (for $\xi < 0$ we rely on the symmetry (33)). From our expression for $\Psi(z)$ a priori one can now determine the rate function for the PDF's in (5) by inverting the Legendre transform (8), which gives the parametric representation

$$\Phi(H) = \Psi(z) - ze^H, \quad \Psi'(z) = e^H \quad (35)$$

and in terms of Z ,

$$\hat{\Phi}(Z) = \Psi(z) - zZ, \quad Z = \Psi'(z). \quad (36)$$

As mentioned in the introduction, the parametric representation (36) can lead to different different branches, i.e. a multi-valuation of $\Psi(z)$. The "optimal" $\Psi(z)$, i.e. solution of the Legendre transform (8), is defined as the minimum over the different branches.

The origin of these different branches can be traced to the ambiguity which remains for $\Psi(z)$ since we have not specified the determination of the

ξ	$0 \leq \xi \leq \xi_1$	$\xi_1 \leq \xi \leq \xi_2$ $z_{c1} < z_{c2} < z_c$	$\xi_2 \leq \xi$ $z_{c1} < z_c < z_{c2}$
$\Delta(z) =$	$\begin{cases} 0, & z_c < z \\ \Delta_1(z), & z < z_c \end{cases}$	$\begin{cases} 0, & z_c < z \\ \Delta_1(z), & z_{c1} < z < z_c \\ \Delta_2(z), & z_{c1} < z < z_{c2} \\ \Delta_3(z), & z < z_{c2} \end{cases}$	$\begin{cases} 0, & z_c < z \\ \Delta_1(z), & z_{c1} < z < z_c \\ \Delta_2(z), & z_{c1} < z < z_c \\ \Delta_2(z) - \Delta_1(z), & z_c < z < z_{c2} \\ \Delta_3(z) - \Delta_1(z), & z_c < z < z_{c2} \\ \Delta_3(z), & z < z_c \end{cases}$

Table I. Determination of the jump function $\Delta(z)$ in the different phases in the case $\xi \geq 0$. One has $z_c = -\frac{2}{\xi}e^{\xi^2/4} \leq 0$ and the points $z = z_{c1}$ and $z = z_{c2}$ are turning points which depend on ξ . In the interval $z \in [z_{c1}, z_{c2}]$, the function $\Delta(z)$ is multi-valued (i.e. it has several branches) due to these turning points. The definition of Δ_ℓ is given in (39).

logarithm in Eq. (31). In practice, the functions $\log(1-x)$, and $\text{Li}_2(x)$ in (32), admit a branch cut for $x > 1$. There are thus branch cuts in the complex plane for q , and for some values of $\{z, \xi\}$ one of these branch cuts may cross the integration axis, see Figures in [37]. These branch cuts originate from the values of q such that the argument of the logarithm in Eq. (31) vanishes. Parameterizing the integration variable as $q = ip$, we then have to find the solutions (i.e. the zeroes) of the following equation

$$e^{-p^2 + \frac{\xi^2}{4}} + z(p + \frac{\xi}{2}) = 0. \quad (37)$$

For $z > z_c$ where $z_c = -\frac{2}{\xi}e^{\xi^2/4} \leq 0$, there is never a branch cut crossing the real axis, see [37], hence Eqs. (31) and (32) are valid in this regime and determine what we call the *main branch*.

For $z < z_c$ all real solutions of Eq. (37) for p are negative and as consequence one branch cut crosses the real axis [37]. It is then necessary to obtain the analytical continuation of Eqs. (31) and (32) to any z by deforming the contour of integration for q to avoid this branch cut. In the easiest case this is possible in the complex plane, and in other cases one needs to consider the Riemann sheets, which leads to more branches and multi-valuation. The analysis is involved and detailed in [37]. Here we summarize the main results. The general formula for $\Psi(z)$ takes the form

$$\Psi(z) = \Psi_0(z) + \Delta(z) \quad (38)$$

where $\Psi_0(z)$ is the same integral as in (32) [44], and $\Delta(z)$ is the jump contribution from the branch cut, which is discussed below. The convention $\Delta(z) = 0$ defines the main branch of $\Psi(z)$. The other branches and the form of $\Delta(z)$ as a function of ξ and z are shown in Table I.

To understand Table I one needs to first discuss the behavior of the real zeroes of (37) which are the relevant one to determine $\Psi(z)$. For $z_c \leq z \leq 0$, there is always one positive zero to (37) denoted $p_1 = p_1(z, \xi)$. For $z < z_c$, the zeroes of (37) are all negative and their number is:

1. for $0 < \xi < \xi_1 = \sqrt{8}$, there is one zero $p_1(z, \xi)$;
2. for $\xi_1 < \xi$ and $z \in]z_{c1}, z_{c2}[$ there are three zeroes $p_1(z, \xi) > p_2(z, \xi) > p_3(z, \xi)$. The zeroes degenerate, i.e. $p_1 = p_2$ for $z = z_{c1}$ and $p_2 = p_3$ for $z = z_{c2}$ which define z_{c1}, z_{c2} . For $z > z_{c2}$, there is only one zero $p_1(z, \xi)$. For $z < z_{c1}$, there is only one zero $p_3(z, \xi)$.

Note that $z_{c1} < z_{c2} < 0$, with $z_{c1} = z_{c2}$ at $\xi = \xi_1$, and their explicit expression and dependence on ξ is given in [37, Eq. (S143)].

To come back to $\Psi(z)$ we now define a jump function for $\ell = \{1, 2, 3\}$ as

$$\Delta_\ell(z) = - \int_z^{z_c} \frac{dz'}{z'} \frac{4p_\ell(z', \xi)}{\xi(2p_\ell(z', \xi) + \xi)} \quad (39)$$

see [37, Eqs. (S133) (S136)] for more explicit formula. Our result, as we now discuss, is that the jump $\Delta(z)$ in Eq. (38) is always a linear combination of the $\Delta_\ell(z)$.

Remarkably, the behavior of $\Psi(z)$ exhibits three "phases" depending on the value of ξ with respect to the two critical values $\xi_1 = \sqrt{8}$ and $\xi_2 \simeq 3.13$ [37, Eq. (S142)], see Table I. The function $\Delta(z)$ is multi-valued (i.e. it has several branches) for $\xi > \xi_1$ and $z \in [z_{c1}, z_{c2}]$. Using the corresponding expressions for $\Psi(z) = \Psi_0(z) + \Delta(z)$ one can compute $\Psi'(z)$ for each branch, which is shown in Fig. 1 (top left). Using the parametric system (35) one obtains the relation between z and H , which reads $Z = e^H = \Psi'(z)$ and is shown in Fig. 1 (top right). Note that

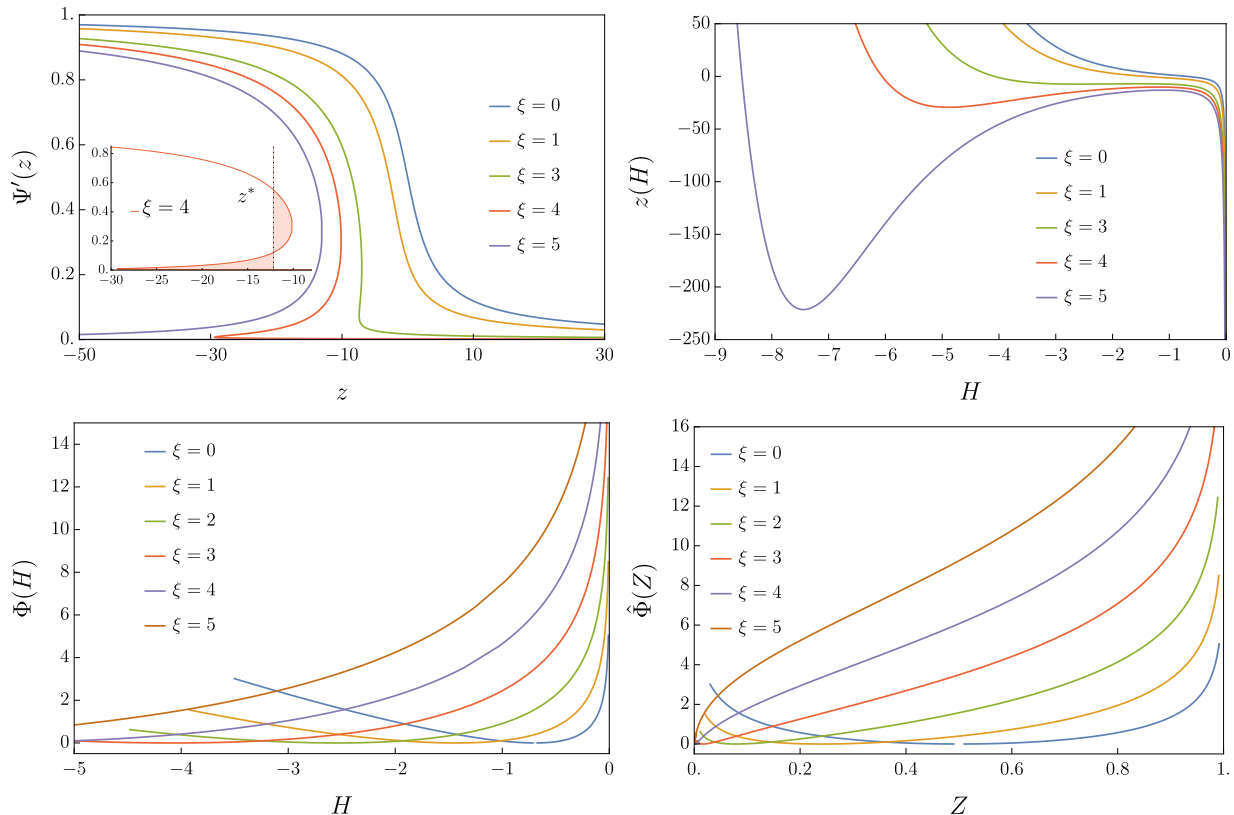


Figure 1. For $\xi = (0, 1, 2, 3, 4, 5)$ we plot the following. **(Top Left)** The derivative rate function $\Psi'(z)$ from Table I as a function of z , with $\Psi'(+\infty) = 0$ and $\Psi'(-\infty) = 1$ (all the branches are shown). For $\xi > \xi_1$ and $z \in [z_{c1}, z_{c2}]$ the function is multi-valued (see text). **(Inset)** First order transition: at $z = z^*$ such that the areas of the two shaded regions become equal the value of (the optimal) $\Psi'(z)$ jumps from one branch to the other, shown for $\xi = 4$. **(Top Right)** The function $z = z(H)$ from the Legendre transform (35). The reciprocal function $H(z)$ is multi-valued for $\xi > \xi_1$ and $z \in [z_{c1}, z_{c2}]$. **(Bottom Left)** The large deviation rate function $\Phi(H)$ versus H , obtained using the parametric representation (35) and Table I. As ξ increases, the location H_{typ} of the minimum at $\Phi(H_{\text{typ}}) = 0$ is shifted towards negative values. **(Bottom Right)** The rate function $\hat{\Phi}(Z)$ versus Z . For $\xi = 0$, it is symmetric around $Z = 0.5$ and one recovers the result of [41] (in general the symmetry is $Z(\xi) \leftrightarrow 1 - Z(-\xi)$). For large values $\xi > \xi_1$, $\hat{\Phi}(Z)$ develops a concave part which is responsible for the first-order phase transition.

$z(H)$ is single-valued but $H(z)$ may not be. One also obtains the rate function $\Phi(H)$, plotted in Fig. 1 (bottom left) and $\hat{\Phi}(Z)$, plotted in Fig. 1 (bottom right). We now comment on these plots.

We start with $\xi < \xi_1$. In that case, see Fig. 1, the function $\Psi'(z)$ is nicely decreasing from $\Psi'(-\infty) = 1$ to $\Psi'(+\infty) = 0$ and it leads to a function $H(z)$ which is single-valued and monotonous. In Table I, the appearance of $\Delta_1(z)$ below z_c is due to the fact that the zero p_1 becomes negative and the branch cut of the logarithm in (31) crosses the real axis.

For $\xi > \xi_1$ the function $\Psi'(z)$ is multi-valued in the interval $z \in [z_{c1}, z_{c2}]$, as can be seen in Fig. 1. Outside of $z \in [z_{c1}, z_{c2}]$, $\Psi'(z)$ is monotonously de-

creasing and it still has the correct limits $\Psi'(-\infty) = 1$ to $\Psi'(+\infty) = 0$. As a consequence of the multi-valuation of $\Psi'(z)$, the corresponding function $z(H)$, shown in Fig. 1, is not monotonous anymore, which implies that H as a function of $z \in [z_{c1}, z_{c2}]$ has three branches, $H_j(z)$, $j = 1, 2, 3$. These correspond to the three extrema of $\Phi(H) + ze^H$, and among these extrema only one is the absolute minimum. In Table I, the appearance of $\Delta_2(z)$ and $\Delta_3(z)$ arise from the fact that (i) at the turning point $z = z_{c1}$ we stop following the first zero p_1 and start following p_2 instead, (ii) at the turning point $z = z_{c2}$ we stop following the second zero p_2 and start following p_3 instead. The turning points are located where the

consecutive zeroes $p_i(z, \xi)$ coalesce.

For $\xi \geq \xi_2$, the ordering between z_c and z_{c2} changes. Hence to follow the second zero p_2 until its coalescence with p_3 , one needs to cross $z = z_c$ where the branch cut of the logarithm in (31) crosses again the real axis, requiring to take into account the jump $\Delta_1(z)$ again.

Multi-valuation and first-order transition. To interpret the S -shape form of $\Psi'(z)$ shown with all its branches in Figure 1 (top left), we recall that the optimal $\Psi'(z) = \langle Z \rangle_z$ is the expectation value of the random variable Z under the z -dependent tilted measure

$$\mathcal{P}(Z)e^{-\sqrt{T}zZ} \sim e^{-\sqrt{T}(\hat{\Phi}(Z)+zZ)} \quad (40)$$

The key point is that for $\xi > \xi_1$ the function $\hat{\Phi}(Z)$ has a concave part, see Fig. 1 (bottom right). As a consequence, for $z \in [z_{c1}, z_{c2}]$ the tilted measure (40) develops three extrema at $Z_j(z) = e^{H_j(z)}$, solutions of $\hat{\Phi}'(Z) = -z$. They lead to the three branches of $\Psi'(z) = Z_j(z)$. Equivalently, there are three extremal values $H_j(z)$ in (8) solutions of (35). The "optimal" $\Psi(z)$ is determined by the minimum in (35), hence it is given by

$$\Psi(z) = \min_{j=1,2,3} [\hat{\Phi}(Z_j) + zZ_j] \quad (41)$$

and the optimal j switches from $j = 1$ to $j = 3$ at $z = z^*(\xi)$ where z^* is the solution of [37]

$$\Delta_1(z^*) = \Delta_3(z^*). \quad (42)$$

It is also the point given by an equal area law on the curve $\Psi'(z)$, as in standard magnetization versus field curve for a first-order phase transition, see Fig. 1 (top left, inset). The points $Z = \{Z_1, Z_3\}$ are "stable" whereas $Z = Z_2$ is "unstable". The optimal rate function $\Psi(z)$ thus exhibits a first-order transition. This type of transition occurs in other large deviation problems [45].

Solitons. Let us discuss the significance of the multiple branches in terms of the nature of the solutions of the interpolating system (11). For any value of ξ , the logarithm in the integrand of Φ_{\pm} in (26) has branch cuts for q in the complex plane. Equivalently, the product $a(k)\tilde{a}(k)$ in (20) vanishes for some complex $k = k_s = ip_c$ where p_c are generic complex solutions of (37), indicating the spontaneous generation of a soliton [12]. This means that additional solutions with a solitonic component are possible, as was the case for the WNT of the KPZ equation [10, 11]. For that problem, by obtaining the exact solution of the $\{P, Q\}$ system for any space-time point, we were able to show that the multi-

valuation of $\Psi(z)$ was equivalent to the coexistence of two solutions (in that case with and without a soliton) for the same mixed-time boundary conditions. Here, for $\xi > \sqrt{8}$ the multi-valuation of $\Psi(z)$ similarly indicates the coexistence of three solutions for $\Lambda g \in [z_{c2}/z_c, z_{c1}/z_c]$ (a ξ -dependent interval), at least two of them being solitonic. Each of these solutions give rise to a different value $Z_j(z)$, i.e. of the value of the right hand side of Eq. (13). The precise nature and interactions of these solitons will be investigated in a subsequent work [46].

Large ξ limit and convergence to KPZ. We now consider the limit where the tracer particle is located extremely far, i.e. $\xi \rightarrow +\infty$. In that limit we can approximate in (32) $\mathbf{i}q - \frac{\xi}{2} \simeq -\frac{\xi}{2}$ and define $\tilde{z} = z\frac{\xi}{2}e^{-\frac{\xi^2}{4}} = -z/z_c$ to obtain

$$\Psi_0(z) \simeq -\int_{\mathbb{R}} \frac{dq}{2\pi} \frac{\text{Li}_2(-z\frac{\xi}{2}e^{-q^2-\frac{\xi^2}{4}})}{(\frac{\xi}{2})^2} = \frac{4}{\xi^2} \Psi_{\text{KPZ}}(\tilde{z}) \quad (43)$$

where

$$\Psi_{\text{KPZ}}(\tilde{z}) = -\frac{1}{\sqrt{4\pi}} \text{Li}_{5/2}(-\tilde{z}) \quad (44)$$

is the main branch of the large-deviation rate function for the height field $h_{\text{KPZ}}(0, T_{\text{KPZ}})$ of the KPZ equation with droplet initial condition. This rate function was obtained in [47] from a Fredholm determinant formula and in [10] from the exact solution of the WNT, i.e. of the $\{P, Q\}$ system. It admits a second branch denoted $\Psi_{\text{KPZ}}(\tilde{z}) + \Delta_{\text{KPZ}}(\tilde{z})$, which is also recovered, see below.

Hence, at the level of the large deviations, the MFT in the regime $Y \sim \sqrt{T}$ recovers, in the large $\xi = \frac{Y}{\sqrt{T}}$ limit, the result of the WNT for the KPZ equation valid for small KPZ time $T_{\text{KPZ}} \ll 1$. Comparing [10, 47] and the present result (43) shows that the correspondence between the MFT time T and the KPZ time T_{KPZ} reads [37]

$$T_{\text{KPZ}} = \frac{Y^4}{16T^3} = \frac{\xi^4}{16T} \quad (45)$$

This can be compared with [20] where it was shown, in the different scaling regime $Y \sim T^{3/4}$, i.e. $T_{\text{KPZ}} = \mathcal{O}(1)$, that in law $Z(Y, T) \simeq \frac{Y}{2T} e^{-\frac{Y^2}{4T}} e^{h_{\text{KPZ}}(0, T_{\text{KPZ}})}$, with the same T_{KPZ} as in (45) (see [37] for details). Since $\tilde{z} = z\frac{\xi}{2}e^{-\frac{\xi^2}{4}}$, the two results match perfectly, showing that no intermediate regime exists between the diffusive scaling $Y \sim \sqrt{T}$ and the of the finite-time KPZ equation scaling $Y \sim T^{3/4}$ (note that the large-time Tracy-Widom KPZ class universality is

seen only for $Y \gg T^{3/4}$).

Finally, as detailed in [37], we obtain the convergence at large ξ of the rate function for the logarithm $H = \log Z$, to the rate function of the reduced KPZ height H_{KPZ}

$$\Phi(H) \simeq \frac{4}{\xi^2} \Phi_{\text{KPZ}}(H_{\text{KPZ}}) \quad (46)$$

with the correspondence $H = -\frac{\xi^2}{4} - \log(\frac{\xi}{2}) + H_{\text{KPZ}}$ and Φ_{KPZ} is the rate function for the KPZ equation, see details and definitions in [37].

We now discuss what happens to the other branches of $\Psi(z)$ at large ξ . We show how the second branch of the KPZ rate function and the value of its jump, Δ_{KPZ} , is recovered in the limit. Recovering this second branch, which exists for $-1 \leq \tilde{z} < 0$, is necessary for (46) to hold for all $H_{\text{KPZ}} \in \mathbb{R}$. To this aim, we first define the rescaled critical values of z as

$$\tilde{z}_c = -\frac{z_c}{z_c}, \quad \tilde{z}_{c1} = -\frac{z_{c1}}{z_c}, \quad \tilde{z}_{c2} = -\frac{z_{c2}}{z_c}. \quad (47)$$

and take their large ξ limit which read

$$\tilde{z}_c \simeq -1, \quad \tilde{z}_{c1} \simeq -1, \quad \tilde{z}_{c2} \simeq 0. \quad (48)$$

From the last column of Table I we now see that, in that limit:

1. the branches $\Delta_1(z)$ and $\Delta_2(z)$ disappear due to the coalescence of z_c and z_{c1} ,
2. the next branch recovers the second branch of the KPZ limit, i.e.

$$\Delta_2(z) - \Delta_1(z) \rightarrow \frac{4}{\xi^2} \Delta_{\text{KPZ}}(\tilde{z}) = \frac{16}{3\xi^2} \log\left(\frac{-1}{\tilde{z}}\right)^{\frac{3}{2}}, \quad (49)$$

which can be explicitly checked [37].

3. When \tilde{z} approaches \tilde{z}_{c2} , we obtain in the large ξ limit that the corresponding value of H_{KPZ} goes to $+\infty$, hence the branches $\Delta_3(z) - \Delta_1(z)$ and $\Delta_3(z)$ disappear at infinity, see Fig. S7. This corresponds to events where $Z = \mathcal{O}(1)$ which become irrelevant in that limit [48].

Fredholm determinant formula. We can now compare our result (32) obtained using the inverse scattering method, to a formula obtained by completely different methods, for a model of sticky Brownian motions [19]. That model, which allows for a rigorous formulation, is believed (up to mathematical subtleties) to be equivalent to the one considered here. The original formula of [19] is valid for any time T and any Y , and here we obtain its

limit in the large deviation diffusive scaling regime. Applied to our model this formula reads

$$\overline{e^{-uZ(Y,T)}} = \det(I - K_u) \quad (50)$$

where the kernel K_u was derived in Ref. [19, Theorem 1.11] and is recalled in Eq. (S191).

We scale $u = \sqrt{T}z$ with $z = \mathcal{O}(1)$ in Eq. (50) so that the l.h.s. of (50) can be identified to the l.h.s. of (7). We perform asymptotic analysis on the kernel K_u and extract the large T large deviation rate function $\Psi(z)$ by using the first cumulant method introduced in [49–51]. The manipulations, sketched in [37] are quite heuristic, but allow to recover nicely the algebraic form of formula (32). It remains open how to make it more controlled.

Extremal diffusions. Consider the rightmost of N independent particles in the same random field, of position $Y_N(T) = \max_{i=1,\dots,N} Y_i(T)$. Without random field and for $N \gg 1$, $Y_N(T)$ has a deterministic part $\simeq 2\sqrt{T \log N}$ plus a "thermal" fluctuation part $\simeq G\sqrt{\frac{T}{\log N}}$, G being a Gumbel random variable. With the random field, for $\log N \sim T \gg 1$, there is also a $\mathcal{O}(1)$ sample-to-sample fluctuation part, with a Tracy-Widom distribution [15, 22]. In the more accessible regime $\log N \sim \sqrt{T} \gg 1$, as shown in [16, 20] this fluctuating term is distributed as $h(0, T_{\text{KPZ}})/\sqrt{\log N}$, the droplet solution of the KPZ equation. These phenomena go beyond the Gaussian nature of Einstein's diffusion. They allow for a detectable fingerprint of the random medium. Recently, these two regimes have been observed numerically [52]. The present results allow to study yet another regime, $\log N \ll \sqrt{T}$, where diffusive scaling holds and the scaled position $y_N(T) = \frac{Y_N(T)}{\sqrt{T}}$ of the maximum converges to

$$y_N(T) \simeq 2\sqrt{\log N} + \frac{G - c_N + \delta H}{\sqrt{\log N}} \quad (51)$$

where for typical environments $\delta H = \mathcal{O}(T^{-1/4})$ is an Edwards-Wilkinson random variable with a computable variance [37], and for rare environments $\delta H = H - H_{\text{typ}}(\xi) = \mathcal{O}(1)$ with the rate function (5) computed here and $\xi = 2\sqrt{\log N}$. We also find that in the regime $N \sim \sqrt{T}$ the disorder average CDF takes the large deviation form $\mathbb{P}(y_N(T) < \xi) \sim e^{-\sqrt{T}\Sigma_\xi(n)}$, with $n = \frac{N}{\sqrt{T}} = \mathcal{O}(1)$ fixed, and $\Sigma_\xi(n)$ a rate function explicitly obtained in [37].

Extension to the SSEP. Our results are relevant within the class of MFT models with quadratic noise

variance $\sigma(\varrho)$. These models enjoy a mapping to the $\{R, Q\}$ DNLS system (S58), see [37, Section XII]. Recently, the exact solution of the MFT of the SSEP was investigated in Ref. [43] using the well-known gauge transformation of Wadati and Sogo, [62, Eq. (4.5)], to map the $\{R, Q\}$ DNLS system to the $\{P, Q\}$ NLS system. The remarkable result of [43] is that under this gauge transformation, the annealed initial condition of the SSEP is mapped onto the initial condition solved by us in [10] (with different coupling constant [53]). The natural extension of [43] would be to study the statistics of a tracer at arbitrary position in an MFT model with quadratic variance and annealed initial condition. The inverse scattering method we have pursued in this work provides the right tools to answer this question.

Conclusion. We have elucidated here in great details the crossover upon adding an asymmetry, between the MFT for diffusive systems and the WNT of the KPZ equation. We have focused on the example of the diffusion of a tracer in a time-dependent random medium in an atypical direction and a "droplet" type initial condition. We have obtained the large-deviation functions in the context of classical integrability using simple, standard and versatile inverse scattering methods. For this model it was based on the integrable crossover between the DNLS and NLS equations. Obtaining the complete solution of this interpolating system (11) beyond the large-deviation observable requires further efforts involving the use of Fredholm determinants similarly to what we have achieved in [10, 11] for the complete solution of the WNT. This is one open question that we leave to subsequent works [46], together with other outstanding questions, such as investigating the MFT-KPZ crossover for more general models, or within the present model, to study (2) for other initial conditions, in particular those identified in [16] to converge in atypical directions to solutions of the KPZ equation for flat and stationary geometries [11].

Note added. After completion, the paper [54] appeared, where the results of [11] are proved rigorously.

Acknowledgments. We thank G. Barraquand for discussions and collaborations on closely related topics. AK acknowledges support from ERC under Consolidator grant number 771536 (NEMO) and PLD from the ANR grant ANR-17-CE30-0027-01 RaMaTraF. This article is based upon work supported by the National Science Foundation under

Grant No. DMS-1928930 while the two authors participated in a program hosted by the Mathematical Sciences Research Institute in Berkeley, California, during the Fall 2021 semester.

Supplementary Material for
The crossover from the Macroscopic Fluctuation Theory to the Kardar-Parisi-Zhang equation controls the large deviations beyond Einstein's diffusion

We give the principal details of the calculations described in the main text of the Letter. We also give additional information about the results displayed in the text.

I. DERIVATION OF THE INTERPOLATING SYSTEM

Let us detail the steps performed in the text to obtain $\Psi(z)$ defined from the expectation value in (7) via the saddle point method. Introducing the standard dynamical path integral representation, one has (where overlines represent averages w.r.t. the random field $\tilde{\eta}$)

$$\overline{e^{-z\sqrt{T}Z(Y,T)}} = \overline{e^{-z\sqrt{T}\int_{\xi}^{+\infty} dx Q_{\tilde{\eta}}(x,t=1)}} \quad (\text{S52})$$

$$= \overline{\int \int \mathcal{D}\tilde{Q}\mathcal{D}\tilde{P}e^{-\int_0^1 dt \int_{\mathbb{R}} dx [\sqrt{T}\tilde{P}(\partial_t\tilde{Q}-\partial_x^2\tilde{Q}-\partial_x\sqrt{2}\tilde{\eta}(x,t)\tilde{Q})]-z\sqrt{T}\int_{\xi}^{+\infty} dx\tilde{Q}(x,t=1)}}} \quad (\text{S53})$$

$$= \int \int \mathcal{D}\tilde{Q}\mathcal{D}\tilde{P}e^{-\sqrt{T}(S[\tilde{P},\tilde{Q}]+z\int_0^1 dt\delta(t-1)\int_{\xi}^{+\infty} dx\tilde{Q}(x,t))} \quad (\text{S54})$$

where the equation of motion (6) has been expressed using the response field $\tilde{P}\sqrt{T}$, and the associated dynamical action is

$$S[\tilde{P},\tilde{Q}] = \int_0^1 dt \int_{\mathbb{R}} dx [\tilde{P}(\partial_t - \partial_x^2)\tilde{Q} - \tilde{Q}^2(\partial_x\tilde{P})^2] \quad (\text{S55})$$

For $T \rightarrow +\infty$ one can use the saddle point method. Here we denote the fields and their saddle point values in the original frame as $\{\tilde{P},\tilde{Q}\}$ to distinguish them from the Galilean transformed fields $\{P,Q\}$ introduced below. Taking the functional derivative w.r.t. $\{\tilde{P},\tilde{Q}\}$ we obtain

$$\partial_t\tilde{Q} = \partial_x^2\tilde{Q} + 2\beta\partial_x(\tilde{Q}^2(\partial_x\tilde{P})) \quad (\text{S56})$$

$$-\partial_t\tilde{P} = \partial_x^2\tilde{P} - 2\beta\tilde{Q}(\partial_x\tilde{P})^2 - z\delta(t-1)\Theta(x-\xi) \quad (\text{S57})$$

with $\beta = -1$. We will keep β as a parameter but for the application to obtain $\Psi(z)$ it is understood that it is set to $\beta = -1$. Initially the upper boundary in time is $t = +\infty$ but since \tilde{P} vanishes for $t > 1$, we can equivalently restrict the equations for $t \in [0,1]$ and interpret the last term in the second equation (which must be integrated backward in time) as a boundary condition $P(x,t=1) = -z\Theta(x-\xi)$ for $\tilde{P}(x,t)$, so it drops from the equation. To make the two equations more symmetric let us now introduce the derivative field $\tilde{R}(x,t) = \partial_x\tilde{P}(x,t)$, leading to

$$\partial_t\tilde{Q} = \partial_x^2\tilde{Q} + 2\beta\partial_x(\tilde{Q}^2\tilde{R}) \quad (\text{S58})$$

$$-\partial_t\tilde{R} = \partial_x^2\tilde{R} - 2\beta\partial_x(\tilde{Q}\tilde{R}^2)$$

with the boundary conditions

$$\tilde{Q}(x,t=0) = \delta(x) \quad , \quad \tilde{R}(x,t=1) = \Lambda_0\delta(x-\xi) \quad , \quad \Lambda_0 = -z \quad (\text{S59})$$

This system is the cousin of the DNLS equation (identical to it upon the change $t \rightarrow \mathbf{it}$).

Now we perform a Galilean transformation $x \rightarrow x - \xi t$ to bring back ξ to zero. Anticipating a bit, let us introduce the interpolating system introduced in the text in (11) which we recall here

$$\begin{aligned} \partial_t Q &= \partial_x^2 Q + 2\beta\partial_x(Q^2 R) + 2gQ^2 R \\ -\partial_t R &= \partial_x^2 R - 2\beta\partial_x(QR^2) + 2gQR^2 \end{aligned} \quad (\text{S60})$$

and notice that if \tilde{Q}, \tilde{R} satisfies this system with couplings (β, g) then

$$Q(x, t) = \tilde{Q}(x - vt, t)e^{-\frac{1}{2}xv + \frac{v^2}{4}t} \quad , \quad R(x, t) = \tilde{R}(x - vt, t)e^{\frac{1}{2}xv - \frac{v^2}{4}t} \quad , \quad (\text{S61})$$

also satisfies the same system with couplings $(\beta, g + \beta\frac{v}{2})$. Thus consider \tilde{Q}, \tilde{R} which satisfy the above DNLS system (S58) with boundary conditions $\tilde{Q}(x, 0) = Q_0(x)$ and $\tilde{R}(x, 1) = \Lambda_0\delta(x - \xi)$. We will choose $v = -\xi$ so that

$$Q(x, t) = \tilde{Q}(x + \xi t, t)e^{\frac{1}{2}x\xi + \frac{\xi^2}{4}t} \quad , \quad R(x, t) = \tilde{R}(x + \xi t, t)e^{-\frac{1}{2}x\xi - \frac{\xi^2}{4}t} \quad , \quad (\text{S62})$$

satisfies the interpolating system (S60) with couplings $(\beta, -\beta\frac{\xi}{2})$ and boundary conditions

$$Q(x, 0) = \tilde{Q}_0(x)e^{\frac{1}{2}x\xi} \quad , \quad R(x, 1) = \Lambda_0\delta(x)e^{-\frac{\xi^2}{4}} \quad , \quad (\text{S63})$$

which for $\tilde{Q}_0(x) = \delta(x)$ gives the result (12) in the text, where we called $\Lambda = \Lambda_0e^{-\frac{\xi^2}{4}}$.

Symmetries. Note that the DNLS equation (S58) is invariant by $x \rightarrow -x$ and $R \rightarrow -R$. The interpolating system $\{R, Q\}$ (S60) is invariant by $x \rightarrow -x$, $R \rightarrow -R$ and $g \rightarrow -g$.

Conserved quantities. Note that the system (S58) admits a series of conserved (i.e. time independent) quantities, the simplest one being $\int_{\mathbb{R}} dx \tilde{Q}(x, t) = 1$ (here its value is fixed to unity by the initial condition (S59)). This conservation law originates from the conservation of probability in the Fokker-Planck equation, $\frac{d}{dt} \int dt q_\eta(x, t) = 0$. Upon a Galilean transformation it becomes

$$\int_{\mathbb{R}} dx Q(x, t)e^{-x\frac{\xi}{2} - \frac{\xi^2}{4}t} = 1 \quad (\text{S64})$$

Note that \tilde{R} also satisfies the conservation law $\int_{\mathbb{R}} dx \tilde{R}(x, t) = \Lambda$ and after a Galilean transformation $\int_{\mathbb{R}} dx R(x, t)e^{x\frac{\xi}{2} + \frac{\xi^2}{4}t} = \Lambda_0 = \Lambda e^{\xi^2/4}$. One can check that this is consistent with the symmetry (14).

Coupling constant. If one compares with Ref. [10] the true coupling constant of the $\{P, Q\}$ (i.e. here $\{R, Q\}$) system used there (called g there) is $\hat{g} = \Lambda g$. Since $\beta\Lambda = ze^{-\xi^2/4}$ and $g = -\beta\frac{\xi}{2}$, this gives $\hat{g} = -z\frac{\xi}{2}e^{-\xi^2/4}$. The special point z_c discussed in the text thus corresponds to $\hat{g} = 1$, as for the case of the WNT of the KPZ equation.

The rate function $\Psi(z)$ from the saddle point. The value of $\Psi(z)$ defined in (7) is then obtained from the saddle point value in (S54). One has

$$\Psi(z) = \left[S[\tilde{P}, \tilde{Q}] + z \int_{\xi}^{+\infty} dx \tilde{Q}(x, 1) \right]_{\text{sp}} \quad (\text{S65})$$

where \tilde{P}, \tilde{Q} must be replaced by the z dependent solutions of the system (S58) with boundary conditions (S59). Taking a derivative w.r.t. z and using the saddle point conditions, only the explicit derivation w.r.t. z remains, and one obtains the formula (13) given in the text

$$\Psi'(z) = \int_{\xi}^{+\infty} dx \tilde{Q}(x, 1) = \int_0^{+\infty} dx Q(x, 1)e^{-\frac{1}{2}x\xi - \frac{\xi^2}{4}} \quad (\text{S66})$$

where $Q(x, 1)$ is the z -dependent solution of the interpolating system (S60) with boundary conditions (12). Since by definition $\Psi(0) = 0$ this equation is sufficient to obtain $\Psi(z)$ if the r.h.s. is known as a function of z .

II. DIRECT SCATTERING SOLUTION FOR THE INTERPOLATING SYSTEM

In this section we derive the formula (17) and (18) for the scattering amplitudes $\{a(k), \tilde{a}(k), b(k), \tilde{b}(k)\}$ given in the text.

Equation for $\bar{\phi}$ at $t = 1$. This equation allows to obtain the relations involving $\tilde{a}(k)$ and $\tilde{b}(k)$. We call $\bar{\phi}_{1,2}(x, t)$ the two components of $\bar{\phi}$ (the dependence in k is implicit). Let us recall that at $x \rightarrow -\infty$, $\bar{\phi} \simeq (0, -e^{\mathbf{i}kx/2})^\top$. The first equation of the Lax pair $\partial_x \bar{v} = U_1 \bar{v}$ with $\bar{v} = e^{-k^2 t/2} \bar{\phi}$ reads in components at $t = 1$, from (15) and using that $R(x, 1) = \Lambda \delta(x)$

$$\partial_x (e^{\mathbf{i}\frac{k}{2}x} \bar{\phi}_1) = -(g + \mathbf{i}\beta k) \Lambda \delta(x) \bar{\phi}_2 e^{\mathbf{i}\frac{k}{2}x}, \quad \partial_x (e^{-\mathbf{i}\frac{k}{2}x} \bar{\phi}_2) = Q(x, 1) \bar{\phi}_1 e^{-\mathbf{i}\frac{k}{2}x} \quad (\text{S67})$$

Let us integrate the first equation from $x = -\infty$ to x . Since $\bar{\phi}_1$ vanishes at $x = -\infty$ it gives

$$\bar{\phi}_1(x, 1) = -(g + \mathbf{i}\beta k) \Lambda e^{-\mathbf{i}\frac{k}{2}x} \Theta(x) \bar{\phi}_2(0, 1) \quad (\text{S68})$$

Taking the limit $x \rightarrow +\infty$, we thus obtain

$$\tilde{b}(k, t = 1) = -(g + \mathbf{i}\beta k) \Lambda \bar{\phi}_2(0, 1) \quad (\text{S69})$$

To determine $\bar{\phi}_2(0, 1)$ we can integrate the second equation in (S67), which gives, using (S68) and (S69)

$$\begin{cases} e^{-\mathbf{i}\frac{k}{2}x} \bar{\phi}_2(x, 1) = \bar{\phi}_2(0, 1) + \tilde{b}(k, 1) \int_0^x dx' Q(x', 1) e^{-\mathbf{i}kx'}, & x > 0 \\ \bar{\phi}_2(x, 1) = -e^{\mathbf{i}\frac{k}{2}x}, & x < 0 \end{cases} \quad (\text{S70})$$

where in the second equation we have used that $\bar{\phi}_2(x, 1) \simeq -e^{\mathbf{i}\frac{k}{2}x}$ for $x \rightarrow -\infty$. Assuming continuity of $\bar{\phi}_2(x, 1)$ at $x = 0$, this leads to $\bar{\phi}_2(0, 1) = -1$ and to

$$\tilde{b}(k, t = 1) = (g + \mathbf{i}\beta k) \Lambda \quad \Rightarrow \quad \tilde{b}(k) = (g + \mathbf{i}\beta k) \Lambda e^{-k^2} \quad (\text{S71})$$

since we recall that $\tilde{b}(k, t) = \tilde{b}(k) e^{k^2 t}$. Taking the $x \rightarrow +\infty$ limit of (S70) and using the asymptotics (16) we also obtain the relation

$$\tilde{a}(k, 1) = \tilde{a}(k) = 1 - (g + \mathbf{i}\beta k) \Lambda \int_0^{+\infty} dx' Q(x', 1) e^{-\mathbf{i}kx'} \quad (\text{S72})$$

Equation for ϕ at $t = 0$. This equation allows to obtain the relations involving $a(k)$ and $b(k)$. We call $\phi_{1,2}(x, t)$ the two components of ϕ (the dependence in k is implicit). Let us recall that at $x \rightarrow -\infty$, $\phi \simeq (e^{-\mathbf{i}kx/2}, 0)^\top$. The first equation of the Lax pair $\partial_x \vec{v} = U_1 \vec{v}$ with $\vec{v} = e^{k^2 t/2} \phi$ reads in components at $t = 0$, from (15) and using that $Q(x, 1) = \delta(x)$.

$$\partial_x (e^{\mathbf{i}\frac{k}{2}x} \phi_1) = -(g + \mathbf{i}\beta k) R(x, 0) \phi_2 e^{\mathbf{i}\frac{k}{2}x}, \quad \partial_x (e^{-\mathbf{i}\frac{k}{2}x} \phi_2) = \delta(x) \phi_1 e^{-\mathbf{i}\frac{k}{2}x} \quad (\text{S73})$$

Integrating the second equation of (S73) from $x = -\infty$ to x . Since ϕ_2 vanishes at $x = -\infty$ it gives

$$\phi_2(x, 0) = e^{\mathbf{i}\frac{k}{2}x} \Theta(x) \phi_1(0, 0) \quad (\text{S74})$$

Taking the limit $x \rightarrow +\infty$, we thus obtain

$$b(k, t = 0) = \phi_1(0, 0) \quad (\text{S75})$$

To determine $\phi_1(0, 0)$ we can integrate the first equation in (S73), which gives, using (S74) and (S75)

$$\begin{cases} e^{\mathbf{i}\frac{k}{2}x} \phi_1(x, 0) = \phi_1(0, 0) - (g + \mathbf{i}\beta k) b(k, 0) \int_0^x dx' R(x', 0) e^{\mathbf{i}kx'}, & x > 0 \\ \phi_1(x, 0) = e^{-\mathbf{i}\frac{k}{2}x}, & x < 0 \end{cases} \quad (\text{S76})$$

where in the second equation we have used that $\phi_1(x, 0) \simeq e^{\mathbf{i}\frac{k}{2}x}$ for $x \rightarrow -\infty$. Assuming continuity of $\phi_1(x, 0)$ at $x = 0$, this leads to $\phi_1(0, 0) = 1$ and to

$$b(k, t = 0) = b(k) = 1 \quad (\text{S77})$$

Taking the $x \rightarrow +\infty$ limit of (S76) and using the asymptotics (16) we also obtain the relation

$$a(k, 0) = a(k) = 1 - (g + \mathbf{i}\beta k) \int_0^{+\infty} dx' R(x', 0) e^{\mathbf{i}kx'} \quad (\text{S78})$$

At this stage we can use the symmetry (14) and obtain

$$a(k) = 1 - (g + \mathbf{i}\beta k)\Lambda \int_{-\infty}^0 dx' Q(x', 1)e^{-\mathbf{i}kx'} \quad (\text{S79})$$

which completes the derivation of the equations (18) and (17) in text. Alternatively one may derive (S79) without using the symmetry (14) by considering the equation for ϕ at $t = 1$. We now present that derivation.

Equation for ϕ at $t = 1$. This equation allows to obtain $a(k)$ in (S79). Let us recall that at $x \rightarrow -\infty$, $\phi \simeq (e^{-\mathbf{i}kx/2}, 0)^\top$. The first equation of the Lax pair, $\partial_x \vec{v} = U_1 \vec{v}$ with $\vec{v} = e^{k^2 t/2} \phi$ as given in the text now reads, in components and at $t = 1$, using that $R(x, 1) = \Lambda \delta(x)$

$$\partial_x (e^{\mathbf{i}\frac{k}{2}x} \phi_1) = -(g + \mathbf{i}\beta k)\Lambda \delta(x) \phi_2 e^{\mathbf{i}\frac{k}{2}x}, \quad \partial_x (e^{-\mathbf{i}\frac{k}{2}x} \phi_2) = Q(x, 1) \phi_1 e^{-\mathbf{i}\frac{k}{2}x} \quad (\text{S80})$$

Integrating these two equations, and using the asymptotics (16) at $x \rightarrow +\infty$ we obtain

$$\begin{aligned} \phi_1(x, 1) &= e^{-\mathbf{i}\frac{k}{2}x} (\Theta(-x) + a(k)\Theta(x)), & a(k) - 1 &= -(g + \mathbf{i}\beta k)\Lambda \phi_2(0, 1) \\ \phi_2(x, 1) &= e^{\mathbf{i}\frac{k}{2}x} \int_{-\infty}^x dx' Q(x', 1) e^{-\mathbf{i}kx'} (\Theta(-x') + a(k)\Theta(x')) \end{aligned} \quad (\text{S81})$$

where we used that $a(k, t) = a(k)$, see the main text. Setting $x = 0$ in the second equation we obtain the relation displayed in the text

$$\phi_2(0, 1) = \int_{-\infty}^0 dx' Q(x', 1) e^{-\mathbf{i}kx'}, \quad a(k) = 1 - (g + \mathbf{i}\beta k)\Lambda \int_{-\infty}^0 dx' Q(x', 1) e^{-\mathbf{i}kx'} \quad (\text{S82})$$

III. DETAILS OF THE CALCULATION OF THE SCATTERING AMPLITUDES

So far the scattering amplitudes $\{a, \tilde{a}\}$ have been expressed as half-Fourier transforms in Eqs. (S72) and (S82). To determine them more explicitly, one wants to solve Eq. (20), namely the normalization relation of the scattering amplitudes, which read here

$$a(k)\tilde{a}(k) = 1 - (g + \mathbf{i}\beta k)\Lambda e^{-k^2} \quad (\text{S83})$$

where $a(k)$ and $\tilde{a}(k)$ satisfy Eq. (18), which we recall reads

$$a(k) = 1 - (g + \mathbf{i}\beta k)\Lambda Q_-(k), \quad \tilde{a}(k) = 1 - (g + \mathbf{i}\beta k)\Lambda Q_+(k), \quad Q_{\pm}(k) = \int_{\mathbb{R}^{\pm}} dx Q(x, 1) e^{-\mathbf{i}kx}. \quad (\text{S84})$$

Clearly for k complex, $Q_+(k)$, hence $\tilde{a}(k)$, is analytic in the lower half-plane, and $Q_-(k)$, hence $a(k)$, is analytic in the upper half-plane. Now we define the parametrization

$$a(k) = a(\infty) e^{\Phi_+(k)}, \quad a(\infty) = 1 + \beta \Lambda Q(0^-, 1), \quad (\text{S85})$$

$$\tilde{a}(k) = \tilde{a}(\infty) e^{\Phi_-(k)}, \quad \tilde{a}(\infty) = 1 - \beta \Lambda Q(0^+, 1), \quad (\text{S86})$$

where $a(\infty)$ and $\tilde{a}(\infty)$ were obtained in Eq. (21), so that $\Phi_{\pm}(k) \rightarrow 0$ as $k \rightarrow \pm\infty$. One can thus rewrite (S83) for real k as

$$1 - (g + \mathbf{i}\beta k)\Lambda e^{-k^2} = e^{\Phi_+(k)} e^{\Phi_-(k)} \quad (\text{S87})$$

where $e^{\Phi_{\pm}(k)}$ are analytic respectively in the UHP/LHP. This is a typical Riemann-Hilbert [55] or Wiener-Hopf problem. In some domain, taking the logarithm of this equation, it can be written as

$$\log(1 - (g + \mathbf{i}\beta k)\Lambda e^{-k^2}) = \Phi_+(k) + \Phi_-(k) + 2\mathbf{i}\pi n(k) \quad (\text{S88})$$

for some integer-valued function $n(k)$. One can check that for $\hat{g} = \Lambda g < 1$ the l.h.s. of (S88) is analytic in a strip around the real axis in k (see Section VII) and decays fast at infinity along the real axis. One can thus apply e.g. [56, Theorem 3.1] (see [57, Chapter 1.3]), which implies that

$$\Phi_{\pm}(k) = \pm \int_{\mathbb{R}} \frac{dq}{2\mathbf{i}\pi} \frac{\log(1 - (g + \mathbf{i}\beta q)\Lambda e^{-q^2})}{q - k \mp \mathbf{i}0^+} \quad (\text{S89})$$

with $n(k) = 0$ in the strip. Hence for $\hat{g} = \Lambda g < 1$ the multi-valuation occurs only outside this strip. The formula for $\Phi_+(k)$ is valid only in the UHP and the one for $\Phi_-(k)$ is valid only in the LHP (at least in a strip around the real axis). This recovers Eq. (26) in the text.

Formally, one can also use as in [41] the well-known Sokhotskyi–Plemelj formula

$$\int_{\mathbb{R}} \frac{dq}{2i\pi} \frac{f(q)}{q - k \pm i0^+} = \mp \int_{\mathbb{R}} \frac{dq}{2i\pi} \frac{f(q)}{q - k} \mp \frac{1}{2} f(k) \quad (\text{S90})$$

which leads to the decomposition of a general function $f(k)$

$$f(k) = \int_{\mathbb{R}} \frac{dk'}{2i\pi} \frac{f(k')}{k' - k - i0^+} - \int_{\mathbb{R}} \frac{dk'}{2i\pi} \frac{f(k')}{k' - k + i0^+} \quad (\text{S91})$$

in parts which are analytic in the UHP and LHP respectively.

Validity. The results above are valid for $\Lambda g < 1$. For their continuation beyond that domain see Section VII below.

Recovering the case $\beta = 0$. If we set $\beta = 0$ in the interpolating system (11) we obtain the $\{P, Q\}$ system extensively discussed in Refs. [10, 11]. Let us show that one then recovers the solution obtained in our previous work [10]. There, we studied a more general initial condition $Q(x, t = 0) = Q_0(x)$, and to identify we must set $g \rightarrow g\Lambda$ (since there $R(x, t = 1) = \delta(x)$ while here $R(x, t = 1) = \Lambda\delta(x)$ while there Λ is set to unity). Taking this into account there we obtained $\tilde{b}(k) = ge^{-k^2}$ which agrees with (17), and

$$a(k) = \sqrt{1 - gb(k)\Lambda e^{-k^2}} e^{-i\varphi(k)} \quad , \quad \varphi(k) = \int_{\mathbb{R}} \frac{dq}{2\pi} \frac{1}{q - k} \log(1 - gb(q)\Lambda e^{-q^2}) \quad (\text{S92})$$

together with $\tilde{a}(k) = a(-k)$ for real k , and $\varphi(-k) = -\varphi(k)$. It is easy to see that it agrees with (S89) for $\beta = 0$ using (S90) with $f(k) = \log(1 - gb(k)\Lambda e^{-k^2})$, that is, in that case for $k \in \mathbb{R}$

$$\Phi_{\pm}(k) = -i\varphi(\pm k) + \frac{1}{2} \log(1 - gb(k)\Lambda e^{-k^2}) \quad (\text{S93})$$

Of course here we restricted to the special case of the droplet initial condition $Q_0(x) = \delta(x)$, where $b(k) = 1$ as found in [10] and recovered here in Eq. (17).

General initial condition for $\beta \neq 0$. Extending the previous discussion we see that the solution of the interpolating system for a more general initial condition $Q(x, 0) = Q_0(x)$ reads

$$\Phi_{\pm}(k) = \pm \int_{\mathbb{R}} \frac{dq}{2i\pi} \frac{\log(1 - (g + i\beta q)\Lambda b(q)e^{-q^2})}{q - k \mp i0^+} \quad (\text{S94})$$

where there is a map between $Q_0(x)$ and $b(q)$ which can be obtained by solving the scattering problem.

IV. BOUNDS AND SYMMETRIES FOR $\Psi(z)$

We give here some properties of the function $\Psi(z)$. Since we start from its definition (7) we are dealing here with what we call in the text the "optimal" $\Psi(z)$, also given by the minimization (8). From its definition (7) the expansion of $\Psi(z)$ in powers of z around $z = 0$ gives the cumulants of $Z = Z(Y, T)$

$$\Psi(z) = -\frac{1}{\sqrt{T}} \log \exp(-z\sqrt{T}Z) = -\sum_{p \geq 1} \frac{(-z)^p}{p!} T^{\frac{p-1}{2}} \overline{Z^p}^c \quad (\text{S95})$$

hence the leading behavior of each cumulants at large time is given by

$$\overline{Z^p}^c \simeq (-1)^{p+1} T^{\frac{1-p}{2}} \Psi^{(p)}(0) \quad (\text{S96})$$

On the other hand, taking derivatives of $\Psi(z)$ w.r.t z for any z lead to

$$\Psi'(z) = \langle Z \rangle_z \quad , \quad \Psi''(z) = -\sqrt{T} \langle Z^2 \rangle_z^c \quad , \quad \langle \mathcal{O} \rangle_z = \frac{\overline{\mathcal{O} \exp(-z\sqrt{T}Z)}}{\exp(-z\sqrt{T}Z)} \quad (\text{S97})$$

where the expectation values are w.r.t. the tilted measure also defined in the text. Since the random variable Z obeys $0 < Z < 1$ it implies

$$0 < \Psi'(z) < 1 \quad , \quad \Psi''(z) < 0. \quad (\text{S98})$$

The function $\Psi(z)$ must thus be concave. Note that some of the branches obtained in the text are not concave hence they do not appear in the optimal $\Psi(z)$. In such cases there is instead a jump of $\Psi'(z)$ from one branch to another one, for $z = z^*$. As discussed in the text, at this point the tilted measure has two degenerate maxima hence the fluctuations are anomalously large, $\sqrt{T} \langle Z^2 \rangle_{z=z^*}^c = +\infty$.

Let us now make the dependence in ξ apparent and denote $Z_\xi = Z(Y, T)$. By definition one has

$$Z_\xi = \int_\xi^{+\infty} dy q_\eta(y, T) \quad , \quad 1 - Z_{-\xi} = \int_{-\infty}^{-\xi} dy q_\eta(y, T) \quad (\text{S99})$$

where $0 < Z_\xi < 1$. The equation (2) is invariant by $y \rightarrow -y$ and $\eta(y, \tau) \rightarrow -\eta(-y, -\tau)$, which leaves the PDF of the noise invariant, hence Z_ξ and $1 - Z_{-\xi}$ have the same PDF. This observation inserted into (7) gives

$$\overline{\exp(-z\sqrt{T}Z_\xi)} \sim \overline{\exp(-\sqrt{T}\Psi_\xi(z))} = \overline{\exp(-z\sqrt{T}(1 - Z_{-\xi}))} = \overline{\exp(-\sqrt{T}(z + \Psi_{-\xi}(-z)))} \quad (\text{S100})$$

hence it implies the symmetry given in the text

$$\Psi_{-\xi}(z) = \Psi_\xi(-z) + z \quad (\text{S101})$$

Remark. To measure Z_ξ and $-Z_{-\xi}$ one can use the DNLS equation with boundary condition $P(x, 1) = \Theta(x - \xi)$ i.e. $R(x, 1) = \delta(x - \xi)$ for the first, and $P(x, 1) = \Theta(-x - \xi)$ i.e. $R(x, 1) = -\delta(-x - \xi)$ for the second. Using the symmetry $x \rightarrow -x$ and $R \rightarrow -R$ one arrives at the same conclusion.

V. DERIVATION OF THE RATE FUNCTION $\Psi(z)$ – MAIN BRANCH

Let us give some more details on how (32) in the text is obtained. Taking a derivative w.r.t. k of (27) at $k = \frac{ig}{\beta}$ and using (28) one obtains

$$\mathbf{i}\beta\Lambda Q_{\mp} \left(\frac{\mathbf{i}g}{\beta} \right) = -\Phi'_{\pm} \left(\frac{\mathbf{i}g}{\beta} \right) \quad (\text{S102})$$

Let us verify that this is consistent with the second equality in (30) (which comes from the conservation of probability). For that let us first recall that (from (S88) with $n(k) = 0$)

$$\log(1 - (g + \mathbf{i}\beta k)\Lambda e^{-k^2}) = \Phi_+(k) + \Phi_-(k) \quad (\text{S103})$$

where $\Phi_{\pm}(k)$ are given in (S89) for k in the complex upper/lower half planes (at least in a strip around the real axis).

Taken at $k = \frac{ig}{\beta}$ (which always belongs to the strip) it again shows that $\Phi_{\pm}(\frac{ig}{\beta})$ are opposite quantities. Taking a derivative w.r.t. k at $k = \frac{ig}{\beta} = -\mathbf{i}\frac{\xi}{2}$ one obtains

$$-\mathbf{i}\beta\Lambda e^{\xi^2/4} = \Phi'_+ \left(\frac{\mathbf{i}g}{\beta} \right) + \Phi'_- \left(\frac{\mathbf{i}g}{\beta} \right) \quad (\text{S104})$$

which is exactly equivalent to the second equality in (30).

One must be careful in computing $\Phi'_{\pm}(k)$ for $k = \frac{ig}{\beta} = -i\xi/2$ since the formula (26) given in the text and above in (S89) for $\Phi_{\pm}(k)$ are valid only for k in the UHP/LHP respectively. There are thus two cases:

1. If $g/\beta > 0$, i.e. $\xi < 0$, we can use (26) for Φ_+ for $\Im(k) \geq 0$ and one obtains

$$\Phi'_+ \left(\frac{ig}{\beta} \right) = \int_{\mathbb{R}} \frac{dq}{2i\pi} \frac{\log(1 - (g + i\beta q)\Lambda e^{-q^2})}{(q - \frac{ig}{\beta})^2} \quad (\text{S105})$$

while, using (S104) one has

$$\Phi'_- \left(\frac{ig}{\beta} \right) = - \int_{\mathbb{R}} \frac{dq}{2i\pi} \frac{\log(1 - (g + i\beta q)\Lambda e^{-q^2})}{(q - \frac{ig}{\beta})^2} - i\beta\Lambda e^{\xi^2/4} \Theta(-\xi) \quad (\text{S106})$$

2. If $g/\beta < 0$, i.e. $\xi > 0$, we can use (26) for Φ_- for $\Im(k) \leq 0$ and one obtains

$$\Phi'_- \left(\frac{ig}{\beta} \right) = - \int_{\mathbb{R}} \frac{dq}{2i\pi} \frac{\log(1 - (g + i\beta q)\Lambda e^{-q^2})}{(q - \frac{ig}{\beta})^2} \quad (\text{S107})$$

while, using (S104) one has

$$\Phi'_+ \left(\frac{ig}{\beta} \right) = \int_{\mathbb{R}} \frac{dq}{2i\pi} \frac{\log(1 - (g + i\beta q)\Lambda e^{-q^2})}{(q - \frac{ig}{\beta})^2} - i\beta\Lambda e^{\xi^2/4} \Theta(\xi) \quad (\text{S108})$$

Putting the two cases together, we obtain from the equality (S102)

$$i\beta\Lambda Q_{\mp} \left(\frac{ig}{\beta} \right) = -\Phi'_{\pm} \left(\frac{ig}{\beta} \right) = \mp \int_{\mathbb{R}} \frac{dq}{2i\pi} \frac{\log(1 - (g + i\beta q)\Lambda e^{-q^2})}{(q - \frac{ig}{\beta})^2} + i\beta\Lambda e^{\xi^2/4} \Theta(\pm\xi) \quad (\text{S109})$$

a result which remains true for $g = \xi = 0$ provided the integrals are then interpreted as principal values and that we use the convention $\Theta(0) = 1/2$.

Now using (30) and inserting $\beta = -1$, $g = -\beta\frac{\xi}{2}$ and $\beta\Lambda = ze^{-\xi^2/4}$ we obtain the result (31) in the text, from which (32) is obtained upon integration over z .

Remark on the Heaviside function. The appearance of the term $\Theta(\pm\xi)$ in (S109) can also be seen as follows. Let us expand (26) in series of Λ

$$\Phi'_{\pm}(k) = \mp \sum_{n \geq 1} \frac{(i\beta\Lambda)^n}{n} \int_{\mathbb{R}} \frac{dq}{2i\pi} \frac{(q - \frac{ig}{\beta})^n e^{-nq^2}}{(q - k \mp i0^+)^2} \quad (\text{S110})$$

Taking $k = \frac{ig}{\beta}$ we can neglect the term $\pm i0^+$ except for $n = 1$. The term $n = 1$ is

$$\mp (i\beta\Lambda) \int_{\mathbb{R}} \frac{dq}{2i\pi} \frac{e^{-q^2}}{q + \frac{i\xi}{2} \mp i0^+} = \mp (i\beta\Lambda) \int_{\mathbb{R}} \frac{dq}{2i\pi} \frac{e^{-q^2}}{q + \frac{i\xi}{2}} - i\beta\Lambda e^{\xi^2/4} \Theta(\pm\xi) \quad (\text{S111})$$

Recovering the typical probability. Similarly the expansion of $z\Psi'(z)$ in powers of z contains a term with a pole at $q = -i\xi/2$ only for $n = 1$. As shown in the text, this term recovers the typical probability $\bar{Z} = Z_{\text{typ}}$. In deriving the equation (34) we have used the identity, for real a

$$\int_{\mathbb{R}} \frac{dq}{2\pi} \frac{1}{iq + a} e^{-q^2} = \frac{1}{2} e^{a^2} (\text{Erfc}(a) - 2\Theta(-a)) \quad (\text{S112})$$

Range of validity As discussed in the text the formula for $\Psi(z)$ presented in this section is what we call the "main branch" valid only for $z/z_c < 1$ with $z_c = -\frac{2}{\xi} e^{\xi^2/4}$. As a result it only allows to determine $\Phi(H)$ for $H < H_c$. To obtain the full solution to the problem we need to consider analytical continuations, to which we now turn.

VI. ANALYTIC CONTINUATION IN THE CASE OF THE WNT FOR THE KPZ EQUATION

Before discussing the intricacies of the analytic continuations for the present problem, we recall here how it works in the case of the WNT for the KPZ equation. It is necessary to do so since we show below that at large ξ the results for KPZ equation are recovered. We present further details than given in Ref. [10] as they will be very useful below. Indeed the situation in the present paper is already quite similar to the one for the KPZ equation where $\Psi_{\text{KPZ}}(\tilde{z})$ admits a second branch for $-1 \leq \tilde{z} < 0$.

For the KPZ equation one first obtains for $\tilde{z} \in [0, +\infty)$

$$\Psi_{\text{KPZ}}(\tilde{z}) = \Psi_{\text{KPZ},0}(\tilde{z}) := -\frac{1}{\sqrt{4\pi}} \text{Li}_{5/2}(-\tilde{z}) \quad (\text{S113})$$

which can be continued for $\tilde{z} \in [-1, +\infty)$. The polylogarithm function $\text{Li}_{5/2}(-\tilde{z})$ is analytic in the complex \tilde{z} plane except on a branch cut for $\tilde{z} \in (-\infty, -1]$. Across this branch cut it has a jump, which leads to

$$\Psi_{\text{KPZ},0}(\tilde{z} + \mathbf{i}0^+) - \Psi_{\text{KPZ},0}(\tilde{z} - \mathbf{i}0^+) = \Delta_{\text{KPZ}}(\tilde{z}) \quad , \quad \Delta_{\text{KPZ}}(\tilde{z}) = \frac{4}{3} \mathbf{i} (\log(-\tilde{z}))^{3/2} \quad (\text{S114})$$

for $z \in (-\infty, -1]$.

Analogy with the logarithm. This situation is analogous to the study of the logarithm which admits different determination in the complex plane. Indeed, along the negative real axis, the logarithm has a jump of value $2\mathbf{i}\pi$. A better understanding of the logarithm is done by considering its domain of definition not in the complex plane but rather on a Riemann surface, see Fig. S2, where it does not have any jump. In the case of the logarithm, the Riemann surface is composed of different sheets joined by winding around the origin and the correct definition of the logarithm on the n -th sheet is $\log z + 2\mathbf{i}\pi n$ where $\log z$ is the principal determination or main branch.

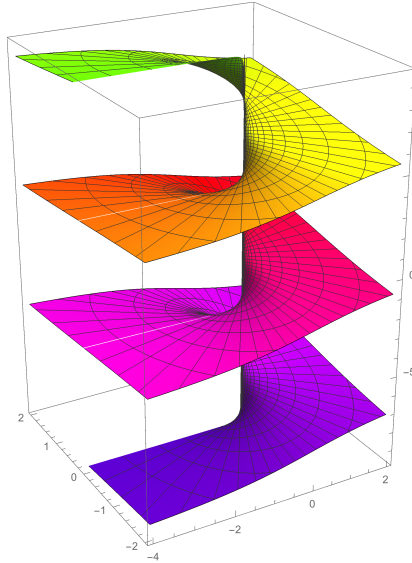


Figure S2. Plot of the Riemann surface of the logarithm $z \mapsto \log z$. This surface is composed of different sheets continuously connected in a staircase manner.

Pursuing the construction of $\Psi_{\text{KPZ}}(\tilde{z})$ on a Riemann surface rather than on the complex plane, we extend continuously the definition $\Psi_{\text{KPZ},0}(\tilde{z})$ to the first Riemann sheet along the branch cut as follows

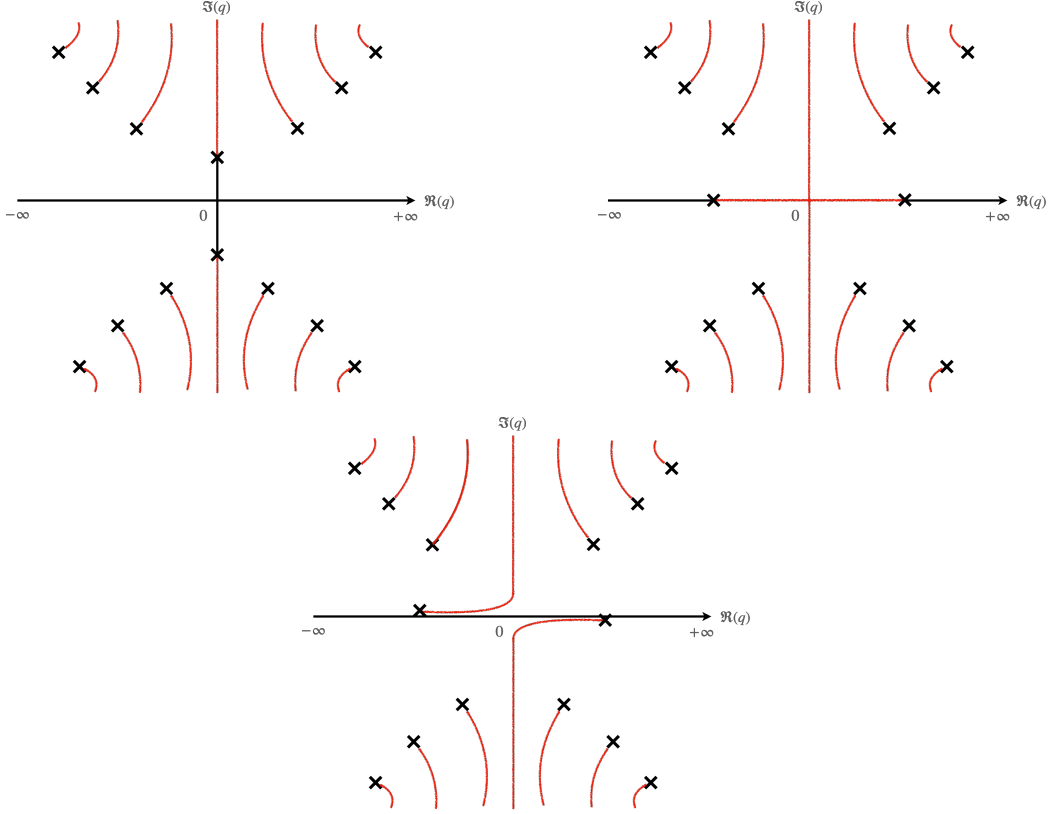


Figure S3. Schematic plot of the argument of the logarithm in Eq. (S117) in the complex q plane for various values of \tilde{z} . **Top left.** $\tilde{z} \geq -1$, $\tilde{z} \in \mathbb{R}$. **Top right.** $\tilde{z} \leq -1$, $\tilde{z} \in \mathbb{R}$. **Bottom** $\Re(\tilde{z}) < -1$, $\Im(\tilde{z}) = 0^+$. The black crosses correspond to the locations where the argument $A_{\text{KPZ}}(q)$ is zero and the red curves correspond to the branch cuts of $\log A_{\text{KPZ}}(q)$.

$$\Psi_{\text{KPZ}}(\tilde{z}) = \begin{cases} \Psi_{\text{KPZ},0}(\tilde{z}), & \Im(\tilde{z}) > 0 \\ \Psi_{\text{KPZ},0}(\tilde{z}) + \Delta_{\text{KPZ}}(\tilde{z}), & \Im(\tilde{z}) < 0 \end{cases} \quad (\text{S115})$$

On the real axis it is multi-valued, i.e. there is a first branch for $\Psi_{\text{KPZ}}(\tilde{z})$ given by the first line, and a second branch given by the second line. One can now continue these two branches for $\tilde{z} \in]-1, 0]$ and one finds that the second branch is

$$\Psi_{\text{KPZ},0}(\tilde{z}) + \Delta_{\text{KPZ}}(\tilde{z}) = -\frac{1}{\sqrt{4\pi}} \text{Li}_{5/2}(-\tilde{z}) + \frac{4}{3} (-\log(-\tilde{z}))^{3/2} \quad (\text{S116})$$

for $\tilde{z} \in]-1, 0]$.

Another route to find the analytic continuation. One can arrive at the same result from the integral representation. Indeed, for $\tilde{z} \in]-1, +\infty[$ one has

$$\tilde{z} \Psi'_{\text{KPZ}}(\tilde{z}) = \int_{\mathbb{R}} \frac{dq}{2\pi} \log(1 + \tilde{z} e^{-q^2}) = \tilde{z} \Psi'_{0,\text{KPZ}}(\tilde{z}) = -\frac{1}{\sqrt{4\pi}} \text{Li}_{3/2}(-\tilde{z}) \quad (\text{S117})$$

Let us plot the argument of the logarithm $A_{\text{KPZ}}(q) = 1 + \tilde{z} e^{-q^2}$ in the complex q plane. This is shown schematically in Fig. S3. For $\tilde{z} > -1$ no branch cut crosses the real axis (integration axis). When \tilde{z} reaches -1 the two symmetric branch cuts along the imaginary axis join. For $\tilde{z} < -1$ they form a "cross" (see Fig. S3 – top right) with ends located at $q = \pm \sqrt{\log(-1/\tilde{z})}$. It is impossible to integrate over the real axis without

crossing them. However suppose now we consider $\tilde{z} \rightarrow \tilde{z} \pm i\epsilon$. We can see that the two branch cuts then avoid each others and it is possible to deform slightly the integration contour to avoid crossing them (see Fig. S3 – bottom). This is consistent with the function $\text{Li}_{3/2}(-\tilde{z})$ being analytic away from the negative real axis for \tilde{z} .

Now one can see that the additional contribution $\Delta_{\text{KPZ}}(z)$ comes for $\tilde{z} < -1$ from the jump across the horizontal part of the "cross" (see Fig. S3 – bottom) and is precisely

$$\tilde{z}\Delta'_{\text{KPZ}}(\tilde{z}) = 2i\pi \int_{-\sqrt{-\log(-1/\tilde{z})}}^{\sqrt{-\log(-1/\tilde{z})}} \frac{dq}{2\pi} = 2i[\log(-\tilde{z})]^{1/2} \quad (\text{S118})$$

while its continuation for $\tilde{z} > -1$ - which enters the second branch - can be obtained as an integral around the complementary of the branch cut in Fig. S3 – top left)

$$\tilde{z}\Delta'_{\text{KPZ}}(\tilde{z}) = 2i\pi \int_{-i\sqrt{\log(-1/\tilde{z})}}^{i\sqrt{\log(-1/\tilde{z})}} \frac{dq}{2\pi} = -2[-\log(-\tilde{z})]^{1/2} \quad (\text{S119})$$

consistent with the previous argument. These considerations will be useful for the next subsection.

VII. ANALYTIC CONTINUATION AND ADDITIONAL BRANCHES OF THE RATE FUNCTION $\Psi(z)$

A. Preliminaries: solutions of Eq. (37) in the text

As mentioned in the text, and for the discussion below about the branch cuts in the integration in the formulas (31) and (32) for $z\Psi'(z)$ and $\Psi(z)$, it is important to study the argument of the logarithm in (31), which we denote $A(q)$

$$A(q) := 1 - z(iq - \frac{\xi}{2})e^{-q^2 - \frac{\xi^2}{4}} \quad (\text{S120})$$

and in particular to find the points where it vanishes, i.e. the zeroes, solutions of $A(q) = 0$. There are many such zeroes but it turns out, see below, that the zeroes on the imaginary axis are the one which play an important role. Setting $q = ip$, it is equivalent to study $A(ip)$ or the function $f_{z,\xi}(p)$ defined as

$$f_{z,\xi}(p) = e^{-p^2 + \frac{\xi^2}{4}} A(ip) = e^{-p^2 + \frac{\xi^2}{4}} + z(p + \frac{\xi}{2}) \quad (\text{S121})$$

and finding its real zeroes, $f_{z,\xi}(p) = 0$, which is Eq. (37) in the text.

We will consider $\xi > 0$ (the case $\xi < 0$ can be studied from the symmetry $(\xi, z) \rightarrow (-\xi, -z)$). Consider also $z < 0$ (see $z > 0$ below). Since $f_{z,\xi}(p) \rightarrow \mp\infty$ as $p \rightarrow \pm\infty$ it has at least one real zero, but in some cases can have three. When there are three zeroes we will denote them $p_1 > p_2 > p_3$ in decreasing order. They are functions of (z, ξ) i.e. $p_i = p_i(z, \xi)$.

The evolution of the zeroes when $z < 0$ is varied is shown in Fig. S4. There are three cases depending in the values of ξ which we now describe. In all three cases the largest zero p_1 vanishes for the value of $z = z_c = z_c(\xi) = -\frac{2e^{\frac{\xi^2}{4}}}{\xi} < 0$. One finds that

1. for $0 < \xi < \xi_1 = \sqrt{8}$, and for all $z < 0$, there is only one zero, $p_1 = p_1(z, \xi)$, see Fig. S4 (top left).
2. for $\xi > \xi_1$ there is an interval of values of z , $z \in]z_{c1}, z_{c2}[$, where there are three zeroes. To find this interval one looks for double zeroes $f_{z,\xi}(p) = f'_{z,\xi}(p) = 0$, i.e.

$$e^{-p^2 + \frac{\xi^2}{4}} = -z(p + \frac{\xi}{2}) = \frac{z}{2p} \quad (\text{S122})$$

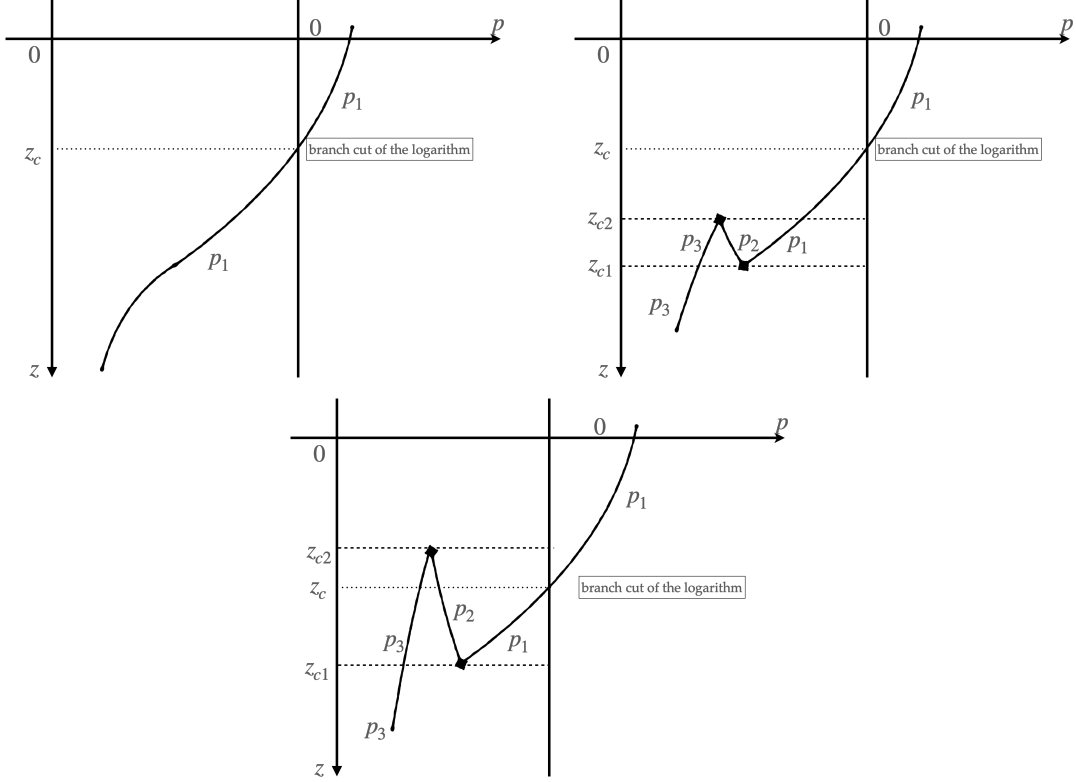


Figure S4. Schematic behavior of the zeroes p_i of the equation $f_{z,\xi}(p_i) = 0$ as a function of $z < 0$ for $\xi > 0$. Top Left: the case $\xi < \xi_1 = \sqrt{8}$ in which case there is a single zero, which changes sign at $z = z_c$. Top Right: the case $\xi_1 < \xi < \xi_2$ in which case there are three zeroes $p_1 > p_2 > p_3$ in the interval $z \in (z_{c1}, z_{c2})$ and $z_{c2} < z_c$. Bottom: the case $\xi > \xi_2$, same but now $z_{c2} > z_c$. The zeroes p_2, p_3 coalesce and annihilate at $z = z_{c2}$ and p_1, p_3 at $z = z_{c1}$. The points z_{c1} and z_{c2} also serve as turning points in the definition of the function $\Psi(z)$.

For a given ξ one can solve these conditions for the couple (z, p) . One finds that there are no real solutions for $\xi < \sqrt{8}$ but that there are two solutions (z_{c1}, p_{c1}) and (z_{c2}, p_{c2}) for $\xi > \xi_1 = \sqrt{8}$. These read, with $z_{c1} < z_{c2}$,

$$z_{c1} = z_{c1}(\xi) = -\frac{1}{2}e^{\frac{1}{8}\left(\xi(\xi+\sqrt{\xi^2-8})+4\right)}\left(\xi - \sqrt{\xi^2-8}\right) \quad , \quad p_{c1} = -\frac{1}{4}\left(\xi - \sqrt{\xi^2-8}\right) \quad (\text{S123})$$

$$z_{c2} = z_{c2}(\xi) = -\frac{1}{2}e^{\frac{1}{8}\left(\xi(\xi-\sqrt{\xi^2-8})+4\right)}\left(\xi + \sqrt{\xi^2-8}\right) \quad , \quad p_{c2} = -\frac{1}{4}\left(\xi + \sqrt{\xi^2-8}\right) \quad (\text{S124})$$

For any $\xi > \xi_1$, and as can be seen in Fig. S4, the two smallest zeroes annihilate at $z = z_{c2}$ where their values are $p_2 = p_3 = p_{c2}$ and the two largest zeroes annihilate at $z = z_{c1}$ where their values are $p_1 = p_2 = p_{c1}$. Note that at $\xi = \sqrt{8}$ the interval is a single point and one has $z_{c1} = z_{c2} = -\sqrt{2}e^{3/2}$ and $p_{c1} = p_{c2} = -1/\sqrt{2}$.

3. It will turn out to be important below to distinguish the cases where $z_{c2} < z_c$ and $z_{c2} > z_c$, see Fig. S4.

Let us determine the value of ξ , denoted $\xi = \xi_2$, at which $z_c(\xi) = z_{c2}(\xi)$. Inserting $z = z_c(\xi) = -\frac{2e^{\frac{\xi^2}{4}}}{\xi}$ into (S122) one gets two equations

$$\xi p e^{-p^2} = -1 \quad , \quad p^2 + \frac{p\xi}{2} = -\frac{1}{2} \quad (\text{S125})$$

where here p should be set to $p = p_{c2}(\xi)$ given in (S124). Combining we obtain a closed equation for $p\xi/2$, i.e.

$$\frac{p\xi}{2} e^{\frac{p\xi}{2}} = -\frac{1}{2} e^{-1/2} \quad \Rightarrow \quad \frac{\xi p_{c2}(\xi)}{2} = W_{-1} \left(-\frac{1}{2\sqrt{e}} \right) \quad (\text{S126})$$

which using $p_{c2}(\xi)$ from (S124) and solving for ξ finally leads to $\xi = \xi_2$ with

$$\xi_2 = -2 \sqrt{\frac{2}{-2W_{-1} \left(-\frac{1}{2\sqrt{e}} \right) - 1}} W_{-1} \left(-\frac{1}{2\sqrt{e}} \right) \simeq 3.13395 \quad (\text{S127})$$

Note that we have discarded the other solution $\xi p_{c2}(\xi) = -1$ of (S126) which does not provide a solution for ξ_2 . Hence, we finally find that for $\xi < \xi_2$ one has $z_{c2} < z_c$ and for $\xi > \xi_2$ one has $z_c < z_{c2}$, see Fig. S4. This will be important below.

B. Continuation and branches of $\Psi(z)$ for $0 < \xi < \xi_1$

We now study the analytical continuations and various branches of $\Psi(z)$. Let us first recall the expressions of $\Psi(z)$ and $\Psi'(z)$ obtained in the text in (31) and (32) for $\xi > 0$

$$z\Psi'(z) = \int_{\mathbb{R}} \frac{dq}{2\pi} \frac{\log(1 - z(\mathbf{i}q - \frac{\xi}{2})e^{-q^2 - \frac{\xi^2}{4}})}{(\mathbf{i}q - \frac{\xi}{2})^2}, \quad \Psi(z) = -\int_{\mathbb{R}} \frac{dq}{2\pi} \frac{\text{Li}_2(z(\mathbf{i}q - \frac{\xi}{2})e^{-q^2 - \frac{\xi^2}{4}})}{(\mathbf{i}q - \frac{\xi}{2})^2} \quad (\text{S128})$$

The argument of the logarithm and polylogarithm is $A(q)$ defined in (S120). The integrand has branch cuts in the complex plane for q when $A(q) \in \mathbb{R}^-$, i.e. is real negative. In the previous subsection we found some of the zeroes (those on the imaginary axis) from which the branch cuts originate. There are additional ones, and the full picture for all $\xi > 0$ is shown schematically in Fig. S5 where the zeroes of $A(q)$ are represented by crosses and the branch cuts by red lines.

Here we examine the simplest case $\xi < \xi_1 = \sqrt{8}$. Then one finds that for $z_c < z < 0$ (top left in Fig. S5) no branch cut crosses the real axis. This corresponds to the regime with a single positive zero $p = p_1$ to Eq. (37). In that regime the formula in (S128) are valid. This is the *main branch*.

For $z \leq z_c(\xi) = -\frac{2e^{\frac{\xi^2}{4}}}{\xi}$ the single zero $p = p_1$ becomes negative hence the branch cut along the positive imaginary axis intersects the real axis at $q = 0$. This is represented in Fig. S5 (top right). In the case however, i.e. for $0 < \xi < \xi_1$, it is always possible (i.e. for any $z \leq z_c$) to deform the integration contour of q away from the real axis to pass below the branch cut (as represented on the Figure). We call this new contour C . This provides a natural analytical continuation to all real z . This leads to

$$\begin{aligned} z\Psi'(z) &= \int_C \frac{dq}{2\pi} \frac{\log(1 - z(\mathbf{i}q - \frac{\xi}{2})e^{-q^2 - \frac{\xi^2}{4}})}{(\mathbf{i}q - \frac{\xi}{2})^2} \\ &= z\Psi'_0(z) + z\Delta'_1(z), \quad z\Psi_0(z) = \int_{\mathbb{R}} \frac{dq}{2\pi} \frac{\log(1 - z(\mathbf{i}q - \frac{\xi}{2})e^{-q^2 - \frac{\xi^2}{4}})}{(\mathbf{i}q - \frac{\xi}{2})^2} \end{aligned} \quad (\text{S129})$$

In the second line we have split the integral into an integral over the real axis which passes right through the branch cut, and a contribution denoted $z\Delta'_1(z)$ which represents the contribution of a contour around the branch cut (taking into account the $2\mathbf{i}\pi$ discontinuity of the logarithm), which reads

$$z\Delta'_1(z) = \int_0^{p_1} \frac{dp}{(p + \xi/2)^2} = \frac{4p_1}{\xi(2p_1 + \xi)} \quad (\text{S130})$$

with $p_1 = p_1(z, \xi)$. The first piece, $z\Psi'_0(z)$ is by definition the integral over \mathbb{R} computed "naively", that is with a jump of the integrand when the argument of the logarithm crosses the negative real axis (which

occurs for $q = 0$) and in such a way that the invariance under the change of variable $\mathbf{i}q \rightarrow -\mathbf{i}q$ ensures that the result is real (in other words one can e.g. replace $\int_{\mathbb{R}} = 2\Re \int_{\mathbb{R}^-}$) and not worry about the branch cut.

We can repeat the same procedure for the formula for $\Psi(z)$ itself in (S128), the branch cut of the Li_2 function being identical to the one of the logarithm with however a different value of the jump

$$\text{Li}_2(t + \mathbf{i}0^+) - \text{Li}_2(t - \mathbf{i}0^+) = -2\mathbf{i}\pi \log t \quad (\text{S131})$$

One obtains

$$\begin{aligned} \Psi(z) &= - \int_C \frac{dq}{2\pi} \frac{\text{Li}_2(z(\mathbf{i}q - \frac{\xi}{2}))e^{-q^2 - \frac{\xi^2}{4}}}{(\mathbf{i}q - \frac{\xi}{2})^2} \\ &= \Psi_0(z) + \Delta_1(z) \quad , \quad \Psi_0(z) = - \int_{\mathbb{R}} \frac{dq}{2\pi} \frac{\text{Li}_2(z(\mathbf{i}q - \frac{\xi}{2}))e^{-q^2 - \frac{\xi^2}{4}}}{(\mathbf{i}q - \frac{\xi}{2})^2} \end{aligned} \quad (\text{S132})$$

with

$$\Delta_1(z) = - \int_0^{p_1} \frac{dp}{(p + \xi/2)^2} \log(-z(p + \frac{\xi}{2})e^{p^2 - \frac{\xi^2}{4}}) \quad (\text{S133})$$

$$= \hat{\Delta}(p_1(z, \xi)) \quad , \quad \hat{\Delta}(p) = \frac{1}{\xi} \left[-(\xi^2 + 2)(\log(\xi) - \log(\xi + 2p)) + 2p(p - \xi) - \frac{4p}{\xi + 2p} \right] \quad (\text{S134})$$

where we have defined a new function $\hat{\Delta}(p)$ which will be useful below. To obtain this expression for $\Delta_1(z)$ one can either compute the contribution of the branch cut, as done above, or integrate the expression (S130) over z . In the latter case one uses the following differential relation for $p_1 = p_1(z)$

$$\frac{dp_1}{dz} = -\frac{1}{z} \frac{p_1 + \frac{\xi}{2}}{1 + 2p_1(p_1 + \frac{\xi}{2})} \quad (\text{S135})$$

and write

$$\Delta_1(z) = - \int_z^{z_c} \frac{dz'}{z'} \frac{4p_1(z')}{\xi(2p_1(z') + \xi)} = \int_0^{p_1} dp \frac{2p}{\xi} \frac{1 + 2p(p + \frac{\xi}{2})}{(p + \frac{\xi}{2})^2} \quad (\text{S136})$$

which also yields (S133), showing that the two methods agree.

The above formula are those used for the plots of $\Psi'(z)$ in the main text for $0 < \xi < \xi_1$. We have checked numerically that for large negative $z \rightarrow -\infty$, $\Psi'(z) \rightarrow 1$ since $p_1 \rightarrow -\frac{\xi}{2} - \frac{1}{z} + o(1/z)$. This gives confidence that this is the correct solution.

Remark. We call $\Psi(z) = \Psi_0(z) + \Delta_1(z)$ for $z < z_c$ a new branch different from the main branch, although in a sense they are the same branch by some choice of integration contour. The important point here is the identification of the jump function $\Delta_1(z)$ which, as we will see now, plays an important role to determine the several other branches for $\xi > \xi_1$.

Remark. The structure of branch cuts in the complex plane discussed here for $\xi > 0$ is already present for $\xi = 0$, although in that case $z_c = -\infty$ (for $\xi \rightarrow 0^+$) so no analytic continuation is needed. There is some interpretation of the corresponding zeroes of $a(k)$ and $\bar{a}(k)$ in terms of additional solitonic solutions of the DNLS equation, as discussed in the main text. For $z > z_c$ these are presumably irrelevant for the large deviations.

C. Continuation and branches of $\Psi(z)$ for $\xi > \xi_1$

Let us consider now the case $\xi > \xi_1 = \sqrt{8}$. First, for $z_c(\xi) < z < 0$ it is still true that no branch cut crosses the real axis. This is because the largest zero p_1 is strictly positive hence the branch cut $q \in [\mathbf{i}p_1, +\mathbf{i}\infty[$ does

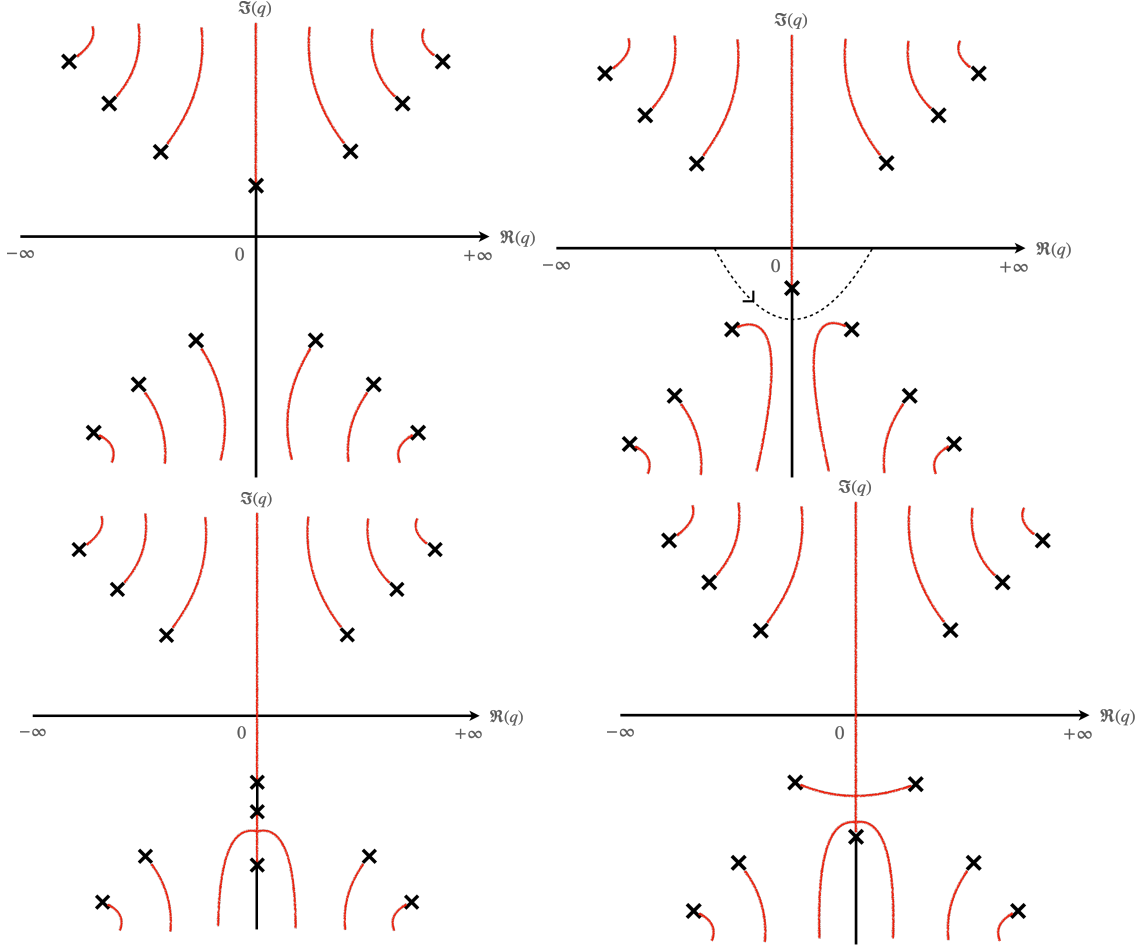


Figure S5. Schematic plots of the argument of the logarithm $A(q)$ given in (S120) as a function of q in the complex plane for $\xi > 0$ and $z < 0$. The crosses indicate the positions of the zeroes of $A(q)$ and the red lines are the branch cuts. **Top Left.** $z_c < z < 0$ for all $\xi > 0$. No branch cut crosses the real axis. **Top Right.** $z < z_c$ for $0 < \xi < \xi_1 = \sqrt{8}$, and $z_{c2} < z < z_c$ for $\xi_1 < \xi < \xi_2$. In that case one branch cut crosses the real axis. The integration contour in q in (S128) can be deformed (dotted lines) to avoid the branch cut. **Bottom Left.** $z_{c1} < z < z_{c2}$ for $\xi_1 < \xi$. It is still possible to avoid the branch cut. **Bottom Right.** $\xi > \xi_1$ and $z < z_{c1}$. In that case the branch cuts have met and form a cross, and there is no way to deform the integration contour to avoid them.

not cross the real axis. Thus the formula in (S128) are valid, and this is again the *main branch*.

Next, as discussed in a previous subsection, see Fig. S4, there is an interval of values of z , $z \in]z_{c1}, z_{c2}[$, where there are three real zeroes $p_1 > p_2 > p_3$ to the equation $A(ip) = 0$. Then there are two sub-cases, for $\xi_1 < \xi < \xi_2$ one has $z_{c2} < z_c$, while for $\xi_2 < \xi$ one has $z_c < z_{c2}$.

In terms of branch cuts, as one can see in Fig. S5, one finds that for $z < z_c$ the branch cut $q \in [ip_1, +i\infty[$ crosses the real axis. However as long as $z > z_{c1}$ there is a way to deform the contour of integration avoid this branch cut. For $z < z_{c1}$ something nasty happens, the upper and lower branch cuts meet and form a cross see Fig. S5 (bottom right). The same happened for the KPZ equation, as discussed in the previous section. In that case, it is not possible anymore to deform the integration contour to avoid these branch cuts. We can now use the "jump" function $\Delta_1(z)$ obtained in the previous section to propose the proper analytical continuations and the ensuing new branches.

When z reaches z_{c1} the zeroes p_1 and p_2 annihilate (corresponding to the merging of the upper and lower branch cuts) and for $z < z_{c1}$ the only remaining zero is p_3 . Thus one would like to write

$$\Psi(z) = \Psi_0(z) + \Delta_3(z) \quad , \quad \Delta_3(z) = \hat{\Delta}(p_3(z)) \quad (\text{S137})$$

where $\hat{\Delta}(p)$ was defined in (S134). This branch appears indeed in the Table I. However since $\Delta_3(z_{c1}) \neq \Delta_1(z_{c1})$ it is not a continuous extension of $\Psi_0(z) + \Delta_1(z)$. This means that there are other branches that will allow a continuous extension. As we now discuss, they will be constructed by first decreasing z from $+\infty$ down to a turning point, increasing it up to a second turning point, and finally decreasing it again down to $-\infty$.

We will thus consider the point $z = z_{c1}$ as the first turning point and start to follow the second zero $p_2 = p_2(z)$. One then proposes the continuous extension defined for $z \in]z_{c1}, z_{c2}[$

$$\Psi(z) = \Psi_0(z) + \Delta_2(z) \quad , \quad \Delta_2(z) = \hat{\Delta}(p_2(z)) \quad (\text{S138})$$

It is a new branch and since $\Psi_0(z) + \Delta_1(z)$ also exists in the same interval $z \in]z_{c1}, z_{c2}[$ the function $\Psi(z)$ is multi-valued in that interval.

When z reaches z_{c2} the zeroes $p_2 = p_2(z)$ and $p_3 = p_3(z)$ annihilate (corresponding to the disappearance of the lower branch-cut as seen in Fig. S5 (top right)). We then again consider $z = z_{c2}$ as a second turning point and start following the third zero p_3 . The candidate for the next continuous extension is therefore

$$\Psi(z) = \Psi_0(z) + \Delta_3(z) \quad , \quad \Delta_3(z) = \hat{\Delta}(p_3(z)) \quad (\text{S139})$$

which is precisely the one in (S137).

This procedure is sufficient for $\xi_1 < \xi < \xi_2$ and leads the third column in the Table I. Using the two turning points one thus obtains a continuous extension, which is multi-valued in the interval $]z_{c1}, z_{c2}[$.

In the case $\xi > \xi_2$ this however is insufficient. Indeed, there is a last feature of the branch cuts to take into account. When z increases from z_{c1} to z_{c2} and then decreases from z_{c2} to $-\infty$ it can cross the value $z = z_c$ depending whether z_c is in the interval $[z_{c1}, z_{c2}]$. This is the case when $\xi > \xi_2$. When z crosses the value z_c , the branch point ip_1 crosses the real axis, either descending from the upper half plane or ascending from the lower half plane. We have observed for the first branch that crossing z_c from above, i.e. $z = z_c + 0^+ \rightarrow z_c + 0^-$ implies that the function Ψ_0 is modified as

$$\Psi_0 \rightarrow \Psi_0 + \Delta_1 \quad (\text{S140})$$

Conversely, crossing z_c from below, i.e. $z = z_c + 0^- \rightarrow z_c + 0^+$ implies that the function Ψ_0 should be modified as

$$\Psi_0 \rightarrow \Psi_0 - \Delta_1 \quad (\text{S141})$$

To obtain the complete solution for $\xi > \xi_2$ one then needs to take into account the coalescence of the zeroes p_1, p_2, p_3 shown in Fig. S4 and also the different crossing of $z = z_c$ independently. This leads to the fourth column of Table I.

Remark. In all these formula $\Psi_0(z)$ denotes the integral (S132) along the real axis which may or may not have a jump in the integrand depending on whether $z < z_c$ or $z > z_c$.

VIII. SUMMARY OF THE RESULTS: DETERMINATION OF $\Phi(H)$

In this Section we summarize the exact results for the large-deviation rate function $\Phi(H)$ of the diffusion in time-dependent random medium for arbitrary position of the tracer $\xi > 0$. The rate function $\hat{\Phi}(Z)$ defined in the text is simply obtained as $\hat{\Phi}(Z) = \Phi(\log Z)$.

A. Exact expressions for all rate functions and critical values

Critical values of ξ . There are two critical values of the position of tracer denoted ξ_1 and ξ_2 . Their value is given as

$$\begin{aligned}\xi_1 &= \sqrt{8} \simeq 2.82843 \\ \xi_2 &= -2 \sqrt{\frac{2}{-2W_{-1}\left(-\frac{1}{2\sqrt{e}}\right) - 1}} W_{-1}\left(-\frac{1}{2\sqrt{e}}\right) \simeq 3.13395\end{aligned}\quad (\text{S142})$$

where W_{-1} is the second real branch of the Lambert function [58].

1. For $\xi \geq \xi_1$ there can be three real zeroes to Eq. (37) depending on z , whereas for $\xi \leq \xi_1$ there is only one real zero.
2. The value ξ_2 is determined as the solution of $z_c(\xi) = z_{c2}(\xi)$. For $\xi \geq \xi_2$, we have the ordering $z_{c1} < z_c < z_{c2}$.

Critical values of z . There are three critical values of the parameter z denoted z_c , z_{c1} and z_{c2} . Their dependence on the tracer position ξ is given as

$$\begin{aligned}z_c(\xi) &= -\frac{2e^{\frac{\xi^2}{4}}}{\xi} \\ z_{c1}(\xi) &= -\frac{1}{2}e^{\frac{1}{8}\left(\xi(\xi+\sqrt{\xi^2-8})+4\right)}\left(\xi - \sqrt{\xi^2-8}\right) \\ z_{c2}(\xi) &= -\frac{1}{2}e^{\frac{1}{8}\left(\xi(\xi-\sqrt{\xi^2-8})+4\right)}\left(\xi + \sqrt{\xi^2-8}\right)\end{aligned}\quad (\text{S143})$$

1. The quantities z_{c1} , z_{c2} are real only for $\xi > \xi_1$. They are determined by the value of p where the function $f_{z,\xi}$ has two degenerate zeroes, i.e. $f_{z,\xi}(p) = f'_{z,\xi}(p) = 0$
2. For $z < z_c$, the largest real zero of $f_{z,\xi}(p)$ is negative whereas for $z > z_c$ it is positive.

Critical values of the zeroes p .

$$p_c = 0 \quad (\text{S144})$$

$$p_{c1} = -\frac{1}{4}\left(\xi - \sqrt{\xi^2-8}\right) \quad (\text{S145})$$

$$p_{c2} = -\frac{1}{4}\left(\xi + \sqrt{\xi^2-8}\right) \quad (\text{S146})$$

The rate function $\Phi(H)$. We obtain the rate function $\Phi(H)$ parametrically. In practice, its numerical determination will be done by parts using all the different branches of $\Psi(z)$. Since $z(H)$ is single-valued, this procedure allows to obtain $\Phi(H)$ in the whole range $]-\infty, 0]$. We provide in the following the representations which were used for the numerical plots.

1. $\xi = 0$

The rate function, see Table II, reads

interval of H	interval of z	$H =$	$\Phi(H) =$
$H \in \mathbb{R}^-$	$z \in \mathbb{R}$	$\log \Psi'_0(z)$	$\Psi_0(z) - z\Psi'_0(z)$

Table II. Case $\xi = 0$

2. $0 < \xi \leq \xi_1$

Defining the critical height $H_c = \log \Psi'_0(z_c)$, the rate function, see Table III, reads

interval of H	interval of z	$H =$	$\Phi(H) =$
$H \leq H_c$	$z_c \leq z$	$\log \Psi'_0(z)$	$\Psi_0(z) - z\Psi'_0(z)$
$0 > H > H_c$	$z_c > z$	$\log(\Psi'_0(z) + \Delta'_1(z))$	$\Psi_0(z) + \Delta_1(z) - z(\Psi'_0(z) + \Delta'_1(z))$

Table III. Case $0 < \xi \leq \xi_1$

3. $\xi_1 < \xi \leq \xi_2$

Defining the three critical heights

$$\begin{aligned}
H_c &= \log \Psi'_0(z_c), \\
H_{c1} &= \log(\Psi'_0(z_{c1}) + \Delta'_1(z_{c1})) = \log(\Psi'_0(z_{c1}) + \Delta'_2(z_{c1})), \\
H_{c2} &= \log(\Psi'_0(z_{c2}) + \Delta'_2(z_{c2})) = \log(\Psi'_0(z_{c2}) + \Delta'_3(z_{c2})),
\end{aligned} \tag{S147}$$

the rate function, see Table IV, reads

interval of H	interval of z	$H =$	$\Phi(H) =$
$H \leq H_c$	$z_c \leq z$	$\log \Psi'_0(z)$	$\Psi_0(z) - z\Psi'_0(z)$
$H_c < H \leq H_{c1}$	$z_{c1} \leq z < z_c$	$\log(\Psi'_0(z) + \Delta'_1(z))$	$\Psi_0(z) + \Delta_1(z) - z(\Psi'_0(z) + \Delta'_1(z))$
$H_{c1} < H \leq H_{c2}$	$z_{c1} < z \leq z_{c2}$	$\log(\Psi'_0(z) + \Delta'_2(z))$	$\Psi_0(z) + \Delta_2(z) - z(\Psi'_0(z) + \Delta'_2(z))$
$H_{c2} < H < 0$	$z_{c2} > z$	$\log(\Psi'_0(z) + \Delta'_3(z))$	$\Psi_0(z) + \Delta_3(z) - z(\Psi'_0(z) + \Delta'_3(z))$

Table IV. Case $\xi_1 < \xi \leq \xi_2$

It is important to note that the expressions for H and for $\Phi(H)$ as a function of z in the second and third line of the above table merge continuously at $H = H_{c1}$ around the turning point at $z = z_{c1}$. This can be seen from (S130) and (S136) as the jumps $\Delta_j(z) = \hat{\Delta}(p_j(z))$, $j = 1, 2$ are the same function of the zeroes $p_j(z)$, hence one has $\Delta_1(z_{c1}) = \Delta_2(z_{c1})$ as well as $\Delta'_1(z_{c1}) = \Delta'_2(z_{c1})$, since $p_1(z) = p_2(z)$ at $z = z_{c1}$. This implies that as z decreases from $+\infty$ down to the turning point z_{c1} and then increases again from z_{c1} , the function $H = H(z)$ smoothly increases, and $\Phi(H)$ is a smooth function of H around H_{c1} . These features can be seen in Fig. 1 (top right) in the text. The same holds for each turning point, and is also valid for the table in the next section.

4. $\xi_2 < \xi$

Defining the five critical heights

$$\begin{aligned}
H_c &= \log \Psi'_0(z_c) \\
H_{c10} &= \log(\Psi'_0(z_{c1}) + \Delta'_1(z_{c1})), \\
H_{c11} &= \log(\Psi'_0(z_c) + \Delta'_2(z_c)), \\
H_{c20} &= \log(\Psi'_0(z_{c2}) + \Delta'_2(z_{c2}) - \Delta'_1(z_{c2})), \\
H_{c21} &= \log(\Psi'_0(z_c) + \Delta'_3(z_c)),
\end{aligned} \tag{S148}$$

the rate function, see Table V, reads

interval of H	interval of z	$H =$	$\Phi(H) =$
$H \leq H_c$	$z_c \leq z$	$\log \Psi'_0(z)$	$\Psi_0(z) - z\Psi'_0(z)$
$H_c < H \leq H_{c10}$	$z_{c1} \leq z < z_c$	$\log(\Psi'_0(z) + \Delta'_1(z))$	$\Psi_0(z) + \Delta_1(z) - z(\Psi'_0(z) + \Delta'_1(z))$
$H_{c10} < H \leq H_{c11}$	$z_{c1} < z \leq z_c$	$\log(\Psi'_0(z) + \Delta'_2(z))$	$\Psi_0(z) + \Delta_2(z) - z(\Psi'_0(z) + \Delta'_2(z))$
$H_{c11} < H \leq H_{c20}$	$z_c < z \leq z_{c2}$	$\log(\Psi'_0(z) + \Delta'_2(z) - \Delta'_1(z))$	$\Psi_0(z) + \Delta_2(z) - \Delta_1(z) - z(\Psi'_0(z) + \Delta'_2(z) - \Delta'_1(z))$
$H_{c20} < H \leq H_{c21}$	$z_c \leq z < z_{c2}$	$\log(\Psi'_0(z) + \Delta'_3(z) - \Delta'_1(z))$	$\Psi_0(z) + \Delta_3(z) - \Delta_1(z) - z(\Psi'_0(z) + \Delta'_3(z) - \Delta'_1(z))$
$H_{c21} < H < 0$	$z_c > z$	$\log(\Psi'_0(z) + \Delta'_3(z))$	$\Psi_0(z) + \Delta_3(z) - z(\Psi'_0(z) + \Delta'_3(z))$

Table V. Case $\xi_2 < \xi$

Optimal rate function $\Psi(z)$ As discussed in the text the "optimal" $\Psi(z)$ follows by definition the minimum of the different branches of $\Psi(z)$ that we have found. For $\xi < \xi_1$ there is no multi-valuation of $\Psi(z)$ hence $\Psi(z)$ follows continuously the two branches $z > z_c$ and $z < z_c$. For $\xi > \xi_1$ there is multi-valuation of $\Psi(z)$ for $z \in]z_{c1}, z_{c2}[$ leading to a discontinuity, i.e. a jump of $\Psi(z)$. The value of z for which $\Psi(z)$ jumps from a branch to the next (see inset of Fig. 1) is given by z^* solution of

$$\Delta_1(z^*) = \Delta_3(z^*) \tag{S149}$$

This value is located between z_{c1} and z_{c2} . We provide in the next two Tables VI the value of the optimal Legendre solution. Note that the jump in the value of Z is always $\Delta'_3(z^*) - \Delta'_1(z^*)$ (jumps between the two maxima of the tilted measure for Z as discussed in the text).

B. Additional plots

In this Section we show the plot of $\Psi(z)$ versus z , as well as the plot of $\Phi(H(z))$ versus z , see Fig. S6.

C. Result for $\xi = 0$ and correspondence with Ref. [41].

We provide in this Section a correspondence between the variables and functions studied in this work and in the work [41] in the particular case $\xi = 0$. In that case $g = 0$. This is summarized in the Table VII.

interval of z	"optimal" $\Psi(z) =$	interval of z	"optimal" $\Psi(z) =$
$z_c \leq z$	$\Psi_0(z)$	$z^* \leq z$	$\Psi_0(z)$
$z^* \leq z < z_c$	$\Psi_0(z) + \Delta_1(z)$	$z_c \leq z < z^*$	$\Psi_0(z) + \Delta_3(z) - \Delta_1(z)$
$z^* > z$	$\Psi_0(z) + \Delta_3(z)$	$z_c > z$	$\Psi_0(z) + \Delta_3(z)$

Table VI. **(Left)** Case $\xi_1 < \xi \leq \xi_2$. In the inversion of the Legendre-Fenchel transform, Z jumps from $\Psi'_0(z^*) + \Delta'_1(z^*)$ to $\Psi'_0(z^*) + \Delta'_3(z^*)$. **(Right)** Case $\xi_2 < \xi$ (assuming $z_c < z^*$). In the inversion of the Legendre-Fenchel transform, Z jumps from $\Psi'_0(z^*)$ to $\Psi'_0(z^*) + \Delta'_3(z^*) - \Delta'_1(z^*)$. Note that $z_c > z^*$ would lead to a jump between the second branch and the last branch with the same jump criterion (S149).

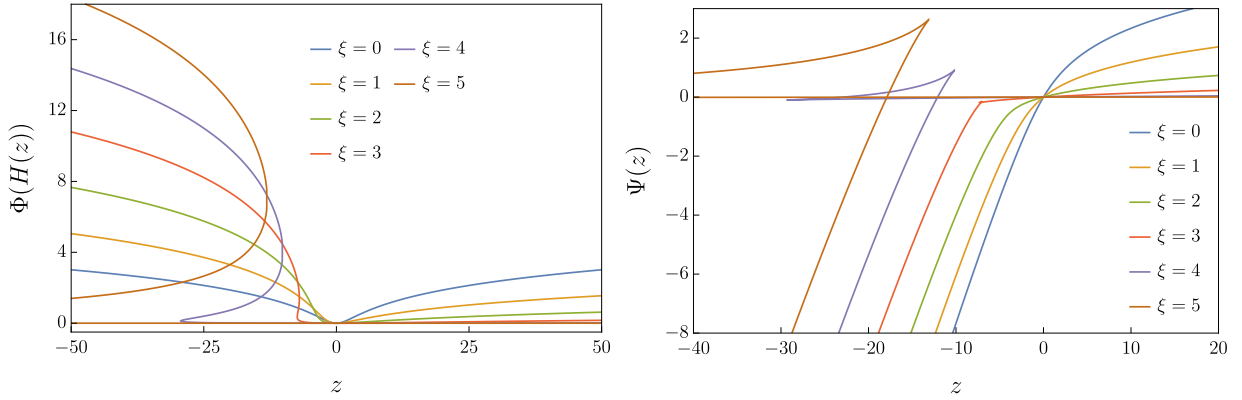


Figure S6. Plots for various values of $\xi = 0, 1, 2, 3, 4, 5$. **(Left)** Large deviation rate function $\Phi(H(z))$ as a function of z using the definition (35). The function is symmetric for $\xi = 0$ and becomes asymmetric for non-zero values of ξ . It satisfies the symmetry $\Phi(H(z))|_{-\xi} = \Phi(H(-z))|_{\xi}$. **(Right)** Large deviation rate function $\Psi(z)$. The minimum branch of $\Psi(z)$ defines the "optimal" solution to the Legendre inversion of Eq. (8). For large negative values of z , the function becomes almost linear, i.e. $\Psi(z) \simeq z$.

This present work	Ref. [41]
$z = \beta\Lambda$	$-\lambda$
βR	v
Q	u
$Z = e^H = \Psi'(z)$	$j + \frac{1}{2}$
$\Phi(H) = \Psi(z) - ze^H = \Psi(z) - z\Psi'(z)$	$s(j)$
$-z = e^{-H}\Phi'(H)$	$\lambda = \frac{ds}{dj}$

Table VII. Correspondence between the variables of this work and Ref. [41] for $\xi = 0$.

Consider the formula (27) and (29) in [41]. Taken together they give

$$s(\lambda) - \lambda j(\lambda) = \int_{\mathbb{R}} \frac{dk}{8\pi k^2} \text{Li}_2(-\lambda^2 k^2 e^{-2k^2}) \quad , \quad \lambda j(\lambda) = \int_{\mathbb{R}} \frac{dk}{4\pi k^2} \log(1 + \lambda^2 k^2 e^{-2k^2}) \quad (\text{S150})$$

From the Table VII we should identify the first result as $\Psi(z) - z/2$ and the second as $z/2 - z\Psi'(z)$. Using the duplication formula for the dilogarithm

$$\text{Li}_2(z) + \text{Li}_2(-z) = \frac{1}{2}\text{Li}_2(z^2) \quad (\text{S151})$$

we indeed find agreement with our formula (32) and (31) with $z = -\lambda$ and using $\Theta(\xi = 0) = 1/2$ as discussed in the text.

D. Cumulant expansion of Z and checks

From its definition (7) the function $\Psi(z)$ encodes the cumulant expansion

$$\Psi(z) = - \sum_{p \geq 1} \frac{(-z)^p}{p!} T^{\frac{p-1}{2}} \overline{Z(Y, T)^p} \quad (\text{S152})$$

We will now check from perturbation theory that the lowest order matches our exact result. Since $Z(Y, T)$ is the cumulative probability (4), from (2) it satisfies the SDE

$$\partial_\tau Z(y, \tau) = \partial_y^2 Z(y, \tau) - \sqrt{2}\eta(y, \tau)\partial_y Z(y, \tau) \quad (\text{S153})$$

which we can call the derivative stochastic heat equation, with initial condition $Z(y, \tau = 0) = \Theta(-y)$. We rescale the space and time variables as $y = x\sqrt{T}$, $\tau = tT$. Here we will abuse notations and use the same letter to denote $Z(y, \tau) = Z(x, t)$. The original variable is recovered at the end. The rescaling yields the dimensionless equation with small noise amplitude

$$\partial_t Z(x, t) = \partial_x^2 Z(x, t) - \sqrt{2}T^{-1/4}\eta(x, t)\partial_x Z(x, t) \quad (\text{S154})$$

with initial condition $Z(x, t = 0) = \Theta(-x)$. Denoting $G(x, t) = \frac{1}{\sqrt{4\pi t}}e^{-x^2/(4t)}$ the free Green's function, this can also be written as

$$Z(x, t) = Z_0(x, t) - \frac{\sqrt{2}}{T^{1/4}} \int_0^t du \int_{\mathbb{R}} dx' G(x - x', t - u)\eta(x', u)\partial_{x'} Z(x', u) \quad , \quad Z_0(x, t) = \int_{\mathbb{R}} dx' G(x - x', t)\Theta(-x') \quad (\text{S155})$$

1. For the first moment one recovers indeed

$$\overline{Z(Y, T)} = \overline{Z(x, 1)} = Z_0(x, 1) = \int_x^{+\infty} dy G(y, 1) = \frac{1}{2}\text{Erfc}\left(\frac{x}{2}\right) = \Psi'(0) \quad (\text{S156})$$

2. To lowest order in $T^{-1/2}$ one finds the second cumulant

$$\overline{Z(x, 1)^2}^c = 2T^{-1/2} \int_0^1 du \int_{\mathbb{R}} dx' G(x - x', 1 - u)^2 (\partial_{x'} Z_0(x', u))^2 + \mathcal{O}(T^{-1}) \quad (\text{S157})$$

Using that $\partial_{x'} Z_0(x', u) = -G(x', u)$ one finds the remarkably simple result

$$\overline{Z(Y, T)^2}^c = \overline{Z(\xi, 1)^2}^c = T^{-1/2} \frac{e^{-\frac{\xi^2}{2}}}{4\sqrt{2\pi}} + \mathcal{O}(T^{-1}) \quad (\text{S158})$$

On the other hand one must have

$$-T^{1/2} \overline{Z(Y, T)^2}^c = \Psi''(0) = -\frac{1}{2} \int_{\mathbb{R}} \frac{dq}{2\pi} e^{-2q^2 - \frac{\xi^2}{2}} = -\frac{1}{4\sqrt{2\pi}} e^{-\frac{\xi^2}{2}} \quad (\text{S159})$$

since $\Psi''(0)$ is the coefficient of z^2 in $z\Psi'(z)$.

This shows that our formula (32) for the large-deviation function $\Psi(z)$ yields correctly the two lowest cumulants, as stated in the text.

E. Cumulants of H

One can obtain the cumulants of H from the derivatives of the rate function $\Phi(H)$ (see e.g. in [59, Sec. 4.2.5 of the Supp. Mat.]). Here they scale as $\overline{H^q} \sim T^{\frac{1-q}{2}}$. The typical value $H = H_{\text{typ}}$ is determined by $\Phi'(H_{\text{typ}}) = 0$, which leads $e^{H_{\text{typ}}} = \Psi'(0)$ (see previous subsection) and the second cumulant reads

$$\overline{H^2}^c = \frac{T^{-\frac{1}{2}}}{\Phi''(H_{\text{typ}})} = -T^{-\frac{1}{2}} \frac{\Psi''(0)}{\Psi'(0)^2} = C_2(\xi) T^{-\frac{1}{2}} \quad , \quad C_2(\xi) = \frac{1}{\sqrt{2\pi}} e^{-\frac{\xi^2}{2}} \left(\text{Erfc}\left(\frac{\xi}{2}\right) \right)^{-2} \quad (\text{S160})$$

Indeed, one can relate the derivatives $\Phi^{(q)}(H_{\text{typ}})$ to those of $\Psi(z)$ around $z = 0$ by differentiating the relations $\Psi'(z) = e^H$ and $\Phi'(H) = -ze^H$. One obtains $\Phi''(H) - \Phi'(H) = -\frac{dz}{dH} e^H = -\frac{e^{2H}}{\Psi''(z)}$. Taken at $z = 0$ and $H = H_{\text{typ}}$ they lead to (S160). One has the asymptotics at small and large ξ

$$C_2(\xi) = \frac{1}{\sqrt{2\pi}} + \frac{\sqrt{2}}{\pi} \xi + \mathcal{O}(\xi^2) \quad , \quad C_2(\xi) = \sqrt{\frac{\pi}{2}} \left(\frac{\xi^2}{4} + 1 \right) + \mathcal{O}\left(\frac{1}{\xi^2}\right) \quad (\text{S161})$$

IX. CONVERGENCE TO THE LARGE DEVIATIONS OF THE KARDAR-PARISI-ZHANG EQUATION

A. Large ξ limit: matching MFT at large time $T \gg 1$ to WNT at small time $T_{\text{KPZ}} \ll 1$

We ought to understand in this Section the behavior of our solution in the large ξ limit. In this regime, one first needs to rescale the variable z as

$$\tilde{z} = z \frac{\xi}{2} e^{-\frac{\xi^2}{4}} = -\frac{z}{z_c} \quad . \quad (\text{S162})$$

Values of the main branch of the large-deviation function $\Psi_0(z)$. Recalling the definition of $\Psi_0(z)$ in (32) for $\xi > 0$, approximating $\mathbf{i}q - \frac{\xi}{2} \sim -\frac{\xi}{2}$ and using the series expansion of the dilogarithm $\text{Li}_2(y) = \sum_{n>0} y^n/n^2$, we obtain that

$$\begin{aligned} \Psi_0(z) &\simeq -\frac{1}{\left(\frac{\xi}{2}\right)^2} \sum_{n=1}^{+\infty} \frac{(-\tilde{z})^n}{n^2} \int_{\mathbb{R}} \frac{dq}{2\pi} e^{-nq^2} \\ &\simeq \frac{4}{\xi^2} \Psi_{\text{KPZ},0}(\tilde{z}) \end{aligned} \quad (\text{S163})$$

To go from the first line to the second one, we performed the Gaussian integral and used the identity

$$\Psi_{\text{KPZ},0}(\tilde{z}) = -\frac{1}{\sqrt{4\pi}} \text{Li}_{5/2}(-\tilde{z}) \quad (\text{S164})$$

Critical values of z . In the same way, we rescale the critical values of z as follows:

$$\tilde{z}_c = -\frac{z_c}{z_c}, \quad \tilde{z}_{c1} = -\frac{z_{c1}}{z_c}, \quad \tilde{z}_{c2} = -\frac{z_{c2}}{z_c} \quad . \quad (\text{S165})$$

and take the $\xi \gg 1$ limit to obtain the limiting values

$$\tilde{z}_c = -1, \quad \tilde{z}_{c1} = -1 + \mathcal{O}\left(\frac{1}{\xi^2}\right), \quad \tilde{z}_{c2} = e^{1-\frac{\xi^2}{4}} \left(1 - \frac{\xi^2}{2} + \mathcal{O}\left(\frac{1}{\xi^2}\right) \right) \quad . \quad (\text{S166})$$

Values of the zeroes p_1, p_2, p_3 . The equation (37) determining the position of the branch cut reads with this variable

$$e^{-p^2} + \tilde{z} \left(1 + \frac{2p}{\xi} \right) = 0 \quad (\text{S167})$$

At the first order at large ξ , the zeroes of this equation read

$$\begin{aligned}
p_1 &\simeq \sqrt{\log\left(\frac{z_c}{z}\right)} = \sqrt{-\log(-\tilde{z})} \\
p_2 &\simeq -\sqrt{\log\left(\frac{z_c}{z}\right)} = -\sqrt{-\log(-\tilde{z})} \\
p_3 &\simeq -\frac{\xi}{2} - \frac{1}{z} = -\frac{\xi}{2} - \frac{\xi}{2\tilde{z}} e^{-\xi^2/4}
\end{aligned} \tag{S168}$$

To study only real zeroes imposes that $\tilde{z} \in [-1, 0]$.

Values of the derivative of the jump function. Recalling that the derivative of the jump function (39) reads

$$\tilde{z}\partial_{\tilde{z}}\Delta_\ell = \frac{4p_\ell}{\xi(2p_\ell + \xi)} \tag{S169}$$

It yields for the different zeroes

$$\begin{aligned}
\tilde{z}\partial_{\tilde{z}}\Delta_1 &\simeq_{\xi \rightarrow \infty} \frac{4}{\xi^2} \sqrt{-\log(-\tilde{z})}, \\
\tilde{z}\partial_{\tilde{z}}\Delta_2 &\simeq_{\xi \rightarrow \infty} -\frac{4}{\xi^2} \sqrt{-\log(-\tilde{z})}, \\
\tilde{z}\partial_{\tilde{z}}\Delta_3 &\simeq_{\xi \rightarrow \infty} z = \frac{2\tilde{z}}{\xi} e^{\frac{\xi^2}{4}}
\end{aligned} \tag{S170}$$

Discussion about which branches remain in the large ξ limit. Recalling the different branches of the large-deviation function $\Psi(z)$ in Table V, we now discuss how the different branches behave in the large ξ limit. Since we have $\tilde{z}_c = \tilde{z}_{c1}$, the branches

$$\begin{aligned}
\Psi(z) &= \Psi_0(z) + \Delta_1(z) \\
\Psi(z) &= \Psi_0(z) + \Delta_2(z)
\end{aligned} \tag{S171}$$

disappear on the \tilde{z} scale. We now explain that the next branch, i.e.

$$\Psi(z) = \Psi_0(z) + \Delta_2(z) - \Delta_1(z) \tag{S172}$$

is the only one, besides the main branch, to remain on the \tilde{z} scale. Indeed, looking at the derivative

$$\begin{aligned}
\tilde{z}\partial_{\tilde{z}}\Psi(z) &= \tilde{z}\partial_{\tilde{z}}\Psi_0(z) + \tilde{z}\partial_{\tilde{z}}\Delta_2(z) - \tilde{z}\partial_{\tilde{z}}\Delta_1(z) \\
&\simeq \frac{4}{\xi^2} \left(\tilde{z}\partial_{\tilde{z}}\Psi_{\text{KPZ},0}(\tilde{z}) - 2\sqrt{-\log(-\tilde{z})} \right)
\end{aligned} \tag{S173}$$

which has a jump function part identical to (S119). Hence that branch converges to the second branch of the KPZ rate function, i.e. to $\Psi_{\text{KPZ}}(\tilde{z}) = \Psi_{\text{KPZ},0}(\tilde{z}) + \Delta_{\text{KPZ}}(\tilde{z})$, as claimed in the text.

Furthermore, as explained in the main text, the last two branches with $\Delta = \Delta_3 - \Delta_1$ and $\Delta = \Delta_3$ disappear in the region $H \sim 0$ or equivalently $Z \sim 1$, which correspond to $H_{\text{KPZ}} \rightarrow +\infty$ see discussion below.

B. Matching to the regime $Y \sim T^{4/3}$

It was predicted in [16, 18], and proved in [20], that the sample-to-sample fluctuations of the probability denoted here as $Z(Y, T) = e^{H(Y, T)}$ – defined in (3) – when seen in an atypical space time direction, are related to those of the random height field $h_{\text{KPZ}}(x, t) = h(x, t)$ solution of the KPZ equation

$$\partial_t h(x, t) = \partial_x^2 h(x, t) + (\partial_x h)^2 + \sqrt{2}\eta(x, t) \tag{S174}$$

with droplet initial condition $e^{h(x,0)} = \delta(x)$, where η is a standard space-time white-noise. The relation to the KPZ solution at finite time, $h_{\text{KPZ}}(0, t)$, holds when one scales $Y \sim T^{3/4}$. The scaling studied here $Y \sim T^{1/2}$ thus corresponds to short KPZ time, while the scaling $Y \sim T$ corresponds to the limit of infinite KPZ time, leading to the Tracy-Widom distribution [15].

Let us recall the result of [20, Section 3.2 Eq. (30)] established in the scaling regime $Y \sim T^{3/4}$ (we consider here $Y > 0$). Setting $y = 0$ and $t = 2T$ there (to account for the different units) it translates into the equality in law in the large T limit (for the diffusion (2))

$$\log \mathbb{P}[y(T) > \tilde{x}(2T)^{3/4}] + \frac{1}{2}\tilde{x}^2(2T)^{1/2} + \frac{1}{4}\log(2T) - \log \tilde{x} = h_{\text{KPZ}}\left(0, \frac{\tilde{x}^4}{2}\right) \quad (\text{S175})$$

where $\tilde{x} = \frac{Y}{(2T)^{3/4}}$. Hence denoting

$$T_{\text{KPZ}} = \frac{Y^4}{16T^3} \quad (\text{S176})$$

we have the equalities in law

$$H(Y, T) = h_{\text{KPZ}}(0, T_{\text{KPZ}}) - \frac{Y^2}{4T} + \log \frac{Y}{2T} \quad \Leftrightarrow \quad Z(Y, T) = \frac{Y}{2T} e^{-\frac{Y^2}{4T}} e^{h_{\text{KPZ}}(0, T_{\text{KPZ}})} \quad (\text{S177})$$

valid a priori in the regime $Y \sim T^{3/4}$. Let us now set $Y = \xi\sqrt{T}$, with $\xi > 0$. One gets

$$Z(Y, T) = \frac{\xi}{2\sqrt{T}} e^{-\frac{\xi^2}{4}} e^{h_{\text{KPZ}}(0, T_{\text{KPZ}})} \quad , \quad T_{\text{KPZ}} = \frac{\xi^4}{16T} \quad (\text{S178})$$

valid a priori in the regime $\xi \sim T^{1/4}$. We now show that it holds beyond that, i.e. in the large deviation regime where ξ is of order one but large, which is also the regime where the KPZ time is small, $T_{\text{KPZ}} \ll 1$. To compare with the known large deviation results for the KPZ equation at short time, it is useful to introduce

$$H_{\text{KPZ}} := h_{\text{KPZ}}(0, T_{\text{KPZ}}) + \log(\sqrt{T_{\text{KPZ}}}) \quad (\text{S179})$$

These results read [47], given here in the form of [10, Eqs. (4) and (22)]

$$\overline{\exp(-\tilde{z}e^{h_{\text{KPZ}}(0, T_{\text{KPZ}})})} = \overline{\exp\left(-\frac{\tilde{z}}{\sqrt{T_{\text{KPZ}}}}e^{H_{\text{KPZ}}}\right)} = \exp\left(-\frac{\Psi_{\text{KPZ}}(\tilde{z})}{\sqrt{T_{\text{KPZ}}}}\right) \quad (\text{S180})$$

where $\Psi_{\text{KPZ}}(\tilde{z}) = \Psi_{\text{KPZ},0}(\tilde{z}) = -\frac{1}{\sqrt{4\pi}}\text{Li}_{5/2}(-\tilde{z})$. While the l.h.s. exists a priori only for $\tilde{z} > 0$ this formula admits an analytic continuation, called the main branch, for $\tilde{z} \in [-1, +\infty]$. Already at this level we can match with the results of the present study. Indeed here we obtained for the main branch for $z > z_c$, see Eqs (43) and (44) in the text

$$\overline{\exp(-z\sqrt{T}Z)} = \exp\left(-\sqrt{T}\frac{4}{\xi^2}\Psi_{\text{KPZ},0}(\tilde{z})\right) \quad , \quad \tilde{z} = z\frac{\xi}{2}e^{-\xi^2/4} \quad (\text{S181})$$

which is in perfect agreement with (S180) using the relations in (S178). Hence the large deviations in the regime $Y \sim T^{3/4}$ and the diffusive regime $Y \sim \sqrt{T}$ match smoothly.

As discussed in [10, 47] one obtains the rate function for the KPZ equation, $\Phi_{\text{KPZ}}(H_{\text{KPZ}})$, upon Legendre inversion in the parametric form

$$\Phi_{\text{KPZ}}(H_{\text{KPZ}}) = \Psi_{\text{KPZ}}(\tilde{z}) - \tilde{z}e^{H_{\text{KPZ}}} \quad , \quad e^{H_{\text{KPZ}}} = \Psi'_{\text{KPZ}}(\tilde{z}) \quad (\text{S182})$$

For the KPZ equation the main branch $\Psi_{\text{KPZ},0}(\tilde{z})$ allows to obtain $\Phi_{\text{KPZ}}(H_{\text{KPZ}})$ only for $H_{\text{KPZ}} < H_{\text{KPZ},c} = \log \frac{\zeta(3/2)}{4\pi}$ which corresponds to the field at which $\tilde{z} = \tilde{z}(H_{\text{KPZ}})$ solution of (S182) with $\Psi_{\text{KPZ}} \rightarrow \Psi_{\text{KPZ},0}$ reaches $\tilde{z} = -1$. For $H_{\text{KPZ}} > H_{\text{KPZ},c}$ one needs to use the second branch $\Psi_{\text{KPZ}} \rightarrow \Psi_{\text{KPZ},0} + \Delta_{\text{KPZ}}(\tilde{z})$ and $\tilde{z}(H_{\text{KPZ}})$ increases again from -1 to 0 as $H_{\text{KPZ}} \rightarrow +\infty$.

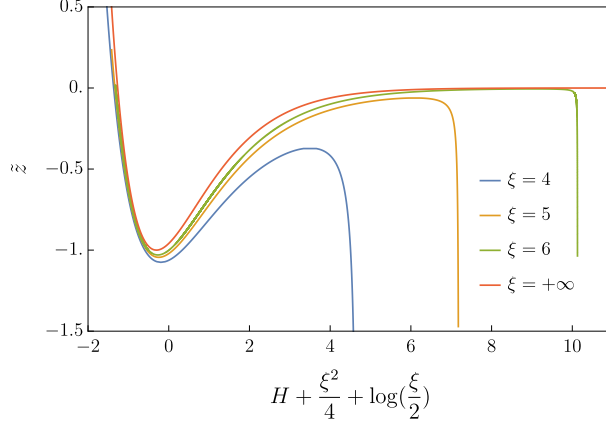


Figure S7. Plot of $\tilde{z} = -z/z_c$ as a function of $H_{\text{KPZ}} = H + \frac{\xi^2}{4} + \log(\frac{\xi}{2})$ for several values of $\xi = 4, 5, 6$ as compared with the asymptotic $\xi = \infty$ KPZ expression. All branches are represented. The convergence to KPZ is excellent. The last two branches in Table I correspond to the sharp decrease to $\tilde{z} \rightarrow -\infty$ and is pushed to $H_{\text{KPZ}} = +\infty$ as $\xi \rightarrow +\infty$. It corresponds to events where $Z \approx 1$ which become irrelevant in that limit.

As we have shown in the previous subsection in the limit $\xi \rightarrow +\infty$ one obtains the convergence

$$\Psi(z) \rightarrow \frac{4}{\xi^2} \Psi_{\text{KPZ}}(\tilde{z}) \quad (\text{S183})$$

not just for the main branch, but for all the branches which survive in that limit. Thus we expect the correspondence between the fields obtained upon Legendre transform

$$H(z) = \log\left(\frac{d\Psi}{dz}\right) \underset{\xi \gg 1}{\simeq} \log\left(\frac{4}{\xi^2} \frac{d\tilde{z}}{dz} \frac{d\Psi_{\text{KPZ}}}{d\tilde{z}}\right) \underset{\xi \gg 1}{\simeq} -\frac{\xi^2}{4} - \log\left(\frac{\xi}{2}\right) + H_{\text{KPZ}}(\tilde{z}) \quad (\text{S184})$$

The prediction is thus that using the results of the present work for $\xi \rightarrow +\infty$, one should have that $\tilde{z} = -z/z_c$ plotted versus $H_{\text{KPZ}} = H + \frac{\xi^2}{4} + \log \frac{\xi}{2}$ reaches a limit curve identical to $\tilde{z}(H_{\text{KPZ}})$ for the KPZ equation. As one can see from (S7) this is indeed the case.

Finally we can check that (S184) is indeed consistent with the correspondence discussed above from the matching to the $Y \sim T^{3/4}$ regime. Indeed, using (S179) and (S178) one has

$$\begin{aligned} H_{\text{KPZ}}(\tilde{z}) &= h_{\text{KPZ}}(0, T_{\text{KPZ}}) + \log(\sqrt{T_{\text{KPZ}}}) \\ &= h_{\text{KPZ}}(0, T_{\text{KPZ}}) - \log(\sqrt{T}) + \log(\xi^2/4) \\ &= H + \frac{\xi^2}{4} + \log \frac{\xi}{2} \end{aligned} \quad (\text{S185})$$

which is identical to (S184).

In conclusion, inserting into the parametric representation of the Legendre transform one obtains for $\xi \gg 1$

$$\Phi(H) \simeq \frac{4}{\xi^2} \Phi_{\text{KPZ}}(H_{\text{KPZ}}) \quad , \quad H_{\text{KPZ}} = H + \frac{\xi^2}{4} + \log \frac{\xi}{2} \quad (\text{S186})$$

as given in the text which means that one can identify the large deviations probabilities

$$\mathcal{P}(H) \sim \exp\left(-\sqrt{T}\Phi(H)\right) \sim \exp\left(-\frac{\Phi(H_{\text{KPZ}})}{\sqrt{T_{\text{KPZ}}}}\right) \sim \mathcal{P}_{\text{KPZ}}(H_{\text{KPZ}}). \quad (\text{S187})$$

X. LARGE-TIME LIMIT OF THE FREDHOLM DETERMINANT RESULT FOR THE STICKY BROWNIAN MOTION

In this section we start from the formula of [19] and study the diffusive limit where T and Y are large with $\xi = Y/\sqrt{T}$ fixed. This leads to a conjectural form for $\Psi(z)$ which agrees with the one derived in the text using inverse scattering. The manipulations in this Appendix are quite heuristic but they have the merit to show that the algebraic structure which emerges from the Fredholm determinant is similar to the one derived in the text from first principles by the inverse scattering method. We hope that it will help to obtain in the future a more precise and rigorous derivation.

In [19] the quantity which corresponds to $Z(Y, T)$ was studied. It was denoted $K_{0,t}(0, [x, +\infty[)$ and called the kernel of the uniform Howitt-Warren flow. The equivalence between the two objects, mathematically very subtle, was discussed in [19, Remark 2.4], see also [60].

Here, the quantity which we define as $Z(Y, T)$ obeys a backward Fokker-Planck equation. Indeed, from the definition

$$Z(Y, \tau) = \int_Y^{+\infty} dy q_\eta(y, \tau) \quad , \quad q_\eta(y, \tau) = -\partial_y Z(y, \tau) \quad (\text{S188})$$

one easily obtain upon integrating Eq. (2)

$$\partial_\tau Z(Y, \tau) = \partial_Y^2 Z(Y, \tau) - \sqrt{2}\eta(Y, \tau)\partial_Y Z(Y, \tau) \quad (\text{S189})$$

with initial condition $Z(Y, \tau = 0) = \Theta(-Y)$. This is equivalent to Ref. [19, Eq. (19)]. The correspondence of notations is that the space and time variables there must be replaced by $t \rightarrow 2T$ and $x = Y$. Note that in Ref. [19, Eq. (19)] the noise term is $-\sqrt{2}\eta(y, T) = \frac{\sqrt{2}}{\sqrt{\lambda}}\hat{\eta}(y, T)$ where $\hat{\eta}$ is standard space time white noise. Hence below λ is set to unity.

The identity proved in [19, Theorem 1.11] reads for u non-negative

$$\mathbb{E}[e^{-uZ(Y, T)}] = \text{Det}(I - K_u)|_{\mathbb{L}^2(C)} \quad (\text{S190})$$

where C is a positively-oriented circle with radius R and centered at R and

$$K_u(v, v') = \frac{1}{2i\pi} \int_{1/2+i\mathbb{R}} \frac{\pi}{\sin \pi s} u^s \frac{g(v)}{g(v+s)} \frac{ds}{s+v-v'} \quad (\text{S191})$$

The definition of $g(v)$ is

$$g(v) = \Gamma(v) e^{aY\psi_0(v) + bT\psi_1(v)} \quad (\text{S192})$$

where $\psi_{0,1}$ denote polygamma functions and $a = \lambda$ and $b = \lambda^2$. Here λ is set to unity.

We now use $\zeta = v + s$ as a variable, for which the integration contour can be chosen as $1/2 + 2R + i\mathbb{R}$ – see remark in [19, Proposition 2.3] – where we recall that C is the integration contour for v, v' . We factorize the kernel (S191) into the following form

$$K_u(v, v') = \int_{1/2+2R+i\mathbb{R}} \frac{d\zeta}{2i\pi} A(v, \zeta) \tilde{A}(\zeta, v'), \quad (\text{S193})$$

$$A(v, \zeta) = \frac{\pi u^{\zeta-v}}{\sin(\pi(\zeta-v))} \frac{g(v)}{g(\zeta)}, \quad \tilde{A}(\zeta, v') = \frac{1}{\zeta - v'}. \quad (\text{S194})$$

We now use the identity

$$\frac{\pi}{\sin(\pi s)} u^s = \int_{\mathbb{R}} dr \frac{u}{u + e^{-r}} e^{-sr} \quad (\text{S195})$$

which, inserted into (S194), allows to factorize the kernel A as

$$A(v, \zeta) = \int_{\mathbb{R}} dr \frac{u}{u + e^{-r}} e^{-(\zeta-v)r} \frac{g(v)}{g(\zeta)} = \int_{\mathbb{R}} dr \sigma(r) A_1(v, r) A_2(r, \zeta) = (A_1 \sigma A_2)(v, \zeta) \quad (\text{S196})$$

where the kernels A_1, A_2 and the function σ read

$$A_1(v, r) = g(v) e^{vr}, \quad A_2(r, \zeta) = \frac{e^{-\zeta r}}{g(\zeta)}, \quad \sigma(r) = \frac{u}{u + e^{-r}}. \quad (\text{S197})$$

Hence using Sylvester's identity

$$\begin{aligned} \text{Det}(I - K_u)|_{\mathbb{L}^2(C)} &= \text{Det}(I - A\tilde{A}) \\ &= \text{Det}(I - A_1 \sigma A_2 \tilde{A}) \\ &= \text{Det}(I - \sigma A_2 \tilde{A} A_1)|_{\mathbb{L}^2(\mathbb{R})} \end{aligned} \quad (\text{S198})$$

This last Fredholm determinant has the typical structure for which the first cumulant method, developed in [49–51] to study the relevant asymptotics (here large T), applies. Defining a determinantal point process $\{a_\ell\}_{\ell \in \mathbb{N}}$ associated to the kernel $A_2 \tilde{A} A_1$, the following identity holds

$$\text{Det}(I - \sigma A_2 \tilde{A} A_1) = \mathbb{E} \left[\prod_{\ell=1}^{\infty} (1 - \sigma(a_\ell)) \right] = \mathbb{E} \left[\prod_{\ell=1}^{\infty} e^{-\varphi(a_\ell)} \right] \quad (\text{S199})$$

where $e^{-\varphi} = 1 - \sigma$. The first cumulant approximation asserts [49, Section 6] that as some parameter goes to infinity (here it will be T , see below), we expect the point process to self-average, i.e.

$$\mathbb{E} \left[\prod_{\ell=1}^{\infty} e^{-\varphi(a_\ell)} \right] \sim e^{-\mathbb{E}[\varphi(a)]} = e^{-\text{Tr}(\varphi A_2 \tilde{A} A_1)} \quad (\text{S200})$$

If the first cumulant method works, we aim to have under the right scaling

$$\text{Det}(I - K_u)|_{\mathbb{L}^2(C)} \sim \exp \left[-\text{Tr}(\varphi A_2 \tilde{A} A_1) \right] \quad (\text{S201})$$

The explicit expression of the kernel $A_2 \tilde{A} A_1$ is obtained as

$$(A_2 \tilde{A} A_1)(r, r') = \int_{1/2+2\mathbb{R}+i\mathbb{R}} \frac{d\zeta}{2i\pi} \int_C \frac{dv'}{2i\pi} \frac{g(v')}{g(\zeta)} \frac{1}{\zeta - v'} e^{r'v' - r\zeta} \quad (\text{S202})$$

taking into account that the measure on the variables v is $\frac{dv}{2i\pi}$. Using that

$$\varphi(r) = \log(1 + ue^r) = -\text{Li}_1(-ue^r) \quad (\text{S203})$$

to apply the first cumulant method we need to calculate the following quantity which only involves the diagonal part of the kernel $A_2 \tilde{A} A_1$

$$\text{Tr}(\varphi A_2 \tilde{A} A_1) = - \int_{\mathbb{R}} dr \int_{1/2+2\mathbb{R}+i\mathbb{R}} \frac{d\zeta}{2i\pi} \int_C \frac{dv'}{2i\pi} \text{Li}_1(-ue^r) \frac{g(v')}{g(\zeta)} \frac{1}{\zeta - v'} e^{r(v'-\zeta)} \quad (\text{S204})$$

We recall that $\Re(\zeta - v') > 0$ by construction. We further proceed to an integration by part with respect to r to obtain

$$\text{Tr}(\varphi A_2 \tilde{A} A_1) = - \int_{\mathbb{R}} dr \int_{1/2+2\mathbb{R}+i\mathbb{R}} \frac{d\zeta}{2i\pi} \int_C \frac{dv'}{2i\pi} \text{Li}_2(-ue^r) \frac{g(v') e^{rv'}}{g(\zeta) e^{r\zeta}} \quad (\text{S205})$$

The boundary terms of the integration by part are zero since $e^{r(1+v'-\zeta)} \rightarrow 0$ for $r \rightarrow -\infty$ and the polylogarithms behave as $\text{Li}_s(e^r) \sim r^s$ at $r \rightarrow +\infty$.

At this stage we proceed to the large-time rescaling to the diffusive regime using the rescaled variables

$$\{Y = \xi\sqrt{T} \quad , \quad v = w\sqrt{T} \quad , \quad \zeta = \omega\sqrt{T} \quad , \quad u = z\sqrt{T}\} \quad (\text{S206})$$

We then rewrite (S204) as

$$\text{Tr}(\varphi A_2 \tilde{A} A_1) = - \int_{\mathbb{R}} dr \text{Li}_2(-ue^r) I(r) = - \int_{\mathbb{R}} dr \text{Li}_2(-ze^r) I(r - \log \sqrt{T}) \quad (\text{S207})$$

where we have shifted the variable r by $-\log \sqrt{T}$, and defined

$$\begin{aligned} I(r - \log \sqrt{T}) &= \int_{1/2+2\mathbb{R}+i\mathbb{R}} \frac{d\zeta}{2i\pi} \int_C \frac{dv' g(v') e^{(r-\log(\sqrt{T}))v'}}{2i\pi g(\zeta) e^{(r-\log(\sqrt{T}))\zeta}} \\ &= \int_{1/2+2\mathbb{R}+i\mathbb{R}} \frac{d\zeta}{2i\pi} e^{-(\log g(\zeta) + (r-\log \sqrt{T})\zeta)} \int_C \frac{dv}{2i\pi} e^{(\log g(v) + (r-\log \sqrt{T})v)} \end{aligned} \quad (\text{S208})$$

The large-time expansion of the function $g(v)$ given in Eq. (S192) reads

$$\begin{aligned} \log g(v) &= aY\psi_0(v) + bT\psi_1(v) + \log \Gamma(v) \\ &= \sqrt{T} \left(\phi(w) + (w + a\xi) \log \sqrt{T} \right) + \chi(w) - \frac{1}{2} \log(\sqrt{T}) + o(T) \end{aligned} \quad (\text{S209})$$

where we defined

$$\phi(w) = \frac{b}{w} - w + (w + a\xi) \log(w) \quad , \quad \chi(w) = \frac{b}{2w^2} - \frac{a\xi}{2w} + \frac{1}{2} \log(2\pi w) \quad (\text{S210})$$

At this stage we will choose the radius of the circle C conveniently to be equal to $R = T/Y$ so that its mapping under the large- T limit is a circle C' of radius $1/\xi$ centered at $1/\xi$ (we assume here and below that $\xi > 0$). Upon the change of variable (S206) in the large T limit, inserting (S209) into (S208) and noting that constant terms cancel from the two integrals we obtain

$$I(r - \log \sqrt{T}) \simeq T \int_{2/\xi+0^++i\mathbb{R}} \frac{d\omega}{2i\pi} e^{-\sqrt{T}(\phi(\omega)+r\omega)-\chi(\omega)} \int_{C'} \frac{dw}{2i\pi} e^{\sqrt{T}(\phi(w)+rw)+\chi(w)} \quad (\text{S211})$$

In the large- T limit these integrals are dominated by saddle points. The saddle point equations read

$$\phi'(w) = -\frac{1}{w^2} + \frac{\xi}{w} + \log(w) = -r \quad (\text{S212})$$

and the same for ω . Since w is on the circle C' we can parameterize it in the following way

$$\frac{1}{w} = -\mathbf{i}q + \frac{\xi}{2} \quad , \quad q \in \mathbb{R} \quad (\text{S213})$$

The saddle point equation becomes

$$e^r = \left(-\mathbf{i}q + \frac{\xi}{2}\right) e^{-q^2 - \frac{\xi^2}{4}} \quad (\text{S214})$$

which is very reminiscent of Eq. (37). To make this saddle point easily attainable, one way is to deform the integration contour of r which is not \mathbb{R} anymore but the image of (S214) as q varies on the real axis, which we call γ . We will assume that this is possible. This is a closed curve for e^r , touching the real axis at values $e^r = 0$ and $e^r = \frac{\xi}{2} e^{-\frac{\xi^2}{4}}$. The solution of (S213) and (S214) defines a function $w(r)$ so that the saddle point evaluation of (S211) gives

$$I(r - \log \sqrt{T}) \simeq -\frac{\sqrt{T}}{2i\pi} \frac{1}{\phi''(w(r))} \quad (\text{S215})$$

where we have also assumed that the integration contour of ω could be deformed to be folded around C' . This ensures that the dominant exponential at the saddle point cancel.

To summarize, the first cumulant (S207) of the Fredholm determinant reads in the large T -limit

$$\text{Tr}(\varphi A_2 \tilde{A} A_1) = \frac{\sqrt{T}}{2i\pi} \int_{\gamma} dr \text{Li}_2(-ze^r) \frac{1}{\phi''(w(r))} \quad (\text{S216})$$

We will now perform the change of variable (S214). Using the saddle point equation $\phi'(w(r)) = -r$ we obtain upon derivation the Jacobian of this change of variable

$$\phi''(w(r)) \frac{dw(r)}{dq} \frac{dq}{dr} = -1, \quad \frac{1}{\phi''(w(r))} dr = -\mathbf{i} \frac{dq}{(\mathbf{i}q - \frac{\xi}{2})^2} \quad (\text{S217})$$

Inserting into (S216) we finally obtain

$$\Psi(z) = \frac{1}{\sqrt{T}} \text{Tr}(\varphi A_2 \tilde{A} A_1) = - \int_{\mathbb{R}} \frac{dq}{2\pi} \frac{\text{Li}_2(z(\mathbf{i}q - \frac{\xi}{2}) e^{-q^2 - \frac{\xi^2}{4}})}{(\mathbf{i}q - \frac{\xi}{2})^2} \quad (\text{S218})$$

which is in agreement with Eq. (32) in the text.

XI. EXTENSION TO THE EXTREMAL DIFFUSION BEYOND EINSTEIN'S DIFFUSION THEORY

In this section we study the position of the maximum of N walkers in the same random field (by sample below we mean one given environment, i.e. random field). Previous works started with Ref. [15, 22] which studied the Beta random walk and pointed out that for $N \gg 1$, and in the regime $\log N \sim T$, the position of the maximum has sample to sample fluctuations given by the Tracy-Widom distribution. Another regime, $\log N \sim \sqrt{T}$, was obtained in [16] and [20] where these fluctuations are described by the solution of the KPZ equation at finite time. Numerical simulations which confirm these regimes have been performed recently [52]. Extending these arguments, our present work allows to study another regime, $\log N \ll \sqrt{T}$, not studied previously.

Consider N independent particles in the same environment. One denotes $Y_N(T) = \max_i Y_i(T)$ with $i = 1, \dots, N$ and $Z_N(Y, T) = \mathbb{P}(Y_N(T) > Y)$. One has the exact relation

$$1 - Z_N(Y, T) = \mathbb{P}(Y_N(T) < Y) = \mathbb{P}(Y(T) < Y)^N = (1 - Z(Y, T))^N \quad (\text{S219})$$

We focus below on the diffusive scaling $Y \sim \sqrt{T}$ at large T , not considered previously in the discussion of the extremal diffusion. We will thus denote $y_N(T) = \frac{1}{\sqrt{T}} Y_N(T)$. There are several observables of interest.

Large deviations of the CDF of the maximum. The first observable is $Z_N = \mathbb{P}(y_N(T) > \xi)$, which is simply the analog of Z for the maximum position of N particles. One can ask, for any finite N , what are the large deviations of the PDF of Z_N for $T \gg 1$. From the above simple relation (S219) one finds for

$$\mathcal{P}(Z_N) \sim \exp\left(-\sqrt{T} \hat{\Phi}_\xi \left(1 - (1 - Z_N)^{1/N}\right)\right) \quad (\text{S220})$$

where the rate function $\hat{\Phi}_\xi(Z)$ is the one obtained in the present work (for $N = 1$). Here and below we indicate explicitly the dependence in ξ of the rate functions.

Averaged CDF of the maximum. Another observable is the following average over the environment

$$\overline{\mathbb{P}(y_N(T) < \xi)} = \int_0^1 dZ e^{N \log(1-Z)} \sim \int_0^1 dZ e^{N \log(1-Z) - \sqrt{T} \hat{\Phi}_\xi(Z)} \quad (\text{S221})$$

where in the last equation we have substituted the large deviation form. Note that considering instead of the average moments of order q is equivalent to substitute $n \rightarrow nq$.

There are several regimes depending on N . If $N \ll \sqrt{T}$ then the second term dominates and implies that $Z \approx Z_{\text{typ}}(\xi)$ so that

$$\overline{\mathbb{P}(y_N(T) < \xi)} \simeq e^{N \log(1 - Z_{\text{typ}}(\xi))} \quad (\text{S222})$$

and the result is identical as the CDF of the maximum position for N particles in the absence of random field.

If $N = n\sqrt{T} \gg 1$ with $n = \mathcal{O}(1)$ fixed, the two terms can balance each others and one finds that this observable takes the large deviation form

$$\overline{\mathbb{P}(y_N(T) < \xi)} \sim e^{-\sqrt{T}\Sigma_\xi(n)} \quad , \quad \Sigma_\xi(n) = \min_Z(\hat{\Phi}_\xi(Z) - n \log(1 - Z)) \quad (\text{S223})$$

with a rate function obtained from a non trivial variational formula. Here for a given ξ the value of Z which realizes the optimum is different from $Z_{\text{typ}}(\xi)$ and thus involves rare environments. Upon some simple manipulations, recalling that $Z = \Psi'(z)$ and $\hat{\Phi}'(Z) = -z$ we obtain $z = \frac{n}{1-Z}$ leading to the parametric representation

$$\Sigma_\xi(n) = \Psi_\xi(z) - z + n - n \log\left(\frac{n}{z}\right) \quad , \quad z(1 - \Psi'_\xi(z)) = n \quad (\text{S224})$$

Note that the approximation $N \log(1 - Z) \simeq -NZ$ valid for $Z = \Psi'_\xi(z) \ll 1$ would instead lead to $z \simeq n$ and $\Sigma_\xi(n) \simeq \Psi_\xi(z)$. Although we leave this study to the future, it is quite likely that a phase transition similar to the one of $\Psi(z)$ for $\xi > \xi_1$ for and for some values of z should also occur here. For $n \rightarrow 0$ one has $n \simeq z(1 - \Psi'_\xi(0)) = z(1 - Z_{\text{typ}}(\xi))$ and one recovers (S222). More precisely one has the expansion

$$\Sigma_\xi(n) = -n \log(1 - \Psi'_\xi(0)) + \frac{\Psi''_\xi(0)n^2}{2(1 - \Psi'_\xi(0))^2} + \mathcal{O}(n^3) \quad , \quad \Psi'_\xi(0) = Z_{\text{typ}}(\xi) \quad (\text{S225})$$

Position of the maximum: typical behavior. One can ask about the position of the maximum and its fluctuations. Let us introduce N i.i.d exponential random variables g_i of PDF $P(g) = e^{-g}\Theta(g)$, and call $G_N = \max_i g_i - \log N$. At large N , $G_N \rightarrow G$ a Gumbel random variable with $\mathbb{P}(G < g) = e^{-e^{-g}}$. For any N one has $\mathbb{P}(G < g) = (1 - \frac{1}{N}e^{-g})^N$. In a given environment one can write

$$\mathbb{P}(Y_N(T) < Y) = e^{N \log(1 - Z(Y,T))} = \overline{\Theta(G_N + \log N + H(Y,T) < 0)}^{G_N} \quad (\text{S226})$$

This formula is valid for any N and for large N one obtains the same formula with $G_N \rightarrow G$ by approximating $e^{N \log(1 - Z)} \simeq e^{-NZ}$. Note that G_N and G in this formula are independent of $H(Y,T)$. As discussed below, the approximation $Z \ll 1$ is also realized for any N with large probability when $\xi = Y/\sqrt{T}$ is large. The random position of the maximum $Y_N(T)$, in a given environment is then given by

$$G_N + \log N + H(Y,T) < 0 \quad \Leftrightarrow \quad Y_N(T) < Y \quad (\text{S227})$$

Note that $G_N + \log N$ is a positive random variable. Since $Z(Y,T)$ and thus $H(Y,T)$ is a positive decreasing function of Y in any sample, one may argue (by taking a derivative w.r.t. Y in (S226)) that (S227) is equivalent to

$$G_N + \log N + H(Y_N(T), T) = 0 \quad (\text{S228})$$

This formula generalizes [20, Eq. (50)] to any N .

Until now this is exact. Let us again consider the diffusive scaling regime $Y \sim \sqrt{T}$ at large T . In a typical environment, one has $H(Y,T) \simeq H_{\text{typ}}(\xi)$ where $\xi = Y/\sqrt{T}$ and $H_{\text{typ}}(\xi) = \log\left(\int_\xi^{+\infty} \frac{e^{-x^2/4}}{\sqrt{4\pi}}\right) = \log\left(\frac{1}{2}\text{Erfc}\left(\frac{\xi}{2}\right)\right) = -\frac{\xi^2}{4} - \log(\sqrt{\pi}\xi) + \mathcal{O}(\xi^{-1})$. Note that $H_{\text{typ}}(\xi)$ varies from 0 for $\xi \rightarrow -\infty$ to $-\infty$ for $\xi \rightarrow +\infty$. Let us denote y_N^{typ} the scaled position of the maximum in a typical environment. At large T it reaches a finite limit in distribution such that

$$G_N + \log N + H_{\text{typ}}(y_N^{\text{typ}}) = 0 \quad \Leftrightarrow \quad y_N^{\text{typ}} = H_{\text{typ}}^{-1}(-G_N - \log N) \quad (\text{S229})$$

where $H_{\text{typ}}^{-1}(h) = \xi$ is the reciprocal function of $H_{\text{typ}}(\xi) = h$. This is correct for any N . The distribution of y_N^{typ} is exactly the same as the one for the maximum of N Brownian motions at time $t = 1$, performing each diffusion $dB_i(t)^2 = 2dt$, started at $B_i(0) = 0$ at $t = 0$, i.e. for the problem without the quenched random

field. For $N \gg 1$, using the asymptotics of $H_{\text{typ}}(\xi)$ one finds the standard result

$$y_N^{\text{typ}} \simeq 2\sqrt{\log N} + \frac{G - \frac{1}{2} \log(4\pi \log N)}{\sqrt{\log N}} + \dots \quad (\text{S230})$$

We can now study the typical fluctuations from sample to sample. To lowest order one should take into account the typical fluctuations of $H(Y, T)$, which are $\delta H = \mathcal{O}(T^{1/4})$. The variance was obtained in (S160) as $\overline{H^2}^c = C_2(\xi)T^{-1/2}$, where the function $C_2(\xi)$ was given there. The position of the maximum is now determined by

$$G_N + \log N + H_{\text{typ}}(y_N) + \sqrt{C_2(y_N)}T^{-1/4}\omega = 0 \quad (\text{S231})$$

where ω is a Gaussian random variable of unit variance. Inverting to leading order at large time we find (an equation valid for any N)

$$y_N = H_{\text{typ}}^{-1} \left(-G_N - \log N - \sqrt{C_2(y_N^{\text{typ}})}T^{-1/4}\omega \right) + o(T^{-1/4}) \quad (\text{S232})$$

$$= y_N^{\text{typ}} - \frac{\sqrt{C_2(y_N^{\text{typ}})}}{H'_{\text{typ}}(y_N^{\text{typ}})}T^{-1/4}\omega + o(T^{-1/4}) \quad (\text{S233})$$

If $N \gg 1$ one finds

$$y_N = 2\sqrt{\log N} + \frac{G - \frac{1}{2} \log(4\pi \log N) + \sqrt{C_2(y_N^{\text{typ}})}T^{-1/4}\omega}{\sqrt{\log N}} + \dots \quad (\text{S234})$$

where we recall that the ω term represents the sample-to-sample fluctuations and the Gumbel variable G the "thermal" fluctuations, the two random variables being uncorrelated.

We can compare this result with Ref. [20, Eqs. (57-58)] setting $D = 1$ and $r_0 = 2$ there, which were obtained when N and T are large with the parameter $g = \frac{\log N}{\sqrt{T}}$ kept fixed. The KPZ time there is $T_{\text{KPZ}} = g^2 = \frac{(\log N)^2}{T}$. This agrees perfectly with the KPZ time in the present work $T_{\text{KPZ}} = \xi^4/(16T)$ where $\xi \sim y_N \sim 2\sqrt{\log N}$ from (S234). For the matching to [20, Eqs. (57-58)] to be perfect we need the variance of the KPZ height field at very short time (i.e. in the Edward-Wilkinson regime for droplet initial condition) which is given by [47]

$$\overline{h(0, T_{\text{KPZ}})^2}^c \simeq C_2^{\text{KPZ}} T_{\text{KPZ}}^{1/2} \quad , \quad C_2^{\text{KPZ}} = \sqrt{\frac{2}{\pi}} \quad (\text{S235})$$

One then easily checks that it exactly matches the amplitude of the fluctuating term $\sim \omega$ in (S234) using the large ξ behavior (S161), $C_2(\xi) \simeq \frac{\xi^2}{4} \sqrt{\frac{2}{\pi}}$.

To summarize, (S232) and (S234) extend the results of [20] about "typical" extremal diffusion to the diffusive regime $Y \sim \sqrt{T}$. In that new regime $\log N \ll \sqrt{T}$, i.e. $T \gg (\log N)^2$ and the fluctuations are of the Edwards-Wilkinson type. If N is large, $\log N$ does not need to be very large. As $(\log N)^2/T$ is increased there is a perfect match to the predictions of [20] in the regime $Y \sim T^{3/4}$ where the sample-to-sample fluctuations are governed by the finite-time KPZ equation.

Remark. The two independent random contributions in (S234) can be separated by considering simultaneously the "quantile" as done in numerical simulations [52], that is, instead of $y_N(T)$, $x_N(T) = \frac{X_N(T)}{\sqrt{T}}$ defined by $\int_{X_N(T)}^{+\infty} dy q_\eta(y, T) = \frac{1}{N}$ in a given sample, or in other words

$$\log H(X_N(T), T) = -\log N \quad , \quad Z(X_N(T), T) = \frac{1}{N} \quad (\text{S236})$$

Position of the maximum: large deviations. Finally, our results yield additional information about the large deviations of extremal diffusion, i.e. for rare environments such that $H - H_{\text{typ}} = \mathcal{O}(1)$. In that case if one heuristically replaces in (S228), $H(Y_N(T), T) \rightarrow H_{\text{typ}}(y_N(T)) + (H - H_{\text{typ}}(y_N^{\text{typ}}))$ one obtains

$$y_N \simeq H_{\text{typ}}^{-1}(-G_N - \log N - (H - H_{\text{typ}})) \quad (\text{S237})$$

and for $N \gg 1$

$$y_N \simeq 2\sqrt{\log N} + \frac{G - \frac{1}{2} \log(4\pi \log N) + (H - H_{\text{typ}}(\xi))}{\sqrt{\log N}} + \dots \quad (\text{S238})$$

with $\xi = 2\sqrt{\log N}$, for rare environments which occur with probability $\sim \exp(-\sqrt{T}\Phi_\xi(H))$. Since ξ is large, rewriting $H = -\frac{\xi^2}{4} - \log \frac{\xi}{2} + H_{\text{KPZ}}$, this is equivalent to extend the estimate of of [20] for the fluctuations of the position of the maximum to the large deviations regime of the KPZ equation (with rare environments occurring with probability $\sim \exp(-\frac{1}{\sqrt{T_{\text{KPZ}}}}\Phi_{\text{KPZ}}(H_{\text{KPZ}}))$ and with $T_{\text{KPZ}} = \frac{\xi^4}{16T} = \frac{(\log N)^2}{T} \ll 1$).

XII. EXTENSION TO GENERAL QUADRATIC MODELS IN THE MFT: DIFFUSION IN RANDOM MEDIUM AND THE SYMMETRIC SIMPLE EXCLUSION PROCESS

One definition of the MFT is as the Langevin equation of a diffusive gas with particle density $q(x, t)$ [61]

$$\partial_t q = \partial_x [D(q)\partial_x q - \sqrt{\sigma(q)}\xi(x, t)] \quad (\text{S239})$$

where $\xi(x, t)$ is a standard space-time white noise. The model solved in this present paper corresponds to $\sigma(q) = 2q^2$ and $D(q) = 1$. Averages of solutions of (S239) over the noise can be obtained from the dynamical action $S[q, p] = \iint dx dt [p\partial_t q - \mathcal{H}(q, p)]$ with Hamiltonian $\mathcal{H}(q, p) = -D(q)\partial_x q\partial_x p + \frac{1}{2}\sigma(q)(\partial_x p)^2$, and where $p(x, t)$ is the response field. At large time these averages can be obtained from the solutions to the saddle point equations $\partial_t q = \frac{\delta \mathcal{H}}{\delta p}$ and $\partial_t p = -\frac{\delta \mathcal{H}}{\delta q}$, which admit the conservation law $\frac{d}{dt} \mathcal{H}(p, q) = 0$.

We will focus below on a subclass of models within the MFT called quadratic models and show how the work of this present paper is relevant to solve them.

A. Mapping of quadratic models in the MFT to the coupled DNLS system

Consider here the quadratic MFT models which have a noise variance parameterized as

$$\sigma(q) = 2Aq(B - q) \quad (\text{S240})$$

and a diffusion constant $D(q) = 1$. This class contains both the SSEP and the present model of diffusion in random medium. The MFT hydrodynamic equations (i.e. the saddle point equations) read

$$\begin{aligned} \partial_t q &= \partial_x [\partial_x q - 2Aq(B - q)\partial_x p] \\ \partial_t p &= -\partial_x^2 p - A(B - 2q)(\partial_x p)^2 \end{aligned} \quad (\text{S241})$$

We introduce the generalized derivative Cole-Hopf transform

$$R(x, t) = A\partial_x p(x, t)e^{ABp(x, t)}, \quad Q(x, t) = q(x, t)e^{-ABp(x, t)}. \quad (\text{S242})$$

The variables $\{R, Q\}$ then verify the coupled DNLS system (S58) with $\beta = 1$

$$\begin{aligned} \partial_t Q &= \partial_x^2 Q + 2\partial_x(Q^2 R) \\ -\partial_t R &= \partial_x^2 R - 2\partial_x(QR^2) \end{aligned} \quad (\text{S243})$$

B. Gauge transformation between NLS and DNLS and relation with the non-local transformation of [43]

Change of variable of Wadati and Sogo. Wadati and Sogo proved in 1982 [62] that the non-linear Schrodinger equation and the derivative non-linear Schrodinger equation were gauge equivalent. Indeed, consider the following systems in the conventions of [62], firstly the coupled NLS

$$\begin{aligned} \mathbf{i}q_{1t} + q_{1xx} - 2r_1q_1^2 &= 0 \\ \mathbf{i}r_{1t} - r_{1xx} + 2r_1^2q_1 &= 0 \end{aligned} \quad (\text{S244})$$

and secondly the coupled DNLS

$$\begin{aligned} q_{2t} - \mathbf{i}q_{2xx} - (r_2q_2^2)_x &= 0 \\ r_{2t} + \mathbf{i}r_{2xx} - (r_2^2q_2)_x &= 0 \end{aligned} \quad (\text{S245})$$

Wadati and Sogo showed that the following change of variables allows to map the coupled DNLS system to the coupled NLS system.

$$\begin{aligned} q_1 &= \frac{q_2}{2} \exp\left(-\mathbf{i} \int_{-\infty}^x r_2 q_2\right) \\ r_1 &= (-\mathbf{i}r_{2x} + r_2^2 q_2/2) \exp\left(\mathbf{i} \int_{-\infty}^x r_2 q_2\right) \end{aligned} \quad (\text{S246})$$

To show the relation with the non-local transformation of [43], one needs to relate the conventions of Wadati to the ones of this present work and of [43]. We first transform the time in (S244) and (S245) as $t \rightarrow \mathbf{i}t$, and choose

$$\begin{aligned} q_1 &= v, & r_1 &= u \\ q_2 &= -2R, & r_2 &= \mathbf{i}Q \end{aligned} \quad (\text{S247})$$

We obtain that (S245) is the $\{R, Q\}$ system with $\beta = 1$ (that is e.g. (11) with $g = 0$ or (S58)) and that (S244) is the $\{P, Q\}$ system with $g = -1$. This $\{P, Q\}$ system is precisely the equations verified by the functions $\{v, u\}$ of [43] (with $v = P$ and $u = Q$).

Now, considering the MFT for the SSEP, we have shown in (S242) that the derivative Cole-Hopf transform of the MFT variables verify the DNLS $\{R, Q\}$ system. Performing the gauge transformation (S246) with our new variables thus leads to

$$\begin{aligned} u &= (Q^2 R + \partial_x Q) \exp\left(2 \int_{-\infty}^x dy QR\right) \\ v &= -R \exp\left(-2 \int_{-\infty}^x dy QR\right) \end{aligned} \quad (\text{S248})$$

We can now go back to the variables q and p of the MFT using the generalized derivative Cole-Hopf transform (S242), and we obtain

$$u = (-Aq(B - q)\partial_x p + \partial_x q) \exp\left(-\int_{-\infty}^x dy A(B - 2q)\partial_y p\right) \quad (\text{S249})$$

$$v = -A\partial_x p \exp\left(\int_{-\infty}^x dy A(B - 2q)\partial_y p\right) \quad (\text{S250})$$

which is valid for any quadratic theory. This recovers the "generalized Cole-Hopf equations" obtained very recently in [43, Eqs. (10)–(11)] (which use the notations $H = p$ and $\varrho = q$). Note however the missing the factor A in the second equation in that work.

C. Stationary measure

The stochastic equation (S239) admits generically a family of stationary measures. For instance if one fixes the boundary conditions as $q(0) = q(L) = \varrho$, and if the problem is taken on a finite-size interval, the stationary measure is [2, 26, 61, 63]

$$\mathcal{P}_{\text{eq}}(\{q(x)\}) \sim e^{-\int_0^L dx (f(q(x)) - f(\varrho) - (q(x) - \varrho) f'(\varrho))} \quad (\text{S251})$$

where $f''(q) = \frac{2D(q)}{\sigma(q)}$. The linear term is determined so that the maximum probability is for $q = \varrho$.

Consider the model of diffusion in a random environment studied here in Eq. (2), with a more general amplitude for the noise. In that case one has $D(q) = 1$ and $\sigma(q) = 2\alpha q^2$, hence $f''(q) = 1/(\alpha q^2)$. This leads to $f(q) = -\frac{1}{\alpha} \log q + kq + c$, and to the stationary measure

$$\mathcal{P}_{\text{eq}}(\{q(x)\}) \propto e^{-\frac{1}{\alpha} \int_0^L dx (-\log(q(x)/\varrho) + \frac{q-\varrho}{\varrho})} \quad (\text{S252})$$

Remark. The stationary measure (S252) is the analog in the continuum of a discrete measure on a lattice defined as a product of independent Gamma variables at each site, i.e. $\prod_x w_x$, with PDF $p(w) \propto w^{\gamma-1} e^{-w}$. Indeed that measure appeared as a stationary measure in the Beta polymer problem, in a (long time) one point version in [18], and for a more general discussion see [64]. For the more general quadratic model parametrized as (S240), in particular for the SSEP, the corresponding discrete stationary measures are instead factorized Bernoulli.

Remark. For the diffusion model, one has $B = 0$ in (S240). Hence $R = A\partial_x p$ and $Q = q$ satisfy the DNLS system with $\beta = 1$. By choosing here $A = -\alpha$ one can vary the exponent γ of the local Gamma distribution to any value in the stationary measure.

D. Extension of [43] to quadratic MFT models with annealed initial condition and tracer away from the origin

Let us consider a model within the MFT where the noise variance is parametrized as (S240). We study here the annealed case where the initial condition of the hydrodynamic equations (S241) is fluctuating according to the stationary measure of the MFT [2, 35, 36]. We choose the initial condition as a local equilibrium configuration with two different densities on the positive and negative axis

$$\mathcal{P}(q(x, 0)) \sim e^{-\sqrt{T}\mathcal{F}(q(x, 0))}, \quad \mathcal{F}(q(x, 0)) = \int_{\mathbb{R}} dx \int_{\tilde{q}(x)}^{q(x, 0)} dz \frac{2D(z)}{\sigma(z)} (q(x, 0) - z) \quad (\text{S253})$$

with $\tilde{q}(x) = q_- \Theta(-x) + q_+ \Theta(x)$ is the step density profile.

We will be interested in the position X_t of a tracer initially located at position $X_0 = 0$ and at final position $X_1 = \xi$. Its position at any time is defined as

$$\int_0^{X_t} dx q(x, t) = \int_0^\infty dx (q(x, t) - q(x, 0)) \quad (\text{S254})$$

If we focus on the generating function of X_1 or the current at the right of X_1 , i.e. $Z(\xi) = \int_\xi^\infty dx (q(x, 1) - q(x, 0))$, then it was shown [26, 35, 36] that the mixed-time boundary conditions of the hydrodynamic system (S240) read

$$p(x, 1) = \lambda \Theta(x - \xi) \quad (\text{S255})$$

$$p(x, 0) = \lambda \Theta(x) + \int_{\tilde{q}(x)}^{q(x, 0)} dr \frac{2D(r)}{\sigma(r)} \quad (\text{S256})$$

for some constant λ . Using the gauge transformation (S250) along with the same manipulations as the ones in [43, below Eqs. (14)-(15)] allows to transform these boundary conditions for $\{p, q\}$ into simple boundary conditions for $\{u, v\}$

$$u(x, 0) = \frac{\omega}{K} \delta(x), \quad v(x, 1) = K \delta(x - \xi). \quad (\text{S257})$$

for some constant K to be determined as in [43]. These boundary conditions have an asymmetry due to the presence of ξ that we can cancel using the same boost transformation as in (S61)

$$U(x, t) = u(x - vt, t) e^{-\frac{1}{2}xv + \frac{v^2}{4}t}, \quad V(x, t) = v(x - vt, t) e^{\frac{1}{2}xv - \frac{v^2}{4}t}, \quad (\text{S258})$$

Note that this boost leaves the coupled NLS system (S244) invariant. We choose $v = -\xi$ so that

$$U(x, t) = u(x + \xi t, t) e^{\frac{1}{2}x\xi + \frac{\xi^2}{4}t}, \quad V(x, t) = v(x + \xi t, t) e^{-\frac{1}{2}x\xi - \frac{\xi^2}{4}t}, \quad (\text{S259})$$

which yields for boundary conditions

$$U(x, 0) = \frac{\omega}{K} \delta(x), \quad V(x, 1) = K e^{-\frac{\xi^2}{4}} \delta(x). \quad (\text{S260})$$

One can then proceed as in this work to complete the scattering analysis and solve the large-deviation problem.

E. Discussion on the quench and annealed initial conditions

The quadratic models of MFT have been investigated through the spectrum of classical integrability in three works and two contexts of initial conditions:

- Reference [43] considered the SSEP with an initial condition in the annealed class and solved the problem through the mapping to the coupled NLS $\{P, Q\}$ system and the use of its scattering theory. The remarkable feature of that work is that the annealed initial condition for the SSEP admits a simple quenched δ, δ mixed-time boundary conditions interpretation in the coupled NLS $\{P, Q\}$ system.
- The present work as well as Ref. [41] considered the diffusion in random media, equivalent to the KMP model, with a quenched initial condition and solved the problem using the scattering theory of the coupled DNLS $\{R, Q\}$ system.

At this stage, the observation is that depending on whether the quench or annealed initial condition is considered, a specific integrable model might be more suited to obtain the exact solution of the problem. Since other gauge transformations between integrable models have been proposed in [62], it would be interesting to investigate whether mappings to other integrable models would allow to answer new questions.

-
- * alexandre.krajenbrink@cambridgequantum.com
- [1] L. Bertini, A. De Sole, D. Gabrielli, G. Jona-Lasinio and C. Landim, *Macroscopic fluctuation theory*. *Reviews of Modern Physics*, **87**(2):593, (2015).
 - [2] B. Derrida, *Non equilibrium steady states: fluctuations and large deviations of the density and of the current* *Journal of Statistical Mechanics: Theory and Experiment*, 2007(07):P07023, (2007).
 - [3] Derrida B, *An exactly soluble non-equilibrium system: the asymmetric simple exclusion process*. *Physics Reports*, **301**(1-3):65–83, (1998).
 - [4] C. A. Tracy and H. Widom. *Asymptotics in ASEP with step initial condition*. *Comm. Math. Phys.*, **290**(1):129–154, (2009).
 - [5] M. Kardar, G. Parisi and Y-C. Zhang, *Dynamic Scaling of Growing Interfaces*, *Phys. Rev. Lett.* **56**, 889, (1986).
 - [6] L. Bertini and G. Giacomin. *Stochastic burgers and KPZ equations from particle systems*. *Communications in mathematical physics*, **183**(3):571–607, (1997).
 - [7] I. V. Kolokolov, S. E. Korshunov, *Explicit solution of the optimal fluctuation problem for an elastic string in random potential*. *Phys. Rev. E* **80**, 031107, (2009); *Universal and non-universal tails of distribution functions in the directed polymer and KPZ problems*. *Phys. Rev. B* **78**, 024206, (2008); *Optimal fluctuation approach to a directed polymer in a random medium*. *Phys. Rev. B* **75**, 140201, (2007).
 - [8] B. Meerson, E. Katzav, A. Vilenkin, *Large Deviations of Surface Height in the Kardar-Parisi-Zhang Equation*, *Physical Review Letters* **116**, 070601, (2016).
 - [9] N. R. Smith, B. Meerson, and A. Vilenkin. *Time-averaged height distribution of the Kardar-Parisi-Zhang interface*. (and references therein) [arXiv:1902.08110](https://arxiv.org/abs/1902.08110), (2019).
 - [10] A. Krajenbrink and P. Le Doussal. *Inverse scattering of the Zakharov-Shabat system solves the weak noise theory of the Kardar-Parisi-Zhang equation*. *Phys. Rev. Lett.*, **127** (6):064101, (2021).
 - [11] A. Krajenbrink and P. L. Doussal. *Inverse scattering solution of the weak noise theory of the Kardar-Parisi-Zhang equation with flat and Brownian initial conditions*. [arXiv:2107.13497](https://arxiv.org/abs/2107.13497), (2021).
 - [12] Shabat, A., and V. Zakharov. *Exact theory of two-dimensional self-focusing and one-dimensional self-modulation of waves in nonlinear media*. *Soviet physics JETP* **34.1** (1972).
 - [13] Ablowitz, M. J., Kaup, D. J., Newell, A. C., and Segur, H. *The inverse scattering transform-Fourier analysis for nonlinear problems*. *Studies in Applied Mathematics*, **53**(4), 249-315, (1974).
 - [14] D. J. Kaup and A. C. Newell. *An exact solution for a derivative nonlinear Schrödinger equation*. *Journal of Mathematical Physics*, **19**(4):798–801, (1978).
 - [15] G. Barraquand and I. Corwin. *Random-walk in beta-distributed random environment*. *Probab. Theory Rel. Fields*, **167**(3):1057–1116, (2017).
 - [16] P. Le Doussal, T. Thiery, *Diffusion in time-dependent random media and the Kardar-Parisi-Zhang equation*, *Phys. Rev. E* **96**, 010102 (2017).
 - [17] I. Corwin and Y. Gu. *Kardar–Parisi–Zhang equation and large deviations for random walks in weak random environments*. *J. Stat. Phys.*, **166**(1):150–168, (2017).
 - [18] T. Thiery, P. Le Doussal, *Exact solution for a random walk in a time-dependent 1D random environment: the point-to-point Beta polymer*, *Journal of Physics A: Mathematical and Theoretical* **50** 4, (2016).
 - [19] G. Barraquand and M. Rychkovsky. *Large deviations for sticky Brownian motions*. [arXiv:1905.10280](https://arxiv.org/abs/1905.10280), (2019).
 - [20] G. Barraquand and P. Le Doussal. *Moderate deviations for diffusion in time dependent random media*. *Journal of Physics A: Mathematical and Theoretical* **53.21**: 215002, (2020).
 - [21] D. Bernard and P. Le Doussal. *Entanglement entropy growth in stochastic conformal field theory and the KPZ class*. *Europhysics Letters*, **131**(1):10007, (2020).
 - [22] G. Barraquand, *Some integrable models in the KPZ universality class*, Probability [math.PR]. Université Paris Diderot – Paris 7, 2015. English. tel-01167855 HAL Id: tel-01167855 <https://tel.archives-ouvertes.fr/tel-01167855>.
 - [23] C. Kipnis, C. Marchioro and E. Presutti, *Heat flow in an exactly solvable model* *J. Stat. Phys.* **27**, 65, (1982)
 - [24] L. Bertini, A. De Sole, D. Gabrielli, G. Jona-Lasinio, and C. Landim, *Current Fluctuations in Stochastic Lattice Gases* *Phys. Rev. Lett.* **94**, 030601 (2005).
 - [25] L. Bertini, D. Gabrielli, and J. L. Lebowitz. *Large deviations for a stochastic model of heat flow*. *Journal of statistical physics*, **121**(5):843–885, (2005).
 - [26] B. Derrida and A. Gerschenfeld, *Current Fluctuations in One Dimensional Diffusive Systems with a Step Initial Density Profile* *J. Stat. Phys.* **137**, 978 (2009).
 - [27] V. Lecomte, A. Imparato, and F. van Wijland, *Current Fluctuations in Systems with Diffusive Dynamics, in and out of Equilibrium* *Prog. Theor. Phys. Suppl.* **184**, 276 (2010).
 - [28] P. L. Krapivsky and B. Meerson, *Fluctuations of current in nonstationary diffusive lattice gases* *Phys. Rev. E* **86**, 031106 (2012).
 - [29] L. Zarfaty and B. Meerson, *Statistics of large currents in the Kipnis–Marchioro–Presutti model in a ring geometry* *J. Stat. Mech.* **033304** (2016).
 - [30] T. Bodineau and B. Derrida, *Distribution of current in nonequilibrium diffusive systems and phase transitions* *Phys. Rev. E* **72**, 066110 (2005)
 - [31] J. Tailleur, J. Kurchan, and V. Lecomte, *Mapping Nonequilibrium onto Equilibrium: The Macroscopic*

- Fluctuations of Simple Transport Models* [Phys. Rev. Lett.](#) **99**, 150602 (2007)
- [32] P. I. Hurtado and P. L. Garrido, *Spontaneous Symmetry Breaking at the Fluctuating Level* [Phys. Rev. Lett.](#) **107**, 180601 (2011). A. Prados, A. Lasanta, and P. I. Hurtado, *Nonlinear driven diffusive systems with dissipation: Fluctuating hydrodynamics* [Phys. Rev. E](#) **86**, 031134 (2012). C. Gutierrez-Ariza and P. I. Hurtado, *The kinetic exclusion process: a tale of two fields* [J. Stat. Mech.](#) **103203** (2019).
- [33] M. A. Peletier, F. H. J. Redig, and K. Vafayi, *Large deviations in stochastic heat-conduction processes provide a gradient-flow structure for heat conduction* [J. Math. Phys.](#) **55**, 093301 (2014).
- [34] O. Shpielberg, Y. Don, and E. Akkermans, *Numerical study of continuous and discontinuous dynamical phase transitions for boundary-driven systems* [Phys Rev E](#) **95**, 032137 (2017).
- [35] A. Grabsch, A. Poncet, P. Rizkallah, P. Illien, and O. Bénichou. Closing and solving the hierarchy for large deviations and spatial correlations in single-file diffusion. [arXiv:2110.09269](#), (2021).
- [36] A. Poncet, A. Grabsch, P. Illien, and O. Bénichou. *Generalized correlation profiles in single-file systems.* [Physical review letters](#), **127(22):220601**, (2021).
- [37] See Supplemental material.
- [38] Since $\hat{\Phi}(Z)$ may not be convex it should be called a Legendre-Fenchel transform, which is not involutive [45].
- [39] We will keep β as a parameter but for the application to obtain $\Psi(z)$ it is understood that it is set to $\beta = -1$.
- [40] Comparing with [10] the "true" coupling constant is in fact $\hat{g} = \Lambda g = -z \xi e^{-\frac{\xi^2}{4}}$, see [37].
- [41] Bettelheim, Eldad, Naftali R. Smith, and Baruch Meerson. *Inverse Scattering Method Solves the Problem of Full Statistics of Nonstationary Heat Transfer in the Kipnis-Marchioro-Presutti Model.* [arXiv:2112.02474](#), (2021).
- [42] Wadati, Miki, Kimiaki Konno, and Yoshi-Hiko Ichikawa. *A generalization of inverse scattering method.* No. IPPJ-381. Nagoya Univ.(Japan). [Inst. of Plasma Physics](#), (1979).
- [43] K. Mallick, H. Moriya, and T. Sasamoto. *Exact solution of the macroscopic fluctuation theory for the symmetric exclusion process.* [arXiv:2202.05213](#), (2022).
- [44] When the integrand has a jump at $q = 0$, one integrates respecting the symmetry $\mathbf{i}q \rightarrow -\mathbf{i}q$, equivalently one integrates on \mathbb{R}^- and take twice the real part.
- [45] Hugo Touchette. *The large deviation approach to statistical mechanics.* [Physics Reports](#), **478(1-3):1-69**, (2009).
- [46] A. Krajenbrink, P. Le Doussal, *In preparation*
- [47] P. Le Doussal, S. N. Majumdar, A. Rosso, G. Schehr, *Exact short-time height distribution in 1D KPZ equation and edge fermions at high temperature,* [Phys. Rev. Lett.](#) **117**, 070403, (2016).
- [48] For the KPZ equation the partition sum $Z_{\text{KPZ}} = e^{H_{\text{KPZ}}}$ is an unbounded random variable. As a result the rate function $\Psi(\tilde{z})$ is undefined for $\tilde{z} < -1$. The present convergence results show precisely how, in the large ξ limit, one goes from a bounded random variable Z to an unbounded one Z_{KPZ} .
- [49] A. Krajenbrink, P. Le Doussal, *Simple derivation of the $(-\lambda H)^{5/2}$ large deviation tail for the 1D KPZ equation,* [J. Stat. Mech.](#) **063210**, (2018).
- [50] A. Krajenbrink, P. Le Doussal, S. Prolhac, *Systematic time expansion for the Kardar-Parisi-Zhang equation, linear statistics of the GUE at the edge and trapped fermions.* [Nuclear Physics B](#), **936** 239-305, (2018).
- [51] Alexandre Krajenbrink. *Beyond the typical fluctuations: a journey to the large deviations in the Kardar-Parisi-Zhang growth model.* [PhD thesis, PSL Research University](#), 2019.
- [52] Ivan Corwin, *Private communication and in preparation.*
- [53] Although it maps to the $\{P, Q\}$ system with $\delta - \delta$ initial conditions, as the WNT of the KPZ equation with droplet initial condition, because of the highly non-local nature of the mapping it does not map SSEP observables to KPZ ones in any obvious way.
- [54] Li-Cheng Tsai, *Integrability in the weak noise theory,* [arXiv:2204.00614](#)
- [55] see e.g. Section 3.3.1. in M. Dunajski. *Solitons, Instantons and Twistors.* [Oxford University Press, Oxford](#), 2009.
- [56] Kisil, Anastasia V. *The relationship between a strip Wiener-Hopf problem and a line Riemann-Hilbert problem.* [IMA Journal of Applied Mathematics](#) **80.5: 1569-1581**, (2015).
- [57] Chapter 1.3 in Noble, B. (1958) *Methods Based on the Wiener-Hopf Technique for the Solution of Partial Differential Equations.* [International Series of Monographs on Pure and Applied Mathematics, vol. 7.](#) New York: Pergamon Press.
- [58] R. M. Corless, G. H. Gonnet, D. E. Hare, D. J. Jeffrey, D. E. Knuth *On the Lambert W function,* [Advances in Computational Mathematics](#), **5** 329-359, (1996).
- [59] A. Krajenbrink, P. Le Doussal, *Exact short-time height distribution in the one-dimensional Kardar-Parisi-Zhang equation with Brownian initial condition,* [Phys. Rev. E](#) **96**, 020102, (2017).
- [60] D. Brockington, J. Warren *The Bethe Ansatz for Sticky Brownian Motions,* [arXiv:2104.06482](#)
- [61] H. Spohn, *Large Scale Dynamics of Interacting Particles* ([Springer, New York](#), 1991)
- [62] M. Wadati and K. Sogo. *Gauge transformations in soliton theory.* [Journal of the Physical Society of Japan](#), **52(2):394-398**, (1983).
- [63] Bertini, L., De Sole, A., Gabrielli, D., Jona-Lasinio, G., Landim, C., *Towards a nonequilibrium thermodynamics: a self-contained macroscopic descrip-*

tion of driven diffusive systems. *J. Stat. Phys.* **135**, 857–872, (2009).

[64] G. Barraquand, M. Rychnovsky, *Random walk on*

nonnegative integers in beta distributed random environment, [arXiv:2201.07270](https://arxiv.org/abs/2201.07270), (2022).